

From (very) Basic Ideas to Rather Complex Gaseous Detector Systems

Maxim Titov, CEA Saclay, Irfu, France

TIPP2023

TECHNOLOGY IN INSTRUMENTATION & PARTICLE PHYSICS CONFERENCE

4 - 8 SEPTEMBER 2023

Topics

- Accelerator-based particle physics
- Non-accelerator particle physics and particle astrophysics
- Experiments with synchrotron radiation and neutrons
- Nuclear physics
- Cosmology
- Instrumentation and monitoring of particle and photon beams
- Applications in photon science, biology, medicine, and engineering

The conference aims to provide a stimulating atmosphere for science and engineering for future experiments and social applications.

International Advisory Committee

Elisabetta Barberio	Manfred Kramer
Ties Behnke	Gobinda Majumder
Sara Bolognesi	Ana Amelia Machado
Shikma Bressler	Petra Merkel
Florencia Canelli	Joachim Mnich
Cinzia Da Via	Nadia Pastore
Marcel Demarteau	Fabrice Retiere
Maria Teresa Dova	Yun Tikhonov
Lattifa Elouadihni	Maxim Titov
Antonio Ferrer	Gigori Trubnikov
Francesco Forti	Niels van Bakel
Ingrid Gregor	Zebion Vilakazi
Borys Grynyov	Jianchun Wang
Kazunori Hanagaki	Yifang Wang
Karl Jakschits	Marc Winter
Antoine Kouchner	

Local Organizing Committee

Shimaa AbuZeid	Oscar Kureba
Jigane Azzouzi	Bruce Mellado (Chair)
Raja Chaerkhaji El Moursli	Pearne Moleka
Sergine Bira Gueye	Amr Radi
Peter Jones	Yahya Tayalati
Naima El Khayati	Michelle Bark
Betty Kibringe	Sahal Yacoub

Cape Town International Convention Centre (CTICC)

science & innovation
Department of Science and Technology
REPUBLIC OF SOUTH AFRICA

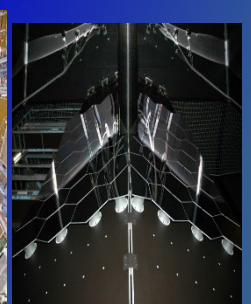
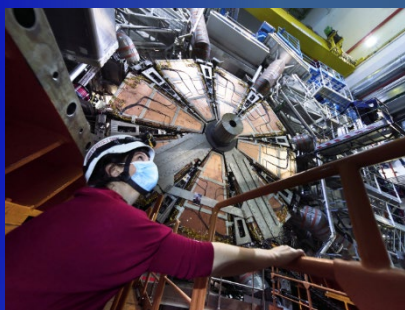
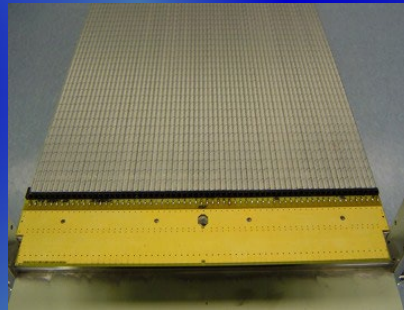
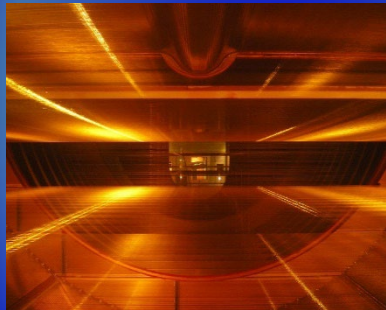
NRF
NATIONAL RESEARCH FOUNDATION
FOR HUMAN-CENTRED RESEARCH

iThemba LABS
International Centre for Data Science
Liaison for Africa

IUPAP
International Union of Pure and Applied Physics

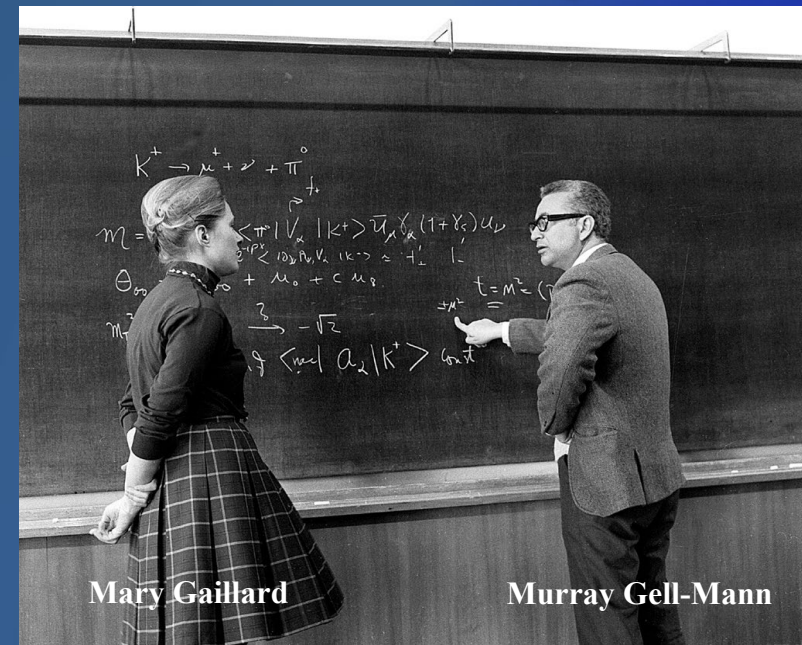
email: tipp2023@tlabs.ac.za

website: <https://indico.tlabs.ac.za/event/112/>



TIPP2023 Instrumentation School in Particle, Nuclear and Medical Physics Instrumentation School, Cape Town, South Africa, Aug. 24 - Sep. 1, 2023

To make a collider experiment, one needs:



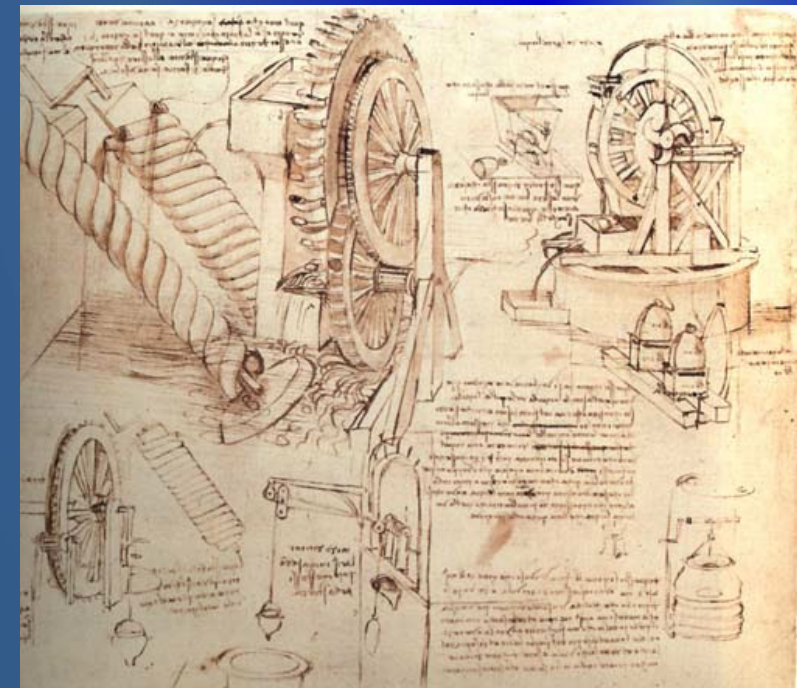
Mary Gaillard

Murray Gell-Mann

A theory:



and a cafeteria



Clear and easy understandable drawings



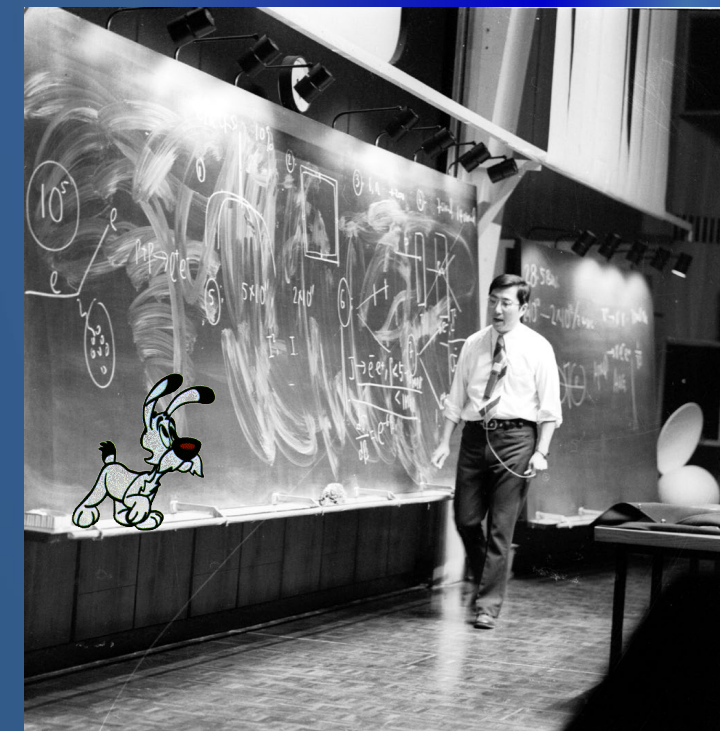
and a tunnel for the accelerator and magnets and stuff



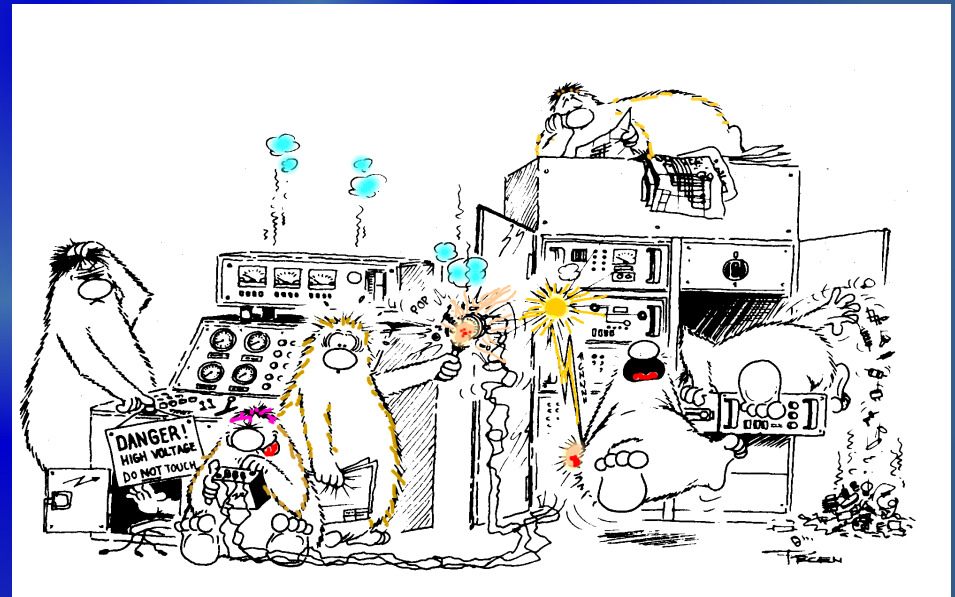
Easy
access
to the
experiment



Physicists to operate detector/analyze data



and a
Nobel
prize



We will just concentrate on
Particle Detectors – “Gaseous Detectors”

Gas-Based Detectors: A Brief History



Geiger Counter
H.Geiger W.Mueller 1928

PPC
Parallel Plate Counter

PC
Proportional Counter

Pestov Counter
V.Pestov 1982

RPC
Resistive Plate Chambers
R.Santonico R.Cardarelli 1981



MWPC
Multiwire Proportional Chamber
G.Charpak et al 1968

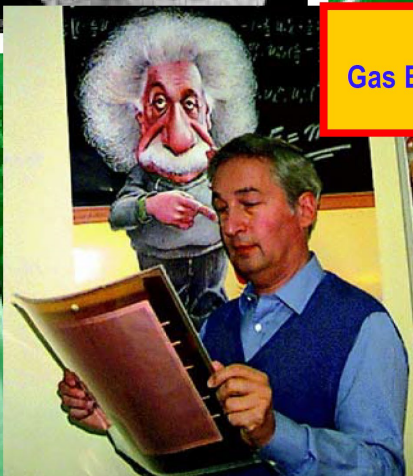
TPC
Time Projection Chamber
D.R.Nygren et al 1974



MSGC
Microstrip Gas Chambers
A.Oed 1988

GEM
Gas Electron Multiplier
F.Sauli 1997

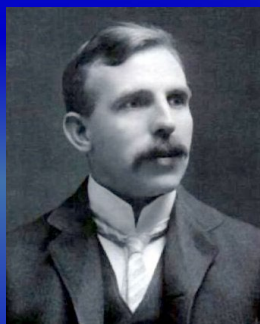
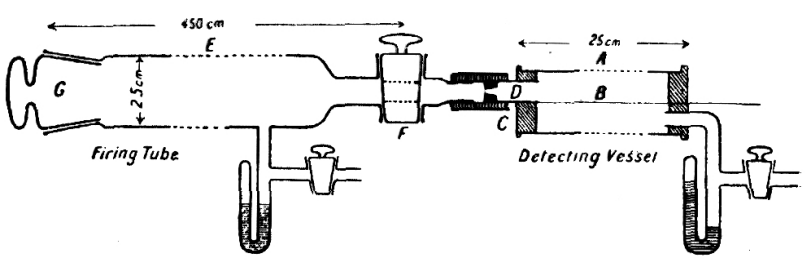
μ M
Micromegas
I.Giomataris et al 1996



Family of Gaseous Detectors with a Glorious Tradition

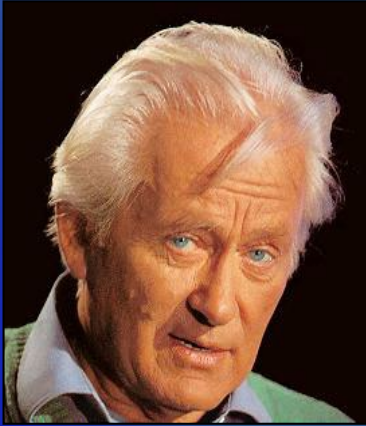
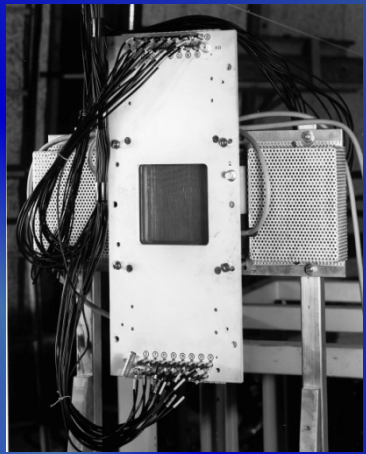
1908: FIRST WIRE COUNTER USED BY RUTHERFORD
IN THE STUDY OF NATURAL RADIOACTIVITY

1968: MULTIWIRE PROPORTIONAL
CHAMBER



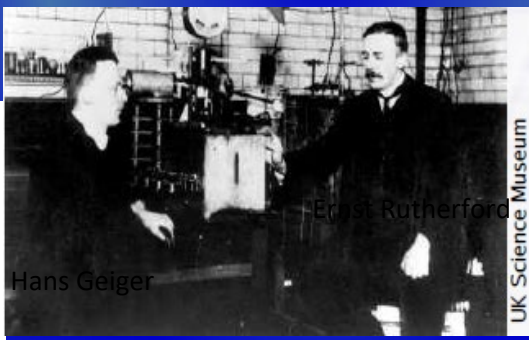
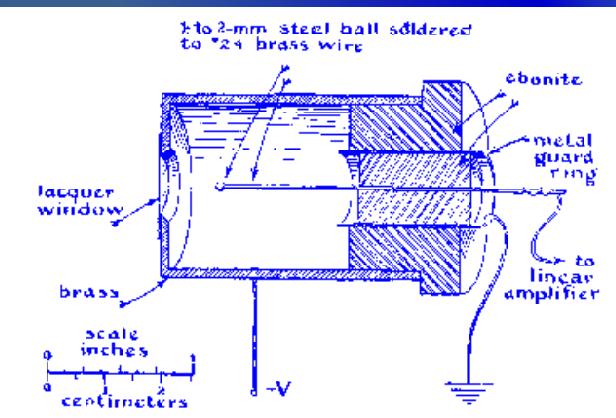
E. Rutherford and H. Geiger, Proc. Royal Soc. A81 (1908) 141

Nobel Prize in Chemistry in 1908



Nobel Prize in Physics 1992

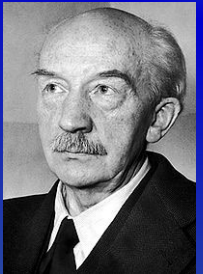
1928: GEIGER COUNTER
SINGLE ELECTRON SENSITIVITY



Hans Geiger

Ernest Rutherford

UK Science Museum



Walther Bothe
Nobel Prize in Physics 1954 for the "coincidence method"

H. Geiger and W. Müller, Phys. Zeits. 29 (1928) 839



George Charpak

Fabio Sauli

Jean-Calude Santiard

G. Charpak, Proc. Int. Symp. Nuclear Electronics (Versailles 10-13 Sept 1968)

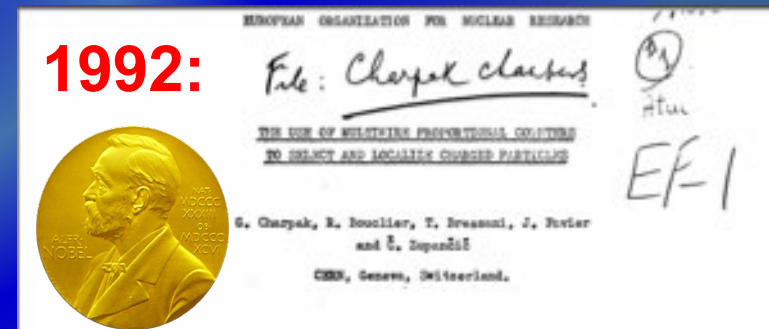
1968: MWPC – Revolutionising the Way Particle Physics is Done



G. Charpak, F. Sauli and J.C. Santiard

Before MWPC: Detecting particles was a mainly a manual, tedious and labour intensive job – unsuited for rare particle decays

1968: George Charpak developed the **MultiWire Proportional Chamber**, (MWPC), which revolutionized particle detection & HEP, **and marked transition from Manual to Electronics era**



“Image” & “Logic (electronics)” tradition combined into the “**Electronics Image**” detectors during the 1970ies

Multi-Wire Proportional Chambers – Particle Physics Spin-Off

Biospace: Company Founded In 1989 by Georges Charpak



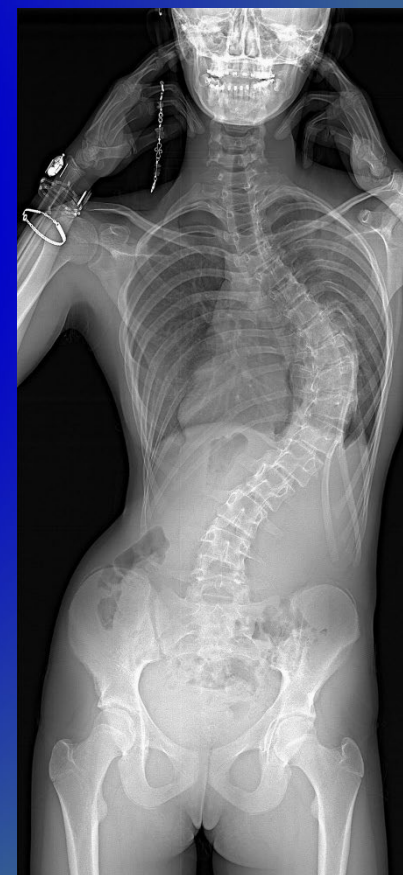
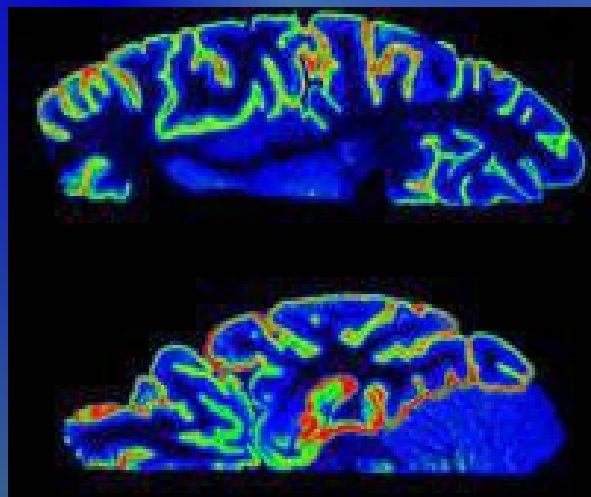
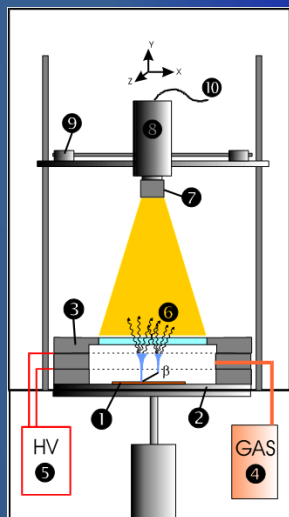
<http://www.biospacelab.com>:

Our digital autoradiography system leverages the gas detection technology invented by our founder Georges Charpak:

Nobel Prize in Physics in 1992.

~ 2000: **LOW-DOSE
3D IMAGING**

COMMERCIAL AUTORADIOGRAPHY SYSTEMS WITH GASEOUS DETECTORS



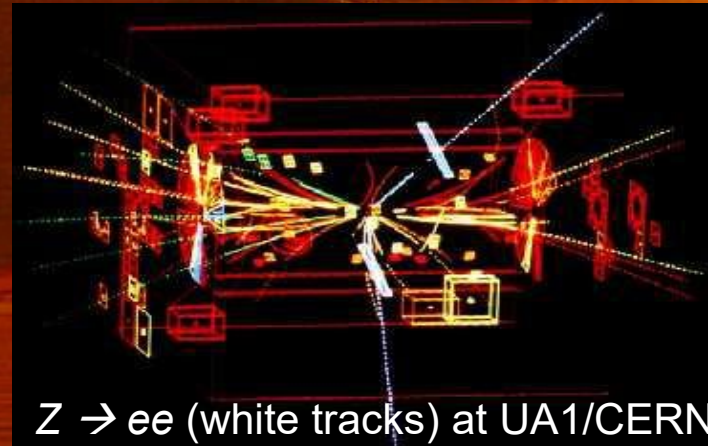
1983/1984: Discovery of W and Z Bosons at UA1/UA2

UA1 used the largest wire / drift chamber of its day (5.8 m long, 2.3 m in diameter)

It can now be seen in the CERN Microcosm Exhibition

Discovery of W and Z bosons
C. Rubbia & S. Van der Meer,

1984:



Z \rightarrow ee (white tracks) at UA1/CERN

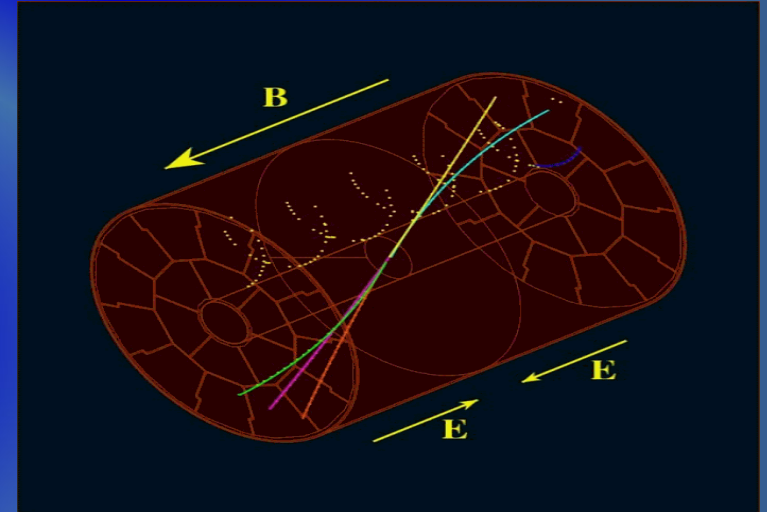
Time Projection Chamber (TPC) in Particle and Ion Physics

PEP4 (SLAC)

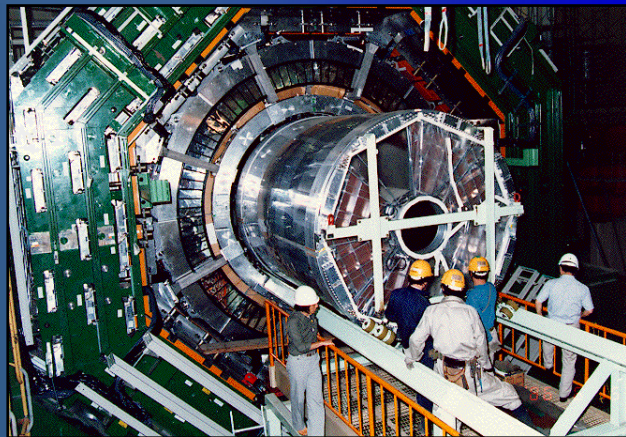


- ✓ Invented by David Nygren (Berkeley) in 1974
- ✓ Proposed as a central tracking device for the PEP-4 detector @ SLAC 1976
- More (and even larger) were built, based on MPWC readout
- New generation of TPCs use MPGD-based readout: e.g. ALICE Upgrade, T2K, ILC, CepC

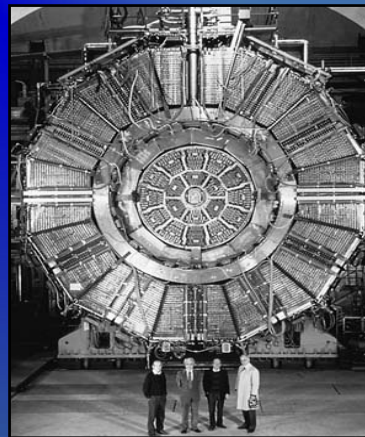
An ultimate drift chamber design is **TPC concept - 3D precision tracking** with low material budget & enables **particle identification** through differential energy loss dE/dx measurement or cluster counting dN_{cl}/dx techniques.



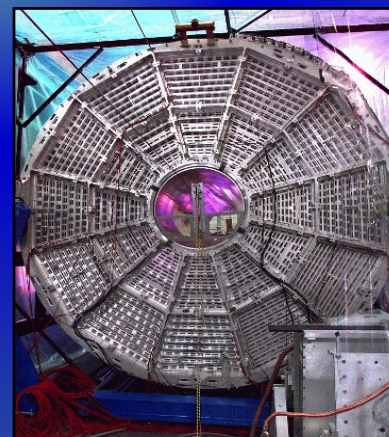
TOPAZ (KEK)



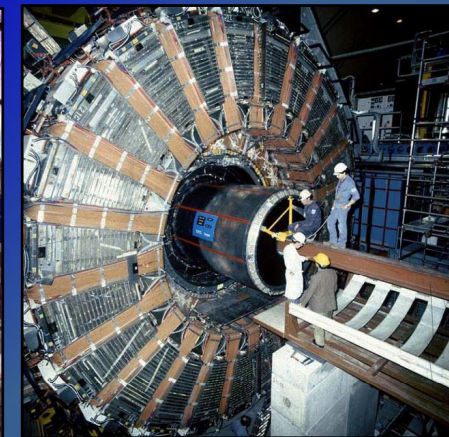
ALEPH (CERN)



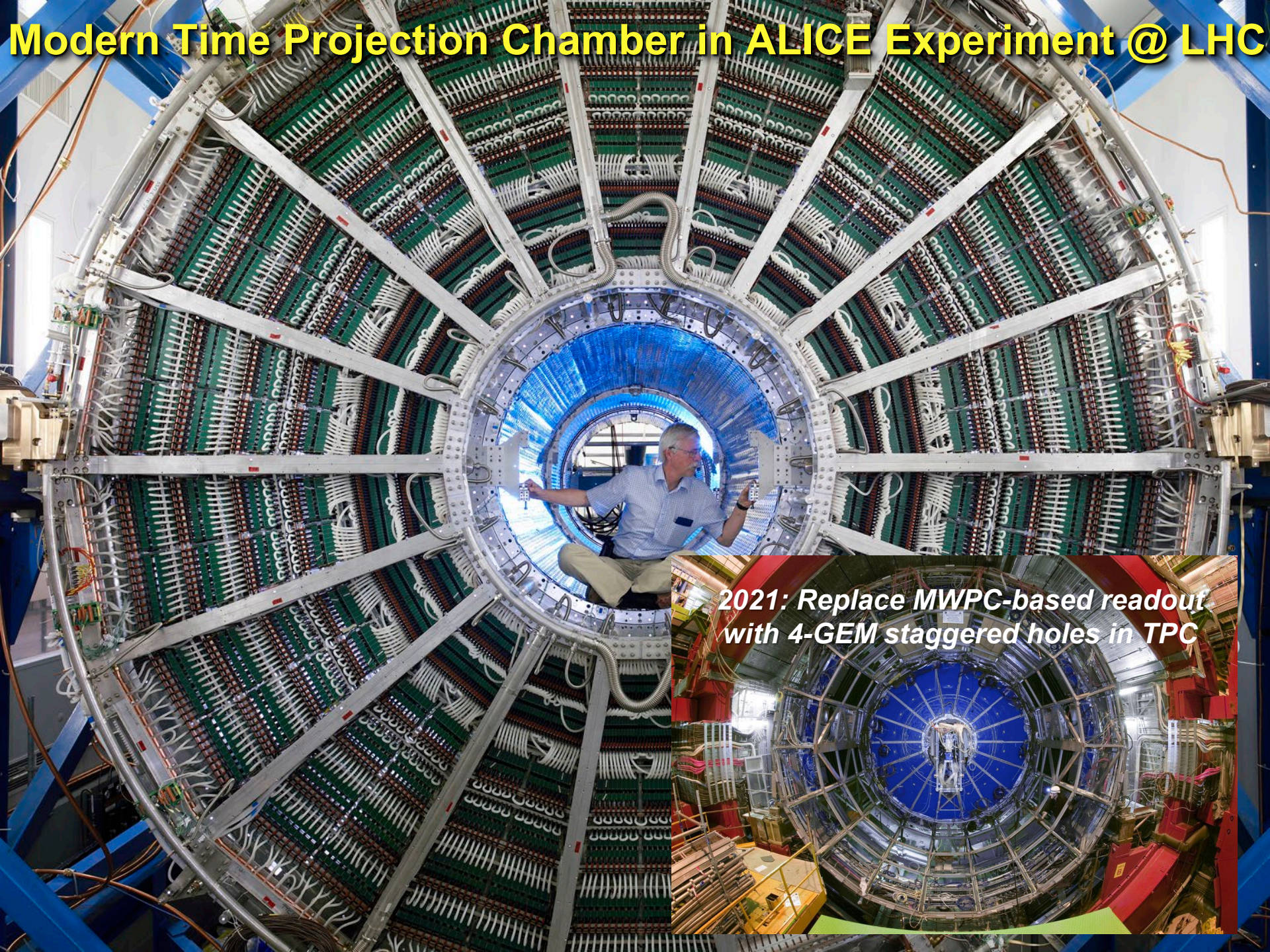
STAR (LBL)



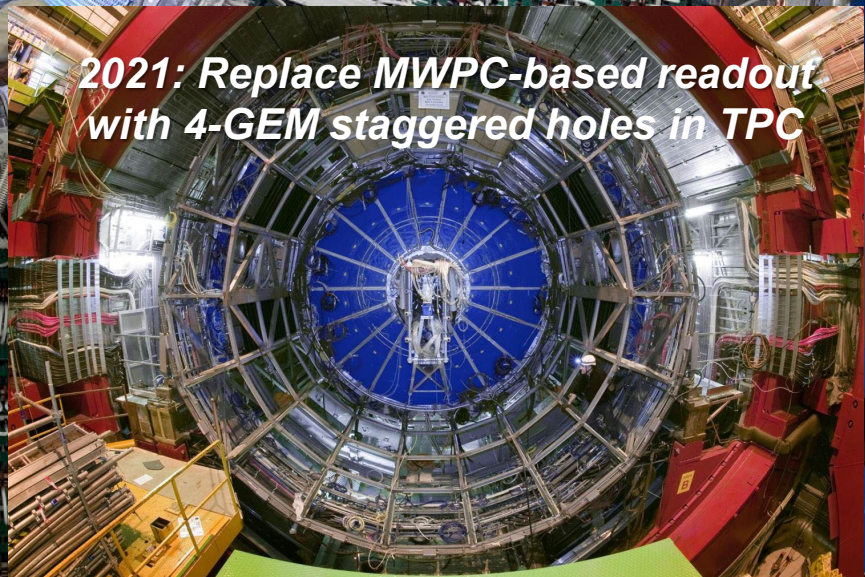
DELPHI (CERN)



Modern Time Projection Chamber in ALICE Experiment @ LHC



2021: Replace MWPC-based readout with 4-GEM staggered holes in TPC

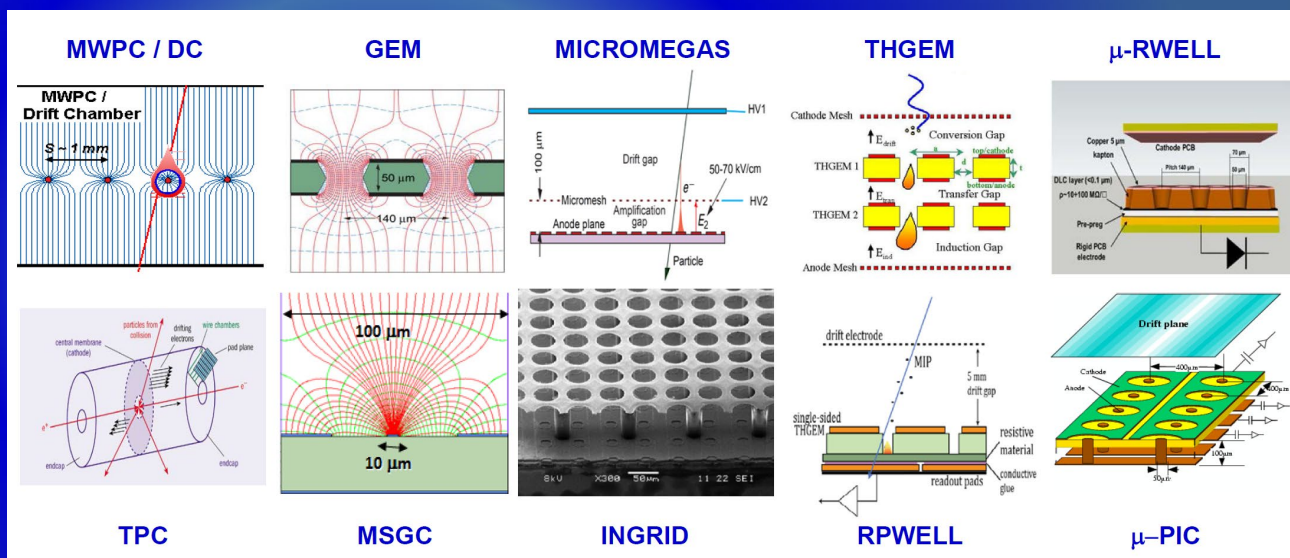
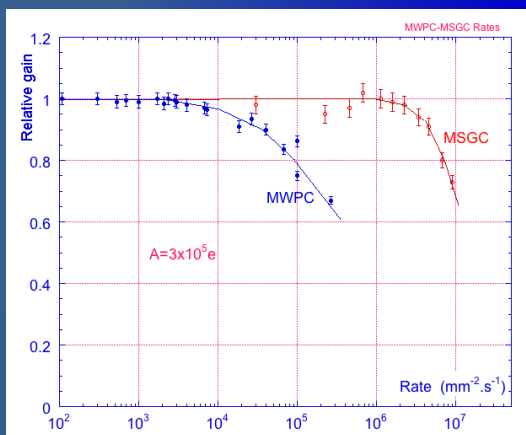


Gaseous Detectors: From Wire/Drift Chamber → Time Projection Chamber (TPC) → Micro-Pattern Gas Detectors

Primary choice for large-area coverage with low material-budget (+ dE/dx measurement)

1990's: Industrial advances in photolithography has favoured the invention of novel micro-structured gas amplification devices (MSGC, GEM, Micromegas, ...)

Rate Capability:
MWPC vs MSGC



HL-LHC Upgrades: Tracking (ALICE TPC/MPGD); Muon Systems: RPC, CSC, MDT, TGC, GEM, Micromegas;

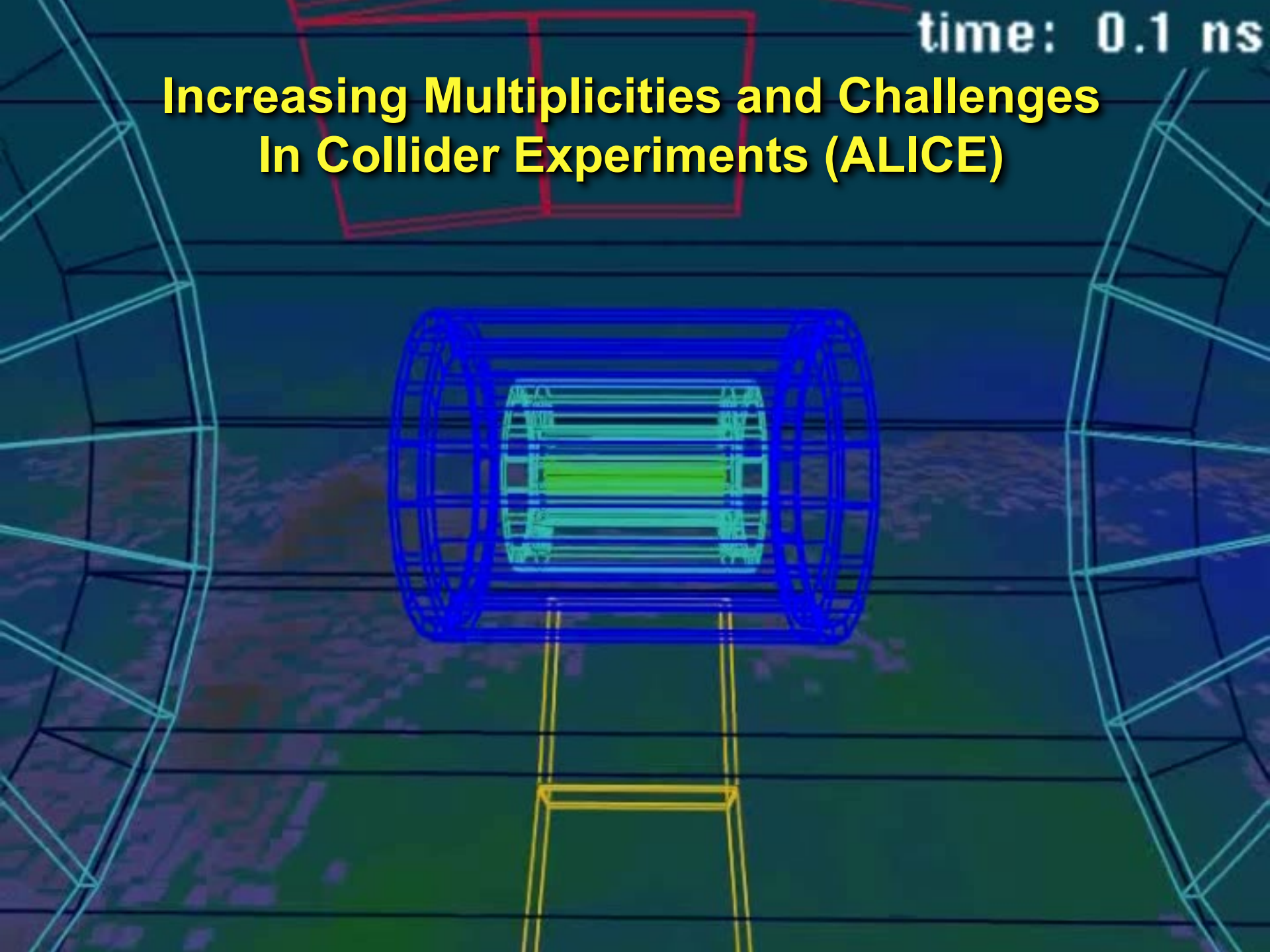
Future Hadron Colliders: FCC-hh Muon System (MPGD - OK, rates are comparable with HL-LHC)

Future Lepton Colliders: Tracking (FCC-ee / CepC - Drift Chambers; ILC / CePC - TPC with MPGD readout)
Calorimetry (ILC, CepC – RPC or MPGD), Muon Systems (OK)

Future Electron-Ion Collider: Tracking (GEM, μWELL; TPC/MPGD), RICH (THGEM), TRD (GEM)

time: 0.1 ns

Increasing Multiplicities and Challenges In Collider Experiments (ALICE)



Tracking Detectors: History and Trends

Cloud Chambers, Nuclear Emulsions + Geiger-Müller tubes

→ dominated until the early 1950s: Cloud Chambers now very popular in public exhibitions related to particle physics

Bubble Chambers had their peak time between 1960 and 1985

→ last big bubble chamber was BEBC at CERN

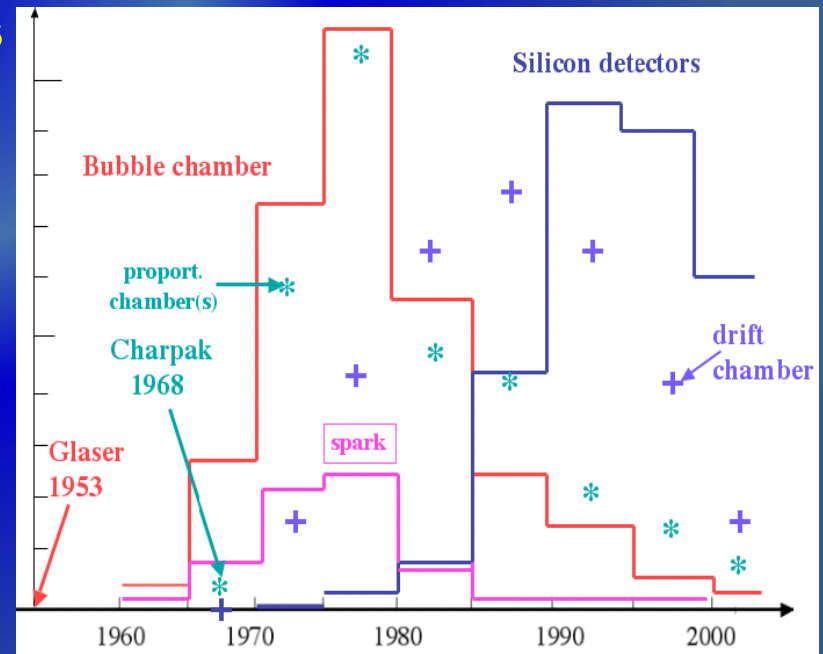
Since 1970s: Wire Chambers (MWPCs and drift chambers) started to dominate; recently being replaced by Micro-Pattern Gas Detectors (MPGD)

Since late 1980s: Solid state detectors are in common use

→ started as small sized vertex detectors (at LEP and SLC)

→ now ~200 m² Si-surface in CMS tracker

Most recent trend: silicon strips & hybrid detectors, 3D-sensors, CMOS Monolithic Active Pixel Sensors (MAPS) → See Frank Hartmann lectures

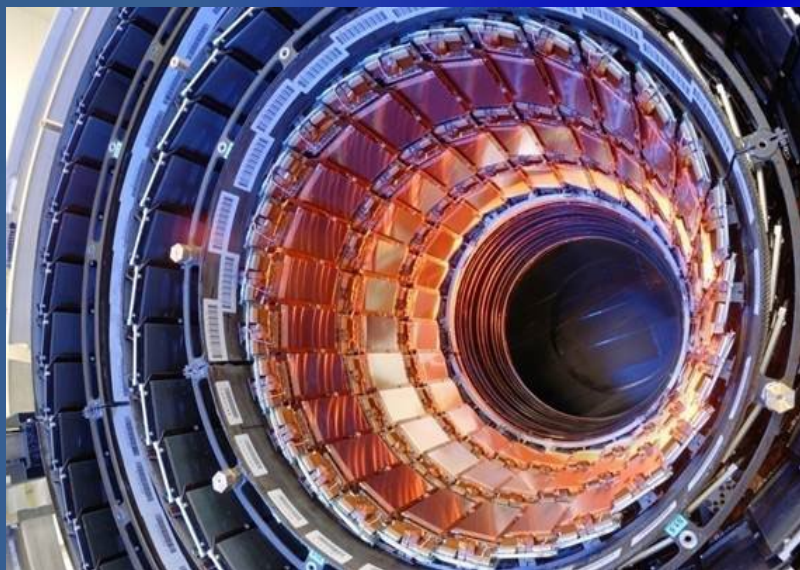


State-of-the-Art in Tracking and Vertex Detectors

Today's 3 major technologies of Tracking Detectors:

Silicon (strips, pixels, 3D, CMOS, monolithic):

→ electron – hole pairs in solid state material

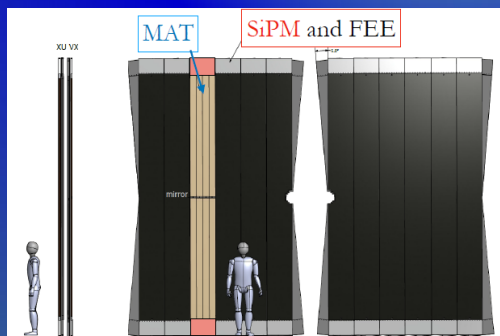
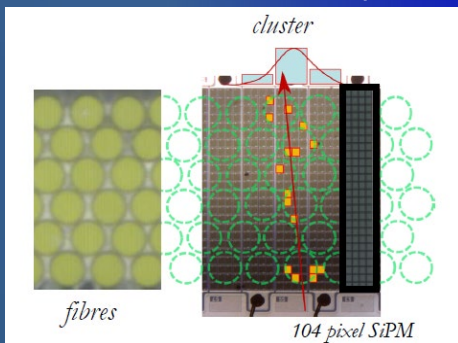


Gaseous (MWPC, TPC, RPC, MPGDs):

→ ionization in gas



Fiber Trackers: → scintillation light detected with photon detectors (sensitive to single electrons)



LHCb Tracker Upgrade (Sci-fibers with SiPM readout):

*J*inst

PUBLISHED BY IOP PUBLISHING FOR SISSA MEDIALAB

RECEIVED: June 12, 2020

ACCEPTED: June 28, 2020

PUBLISHED: October 22, 2020

INTERNATIONAL CONFERENCE ON INSTRUMENTATION FOR COLLIDING BEAM PHYSICS
NOVOSIBIRSK, RUSSIA
24–28 FEBRUARY, 2020

M. Titov, JINST15 C10023 (2020)

**Next frontiers in particle physics detectors: INSTR2020
summary and a look into the future**

M. Titov

Commissariat à l'Énergie Atomique et Énergies Alternatives (CEA) Saclay, DRF/IRFU/DPHP,
91191 Gif sur Yvette Cedex, France

E-mail: maxim.titov@cea.fr

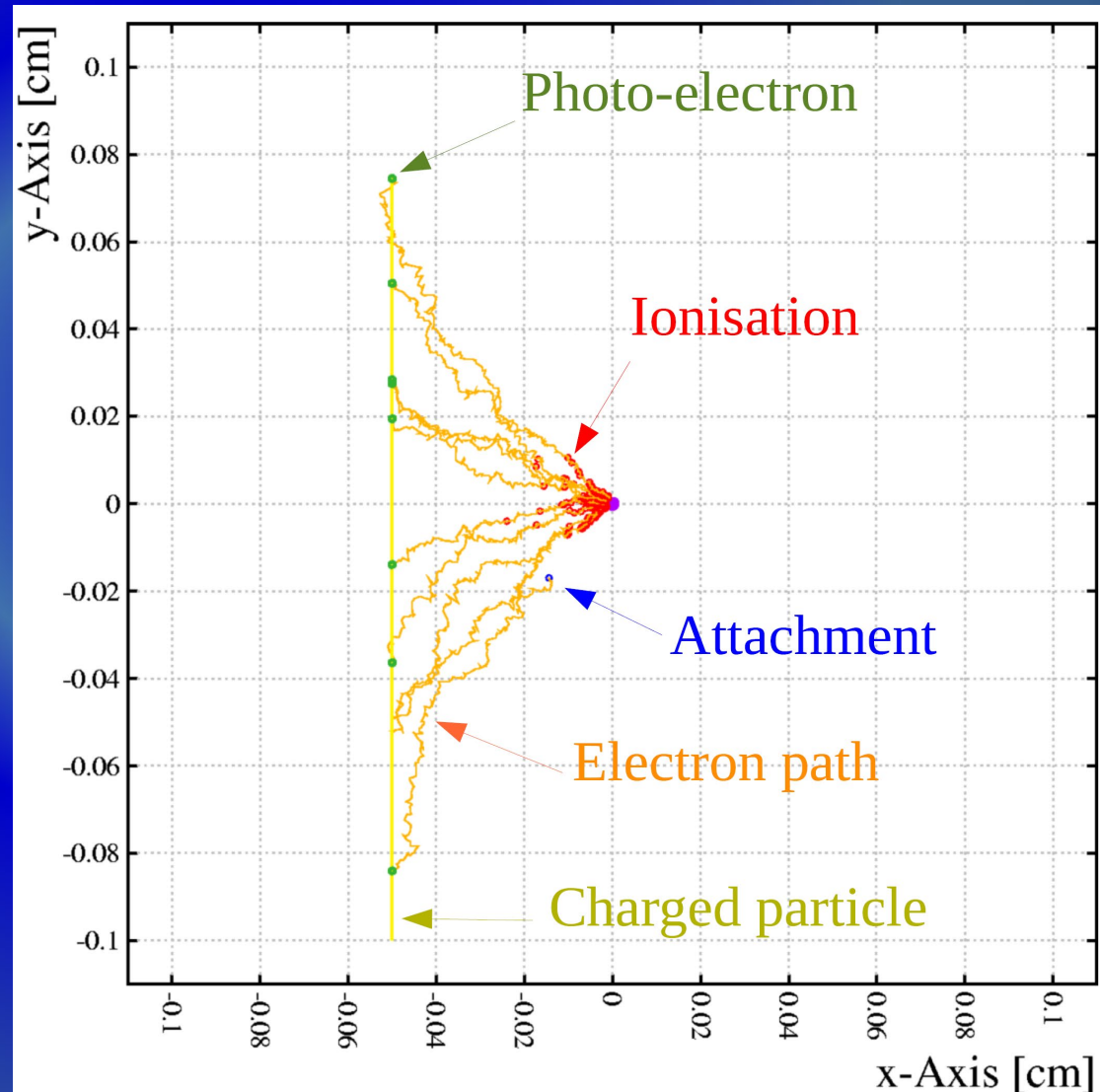
Gaseous Detectors: Working Principle

- ✓ a **charged particle** passing through the gas **ionizes** a few gas molecules;
- ✓ the **electric field** in the gas volume **transports** the ionisation electrons and provokes **multiplication**;
- ✓ the movement of electrons and ions leads **to induced currents** in electrodes;
- ✓ the **signals** are processed and recorded.

Example:

- 10 GeV muon crossing
- Gas mixture: Ar/CO₂ (80:20) %
- Electron are shown every 100 collisions, but have been tracked rigorously.
- Ions are not shown.

At the 100 μm – 1 mm scale:



Gas Detectors: Why Use Gas as a Medium for Ionization ?

- ✓ Effectively quite light in terms of gm/cm^2 , requirement for reducing multiple scattering in particle physics
- ✓ Few other technologies can easily realize detectors with as large a sensitive area as gas-filled devices
- ✓ Gas-filled detectors are relatively cheap in terms of \$ per unit area/volume
- ✓ There are optimized gas mixtures for **charged particles detection** (high energy and nuclear physics), **X-rays** (synchrotron physics, astronomy) and **neutrons** (neutron scattering, national security)
- ✓ **Electron transport characteristics** are favorable and well characterized
- ✓ **Gas gain, M** (electron multiplication factor), can be achieved, over many orders of magnitude (**large dynamic range**)
- ✓ **Ionization collection or fluorescence emission can form the signal**

Gaseous Detectors: Signal Generation

✓ Ionization statistics in gas

✓ Charge transport in gas

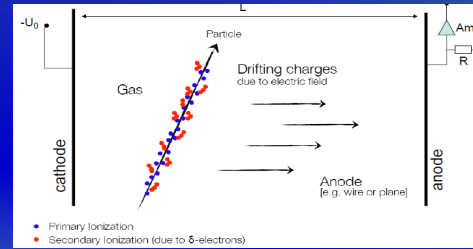
a) Diffusion

b) Electron and ion mobility

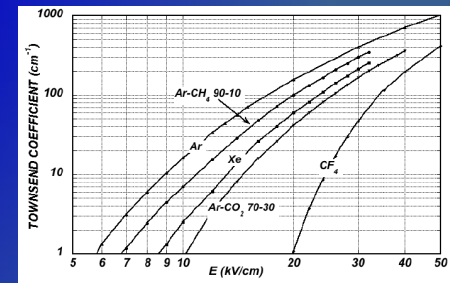
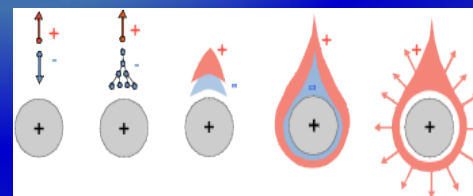
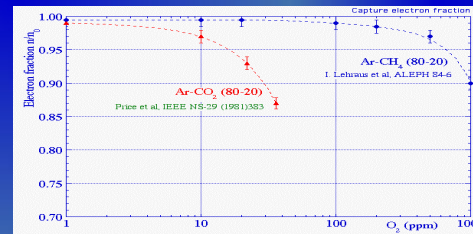
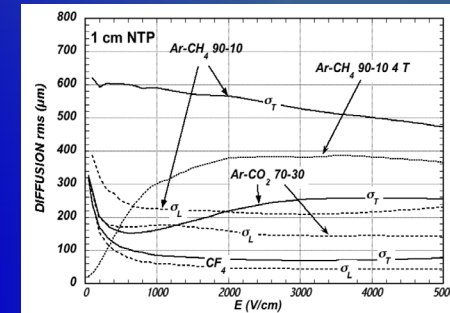
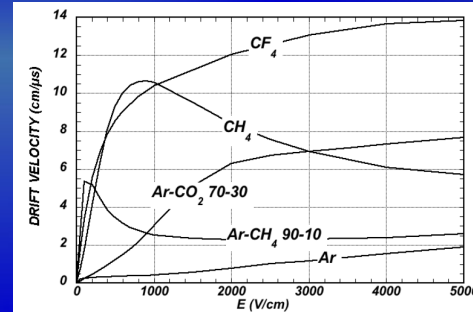
c) Drift velocity

✓ Loss of Electrons / Attachment

✓ Charge multiplication / Gas Amplification



Gas	Density, mg cm^{-3}	E_z eV	E_I eV	W_I eV	dE/dx_{min} keV cm^{-1}	N_P cm^{-1}	N_I cm^{-1}
H ₂	0.084	10.8	13.6	37	0.34	5.2	9.2
He	0.179	19.8	24.6	41.3	0.32	3.5	8
Ne	0.839	16.7	21.6	37	1.45	13	40
Ar	1.66	11.6	15.7	26	2.53	25	97
Xe	5.495	8.4	12.1	22	6.87	41	312
CH ₄	0.667	8.8	12.6	30	1.61	28	54
C ₂ H ₆	1.26	8.2	11.5	26	2.91	48	112
iC ₃ H ₁₀	2.49	6.5	10.6	26	5.67	90	220
CO ₂	1.84	7.0	13.8	34	3.35	35	100
CF ₄	3.78	10.0	16.0	35-52	6.38	52-63	120

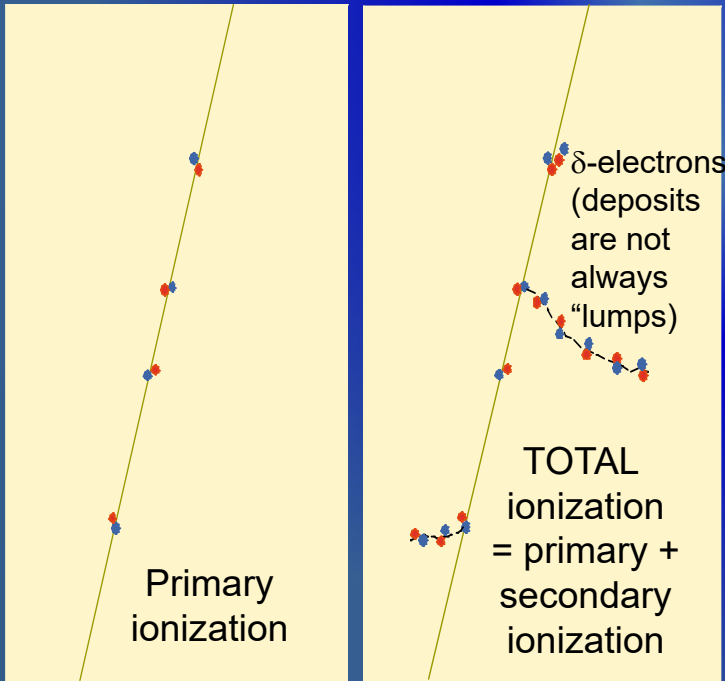


Efficient Gaseous Detector development (*energy deposit, electric fields, drift velocity & diffusion, attachment and amplification*) is today possible with *existing precise and reliable simulation tools*

Gaseous Detectors: Ionization Statistics (I)

TOTAL IONIZATION:

- **Primary electron-ion pairs**
 - Coulomb interactions of charged particles with molecules
 - typically ~ 30 primary ionization clusters /cm in gas at 1 bar
- **Secondary ionization: clusters and delta-electrons** → on average 90 electrons/cm in gas at 1 bar



The actual number of **primary electron/ion pairs** (n_p) is **Poisson distributed**:

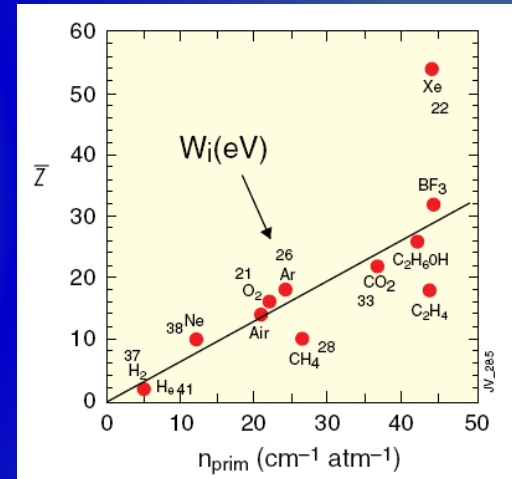
$$P(n_p, \langle n_p \rangle) = \frac{\langle n_p \rangle^{n_p} e^{-\langle n_p \rangle}}{n_p!}$$

σ_I : Ionization x-Section
 n_e : Electron density
 L : Thickness

$$\langle n_p \rangle = L/\lambda$$

$$\lambda = 1/(n_e \sigma_I)$$

Number of primary electron/ion pairs in frequently used gases:



Detection efficiency of a perfect detector is limited to:

→ for thin (L) layers ϵ can be significantly lower than 1

$$\epsilon = 1 - e^{-n_p}$$

$$\langle n_p \rangle = L/\lambda$$

GAS (STP)	thickness	ϵ (%)
Helium	1 mm	45
	2 mm	70
Argon	1 mm	91.8
	2 mm	99.3

Ionization Statistics: Table for Most Common Gases

Table 35.1: Properties of noble and molecular gases at normal temperature and pressure (NTP: 20° C, one atm). E_X , E_I : first excitation, ionization energy; W_I : average energy for creation of ion pair; $dE/dx|_{\min}$, N_P , N_T : differential energy loss, primary and total number of electron-ion pairs per cm, for unit charge minimum ionizing particles. Values often differ, depending on the source, and those in the table should be taken only as approximate.

F. Sauli, M. Titov,
Review of Particle Physics,
Particle Data Group (2022)

Gas	Density, mg cm ⁻³	E_x eV	E_I eV	W_I eV	$dE/dx _{\min}$ keV cm ⁻¹	N_P cm ⁻¹	N_T cm ⁻¹
H ₂	0.084	10.8	13.6	37	0.34	5.2	9.2
He	0.179	19.8	24.6	41.3	0.32	3.5	8
Ne	0.839	16.7	21.6	37	1.45	13	40
Ar	1.66	11.6	15.7	26	2.53	25	97
Xe	5.495	8.4	12.1	22	6.87	41	312
CH ₄	0.667	8.8	12.6	30	1.61	28	54
C ₂ H ₆	1.26	8.2	11.5	26	2.91	48	112
iC ₄ H ₁₀	2.49	6.5	10.6	26	5.67	90	220
CO ₂	1.84	7.0	13.8	34	3.35	35	100
CF ₄	3.78	10.0	16.0	35-52	6.38	52-63	120

Ar/CO₂ (70/30):

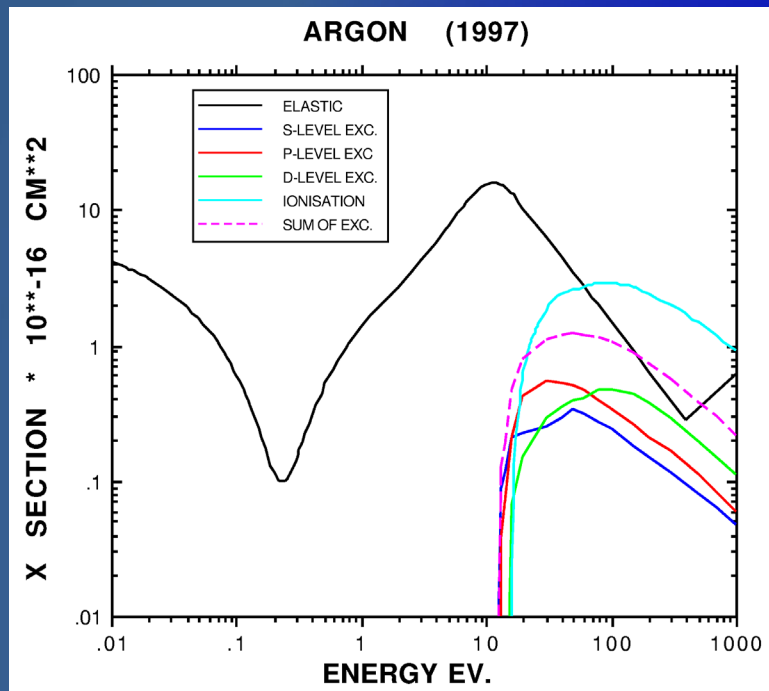
$$N_P = 25 \cdot 0.7 + 35 \cdot 0.3 = 28 \frac{\text{pairs}}{\text{cm}}; \quad N_T = \frac{2530}{26} \cdot 0.7 + \frac{3350}{35} \cdot 0.3 \approx 97 \frac{\text{pairs}}{\text{cm}}$$

$N_T \sim 100$ e-ion pairs during ionization process (typical number for 1 cm of gas) is not easy to detect \rightarrow typical noise of modern pixel ASICs is $\sim 100e^-$ (ENC)

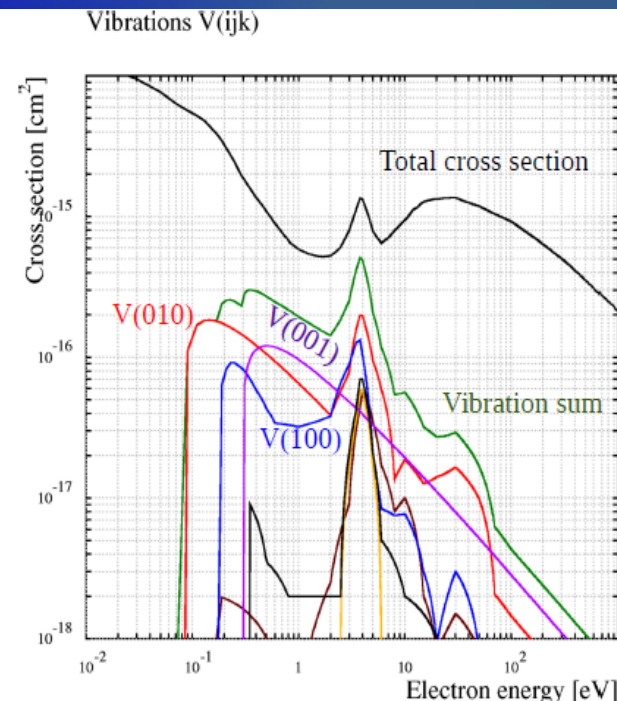
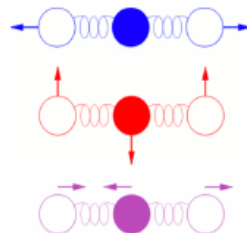
Need to increase number of e-ion pairs \rightarrow ... ☹ ... how ??? \rightarrow GAS AMPLIFICATION

Transport of Electrons in Gases: Drift Velocity

CHARGE TRANSPORT DETERMINED BY ELECTRON-MOLECULE CROSS SECTION:



- ▶ CO₂ is linear:
 - ▶ O - C - O
- ▶ Vibration modes are numbered V(ijk)
 - ▶ i: symmetric,
 - ▶ j: bending,
 - ▶ k: anti-symmetric.



Magboltz: microscopic e⁻ transport

- ▶ A large number of cross sections for 60 molecules...
 - ▶ Numerous organic gases, additives, e.g. CO₂:
 - ▶ elastic scattering,
 - ▶ 44 inelastic cross sections (5 vibrations and 30 rotations + super-elastic and 9 polyads),
 - ▶ attachment,
 - ▶ 6 excited states and
 - ▶ 3 ionisations.
 - ▶ noble gases (He, Ne, Ar, Kr, Xe):
 - ▶ elastic scattering,
 - ▶ 44 excited states and
 - ▶ 7 ionisations.

LXcat (pronounced *elecscat*) is an open-access website for collecting, displaying, and downloading ELECTron SCATtering cross sections and swarm parameters (mobility, diffusion coefficient, reaction rates, etc.) required for modeling low temperature plasmas. [...]"

Lxcat:

<http://www.lxcat.laplace.univ-tlse.fr/>

Magboltz:

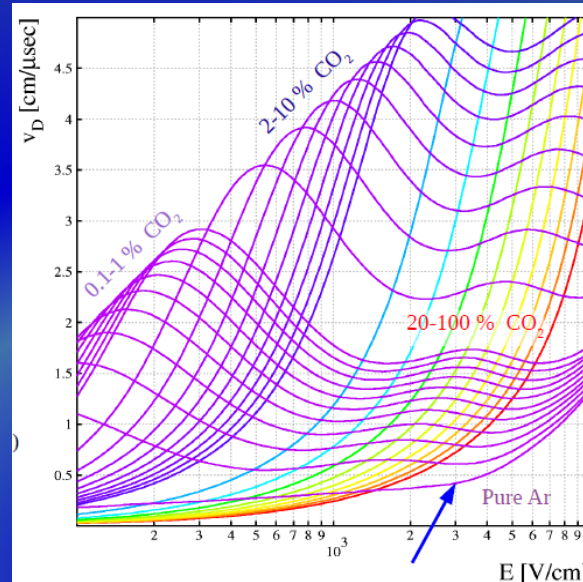
S. Biagi, Nucl. Instr. and Meth. A421 (1999) 234
<http://magboltz.web.cern.ch/magboltz/>

Transport of Electrons in Gases: Drift Velocity

Large drift velocities are achieved by adding polyatomic gases (usually hydrocarbons, CO₂, CF₄) having large inelastic component at moderate energies of a few eV → electron "cooling" into the energy range of the Ramsauer-Townsend minimum (at ~0.5 eV) of the elastic cross-section.

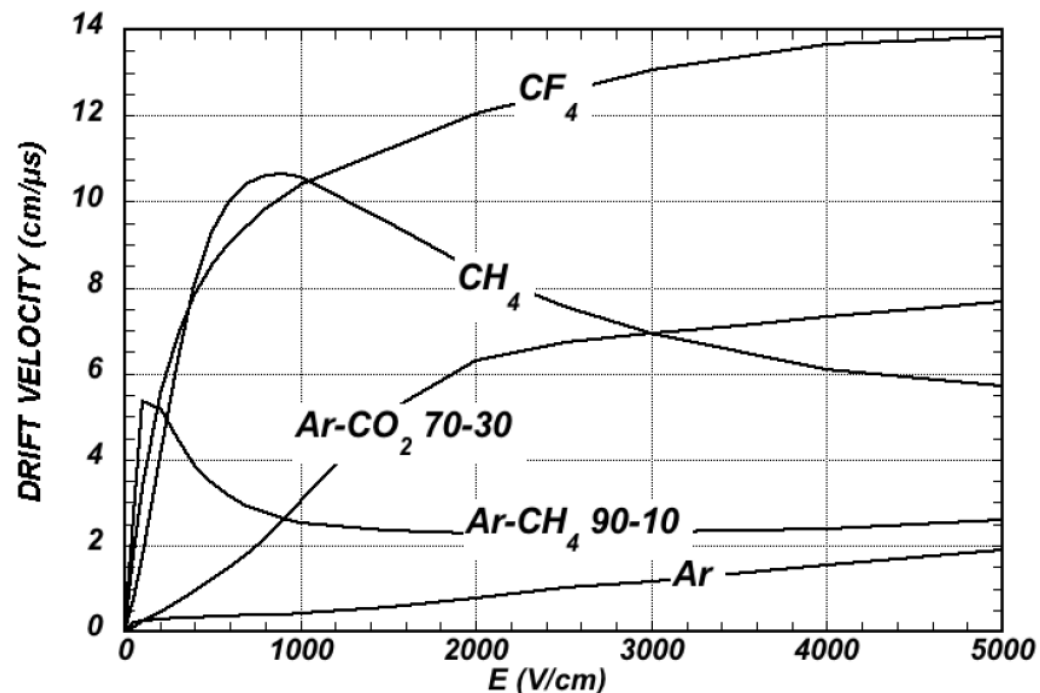
Large range of drift velocities in gases: 1 ... 10 cm/μs; typical categories:

- ✓ "slow" gases, e.g. Ar/CO₂ mixtures 1-2 cm/μs, almost linear dependence on E-field
- ✓ "fast" gases, e.g. Ar/CF₄ mixtures ~10-15 cm/μs
- ✓ "saturated" gases, e.g. Ar/CH₄; - e.g. Ar/CH₄ (90/10) – drift velocity less sensitive to E-field variations and nearly constant (useful for drift chamber operation)



Even small addition of CO₂ to Ar makes gas dramatically faster

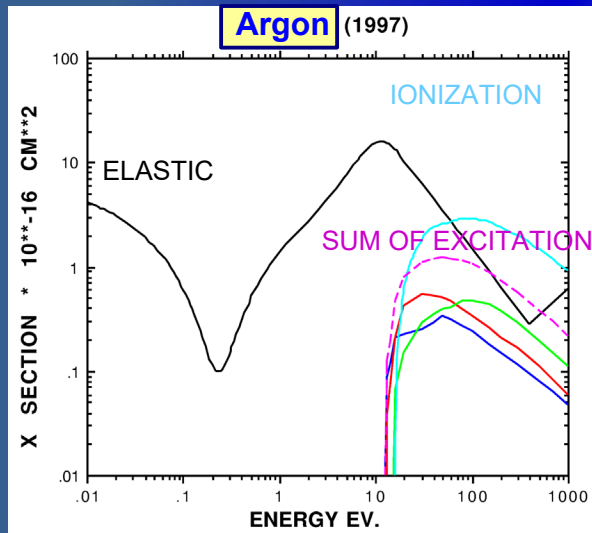
Additives like CO₂ & hydrocarbons are called "quencher" or "admixture"



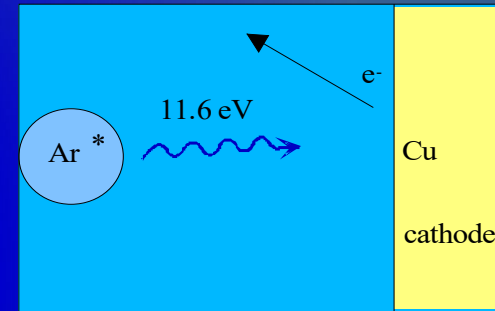
Selection of Gas Mixture: Quenching of Photons

● Slight problem in gas avalanche

- Argon atoms can be ionized but also can be brought into excited states
- Excited Argon atoms can only de-excite by emission of high-UV photons



consequence: UV photons (>11.6 eV) hit surface of metals (cathode) and free new electrons, ionization energy of Cu = 7.7 eV

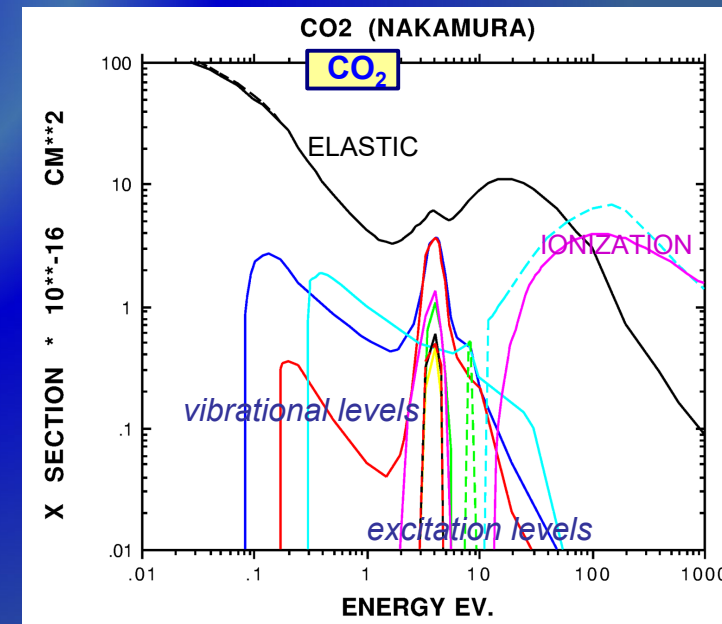


↓

VERY unstable operation

● Solution

- Add gases with many vibrational and rotational energy levels: CO₂, CH₄
- Absorption of UV photons over a wide energy range; dissipation by collisions or dissociation into smaller molecules (see aging effects)



Transport of Electrons in Gases: Diffusion

An initially point like cloud of electrons will 'diffuse' because of multiple collisions and assume a Gaussian shape. The diffusion depends on the average energy of the electrons. The variance σ^2 of the distribution grows linearly with time. In case of an applied electric field it grows linearly with the distance.

$$n(x) = \left(\frac{1}{\sqrt{4\pi Dt}} \right)^3 e^{-\frac{(x-v_D t)^2}{4Dt}}$$

$$v_D = \frac{\Delta s}{\Delta t}$$

$$\sigma_x = \sqrt{2Dt} = \sqrt{2D \frac{s}{v_D}}$$

Solution of the diffusion equation (l =drift distance)

$$D = \frac{2}{3} \frac{v}{eE} \epsilon \quad \sigma_x = \sqrt{\frac{4}{3} \frac{l}{eE} \epsilon}$$

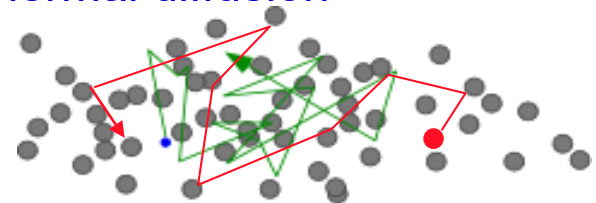
'Cold' gases are close to the thermodynamic limit i.e. gases where the average microscopic energy $\epsilon = 1/2 m u^2$ is close to the thermal energy $3/2 kT$.

CH_4 has very large fractional energy loss \rightarrow low $\epsilon \rightarrow$ low diffusion.

Argon has small fractional energy loss/collision \rightarrow large $\epsilon \rightarrow$ large diffusion.

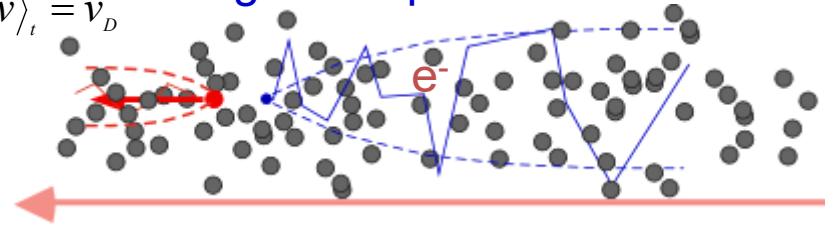
$E=0$: thermal diffusion

$$\langle v \rangle_{A^+} = 0$$

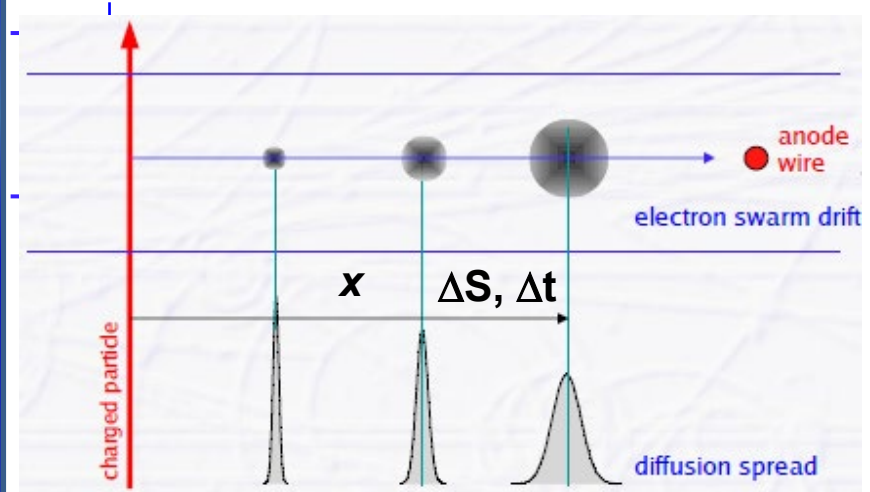


$E>0$: charge transport and diffusion

$$\langle v \rangle_t = v_D$$



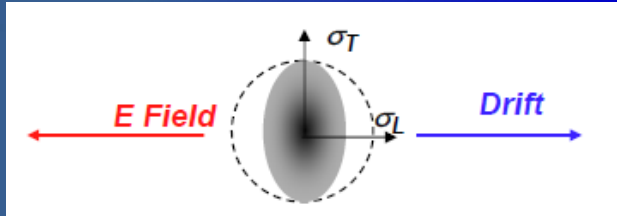
Electric Field



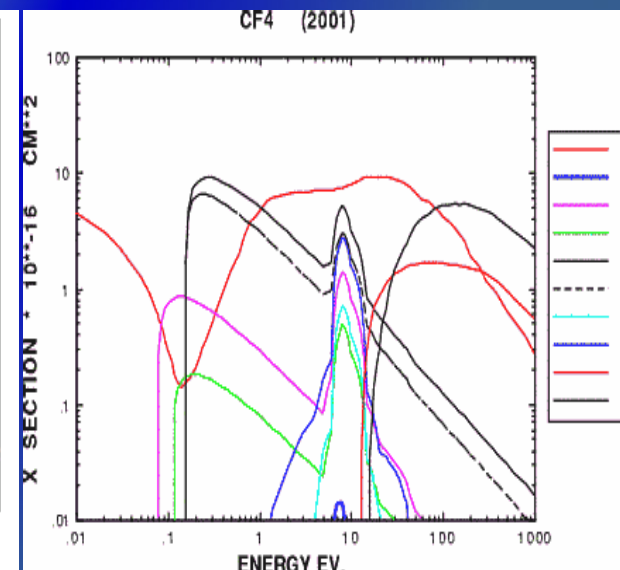
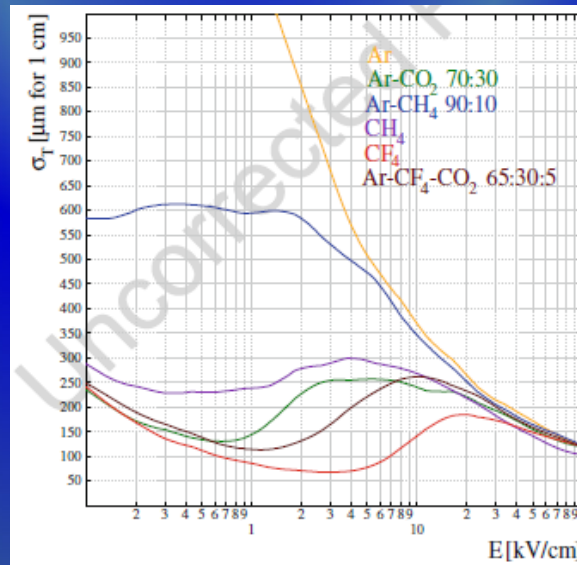
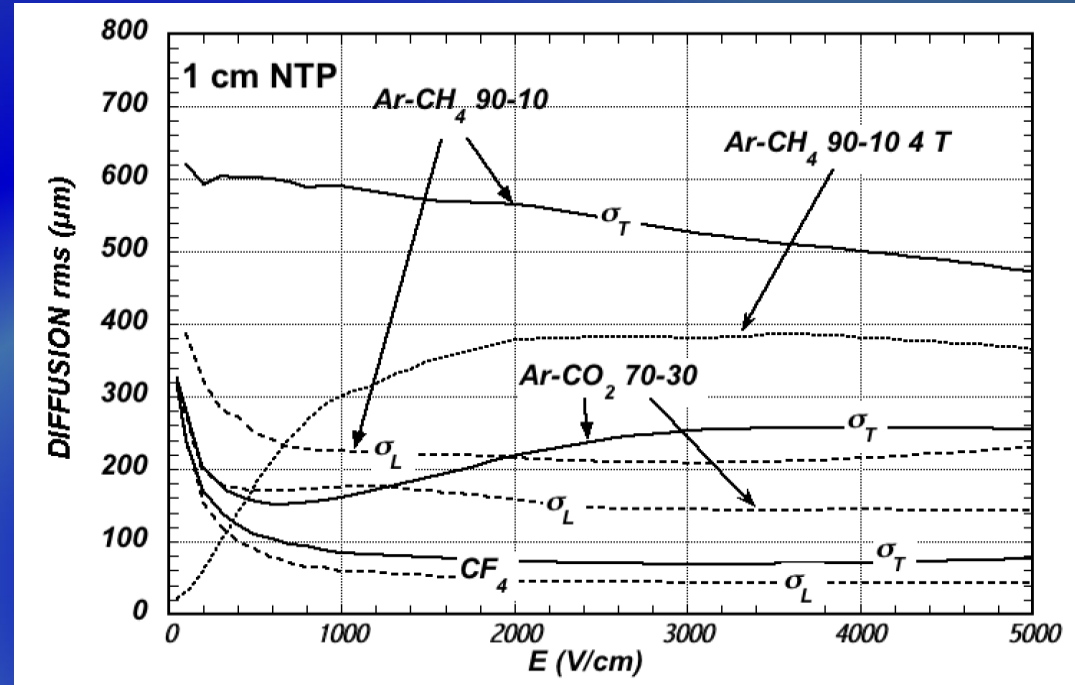
Transport of Electrons in Gases: Diffusion

Electric field alters the diffusion so that it is necessary to introduce two diffusion coefficients:

longitudinal diffusion (σ_L) and **transverse diffusion (σ_T)**



- ✓ **CO₂** is much cooler gas than CH₄ at low electric fields → allows to optimize separately diffusion properties in the drift and multiplication regions (but, CH₄ is much better quencher than CO₂)
- ✓ **CF₄** has the largest drift velocity
- ✓ & lowest electron diffusion among known gases due to the sizeable Ramsauer-Townsend dip in the elastic cross-section which coincides with a very large vibrational modes (but, **CF₄** has a small quenching cross-section of excited Ar states and emits light from the far UV to the visible light)



Gaseous Detectors: Software and Simulation Tools

Garfield, together with HEED, Degrad, Magboltz, SRIM, ANSYS, COMSOL, and neBEM software packages represent the core simulation tools for microscopic modelling of gaseous detector response.

Monte Carlo approach – a way out ?

- ▶ Analytic models are precious for the insight they afford.
- ▶ But the complexity of real gases and detectors make realistic models unwieldy:
 - ▶ inelastic collisions (vibrations, rotations, polyads);
 - ▶ excitations and Penning transfers;
 - ▶ ionisation;
 - ▶ attachment;
 - ▶ intricate, position-dependent E and B fields.
- ▶ Predictions for experiments are more practical using a Monte Carlo approach, here based on Magboltz.

- ✓ **HEED** – energy loss, a photo-absorption and ionization model
- ✓ **DEGRAD** – electron transport, cluster size distribution
- ✓ **Magboltz** – electron transport properties: drift, diffusion, multiplication, attachment
- ✓ **ANSYS, COMSOL, neBEM** – electric field maps in 2D / 3D
- ✓ **Garfield** – fields, drift properties, signals (interfaced to above)

Some recent highlights:

- **Garfield++ et al.** (new development and maintenance of codes, documentation, examples)
- **Garfield++ and delayed weighting fields in the calculation of the induced signal (resistive electrodes)**
- **Greenhouse gases**
- **Improving accuracy of the modelling and the detector physics understanding: Penning transfer, Non equilibrium effect in gaseous detectors, Ions and cluster ions**

Garfield ++ Package: Software Simulation and Tools

Garfield++ Installation Examples Documentation

Garfield++ *Heinrich Schindler, Rob Veenhof*

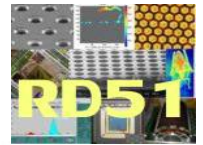
About
Garfield++ is a toolkit for the detailed simulation of particle detectors based on ionisation measurement in gases and semiconductors. The main... with the [Garfield](#) program. The main differences are the more up-to-date treatment of electron transport, the possibility to simulate silicon sensors...

More... **Support of Garfield++ package (maintenance and new developments)- a unique software package for microscopic modeling of small-scale structures -**

- Installation
- Examples
- Documentation (User Guide, Doxygen, FAQ)

Support
If you have any questions, please send a mail to garfield-support@cern.ch (or contact [Heinrich Schindler](#) or [Rob Veenhof](#) directly).
To receive (infrequent) announcements about updates of the code, please subscribe to the mailing list garfield-users@cern.ch on E-G...
Issues can be reported on [JIRA](#) or [GitLab](#).

Related calculations
Modelling of [avalanches](#) and [streamers](#) with COMSOL.



Examples

Tutorials

First steps

- Simulating a drift tube: gas tables, analytic fields, Runge-Kutta-Fehlberg integration of drift lines, signals
- Simulating a GEM: finite element model, microscopic tracking of electrons
- Simulating a silicon sensor: user-parameterized fields, strip/pixel weighting fields, Monte Carlo integration of drift lines, signals
- Simulating a Resistive Plate Chamber

Primary ionization

- Simulating charged-particle tracks using [Heed](#).
- Simulating ion tracks using tables computed with SRIM or the TRIM interface.

Transport properties

- Generating gas tables and dealing with gas files.
- Penning transfer.
- Cross-sections used by Magboltz.

Electric fields

- Importing finite-element field maps calculated using
 - Elmer and Gmsh,
 - ANSYS, for two-dimensional and three-dimensional problems,
 - COMSOL,
 - CST.
- Importing TCAD field maps.
- Computation of electric fields using the nearly exact Boundary Element Method (neBEM).

Signals

- Weighting fields and induced currents

Applications

Micropattern gas detectors

- Movies of avalanches in a single GEM
- Movies of avalanches in a triple GEM
- Timing up of a GEM
- Photon detection with a Thick GEM
- Energy pion detection with a Micromegas
- Timing with Geant4

Chambers

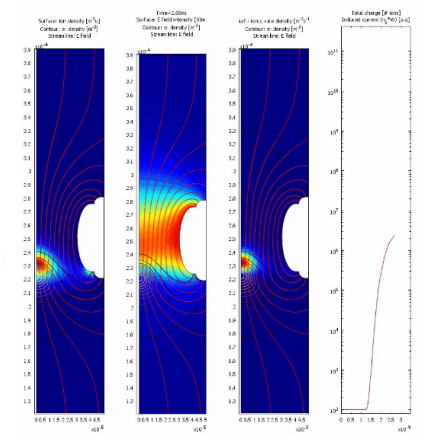
Simulation of the ALICE TPC

Diodes

Photoluminescence

Gas properties

- Paschen curves

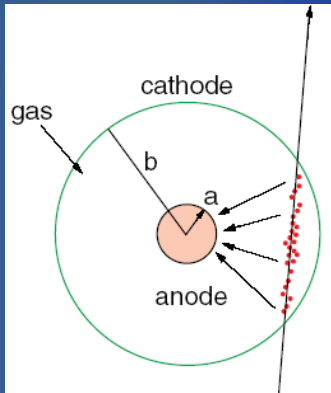


Gitlab Repository

<https://gitlab.cern.ch/garfield/garfieldpp>

Single Wire Proportional Counter: Avalanche Development

Thin anode wire (20 – 50 μm)
coaxial with cathode

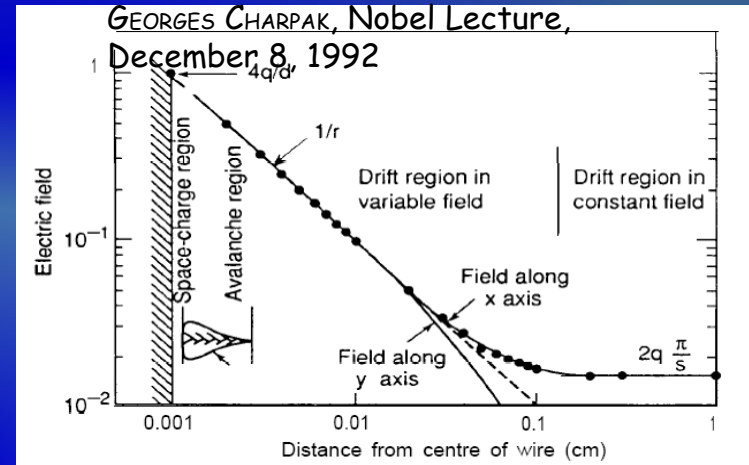


Electric field:

$$E(r) = \frac{CV_0}{2\pi\epsilon_0 r}$$

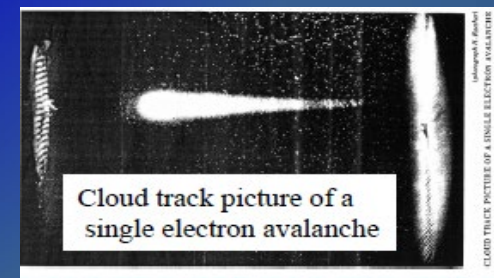
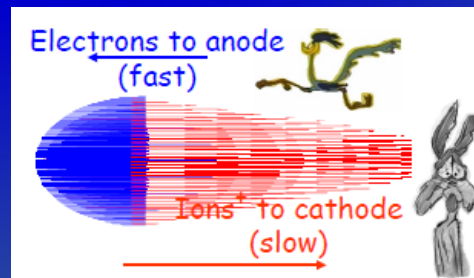
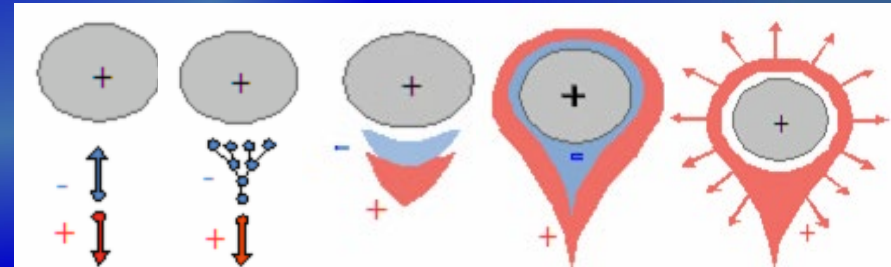
$$C = \frac{2\pi\epsilon_0}{\ln(b/a)}$$

Avalanche development in the high electric field
around a thin wire (multiplication region $\sim < 50 \mu\text{m}$):



- **Strong increase of E-field close to the wire**
→ electron gains more and more energy
- Above some threshold ($>10 \text{ kV/cm}$)
→ **electron energy high enough to ionize** other gas molecules
→ newly created electrons also start ionizing
- **Avalanche effect:** exponential increase of electrons (and ions)
- **Measurable signal on wire**
→ organic substances responsible for “quenching” (stopping) the discharge

Different stages in the gas amplification process next to the anode wire.



Ionization Cross Section: Townsend Coefficient

Multiplication of ionization is described by the first Townsend coefficient - $\alpha(E)$

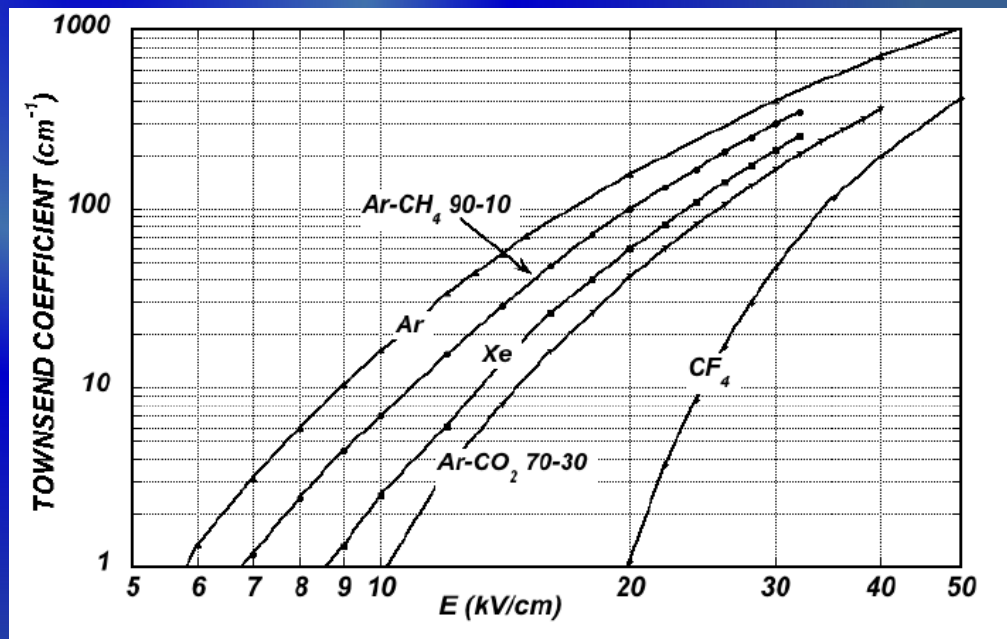
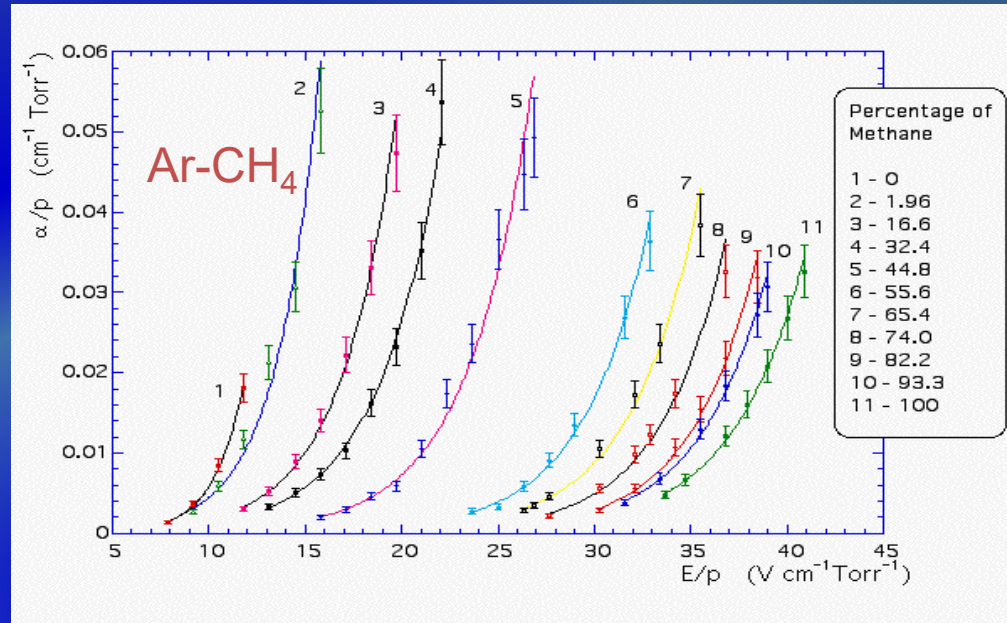
$$dn = n \alpha dx \quad \alpha = \frac{1}{\lambda} \quad \lambda - \text{mean free path}$$

$$n = n_0 e^{\alpha(E)x} \quad \text{or} \quad n = n_0 e^{\alpha(r)x}$$

- ✓ $\alpha(E)$ is determined by the excitation and ionization cross sections of the electrons in the gas.
- ✓ It depends also on various and complex energy transfer mechanisms between gas molecules.
- ✓ There is no fundamental expression for $\alpha(E)$ → it has to be measured for every mixture.

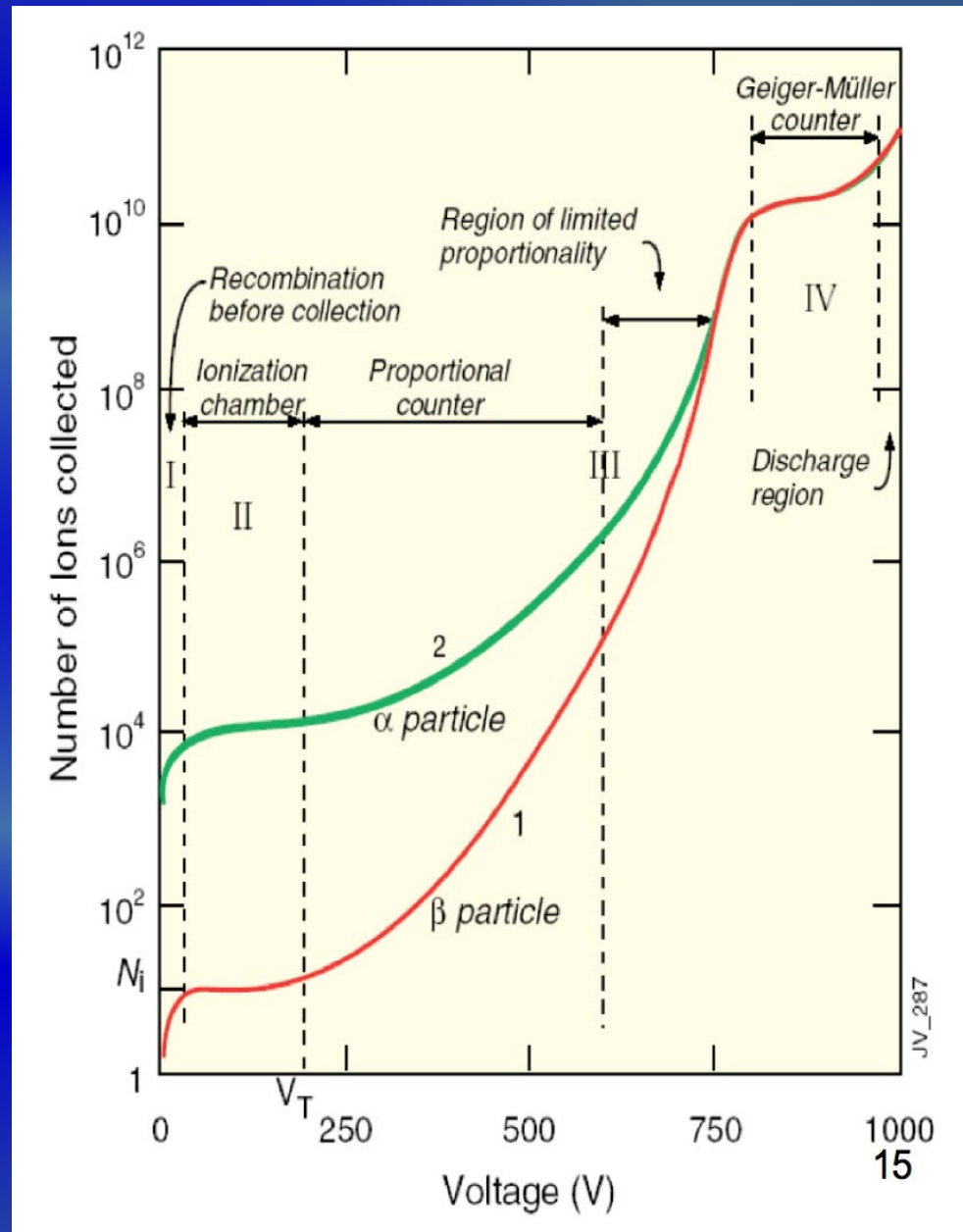
$$M = \frac{n}{n_0} = \exp \left[\int_a^{r_c} \alpha(r) dr \right]$$

Amplification factor or Gain



Operation Modes of Gas Detector: Gain-Voltage Characteristics

- ✓ **Ionization mode (II):**
→ full charge collection, but no multiplication – gain = 1
- ✓ **Proportional mode (IIIA):**
→ Multiplication of ionization starts; detected signal proportional to original ionization → possible energy measurement (dE/dx)
→ proportional region (gain $\sim 10^3 - 10^4$)
→ semi-proportional region (gain $\sim 10^4 - 10^5$), space charge effects
→ secondary avalanches need quenching
- ✓ **Limited proportional mode (saturated, streamer) (IIIB):**
→ saturation (gain $> 10^6$), independent of number of primary electrons
→ streamer (gain $> 10^7$), avalanche along the particle track
- ✓ **Geiger mode (IV):**
→ Limited Geiger region: avalanche propagated by UV photons;
→ Geiger region (gain $> 10^9$), avalanche along the entire wire



Wire Proportional Counter: Signal Development

Incremental charge induced by Q moving through dV :

$$dQ = \frac{Q}{V_0} dV = \frac{Q}{V_0} \frac{dV}{dr} dr$$

Assuming that the total charge of the avalanche Q is produced at a (small) distance l from the anode, the electron and ion contributions to the induced charge are:

$$q^- = \frac{Q}{V_0} \int_a^{a+\lambda} \frac{dV}{dr} dr = -\frac{QC}{2\pi\epsilon_0} \ln \frac{a+\lambda}{a}$$

and

$$q^+ = \frac{Q}{V_0} \int_{a+\lambda}^b \frac{dV}{dr} dr = -\frac{QC}{2\pi\epsilon_0} \ln \frac{b}{a+\lambda}$$

The total induced signal is $q = q^- + q^+ = -\frac{QC}{2\pi\epsilon_0} \ln \frac{b}{a} = -Q$ on the anode ($+Q$ on the cathode)

The ratio of electron and ion contributions:

$$\frac{q^-}{q^+} = \frac{\ln(a+\lambda) - \ln a}{\ln b - \ln(a+\lambda)}$$

For a counter with $a=10\mu\text{m}$, $b=10\text{ m}$: $q^-/q^+ \sim 1\%$ The electron-induced signal is negligible

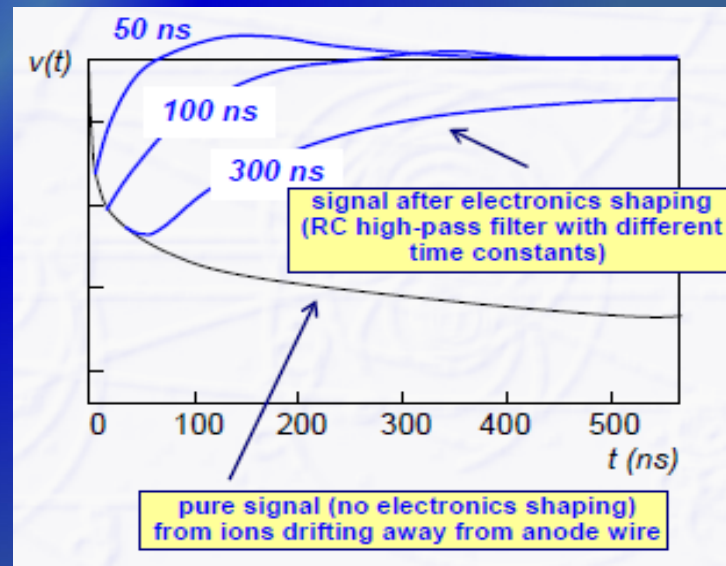
Neglecting electrons, and assuming all ions leave from the wire surface:

$$q(t) = q^+(t) = -\int_0^t dq = -\frac{QC}{2\pi\epsilon_0} \ln \frac{r(t)}{a} \quad \frac{dr}{dt} = \mu^+ E = \frac{\mu^+ CV_0}{2\pi\epsilon_0} \frac{1}{r}$$

$$q(t) = -\frac{QC}{2\pi\epsilon_0} \ln \left(1 + \frac{\mu^+ CV_0}{2\pi\epsilon_0 a^2} t \right) = -\frac{QC}{2\pi\epsilon_0} \ln \left(1 + \frac{t}{t_0} \right) \quad i(t) = -\frac{QC}{2\pi\epsilon_0} \frac{1}{t_0 + t}$$

Total ions drift time:

$$T^+ = \frac{\pi\epsilon_0 (b^2 - a^2)}{\mu^+ CV_0} \quad q(T^+) = -Q$$



Useful Write-Ups on Gaseous Detectors

Wire & Drift Chamber Basics

More on signal theorems, readout electronics etc. can be found in:

CERN 77-09
3 May 1977

ORGANISATION EUROPÉENNE POUR LA RECHERCHE NUCLÉAIRE
CERN EUROPEAN ORGANIZATION FOR NUCLEAR RESEARCH

PRINCIPLES OF OPERATION OF MULTIWIRE
PROPORTIONAL AND DRIFT CHAMBERS

F. Sauli

Lectures given in the
Academic Training Programme of CERN
1975-1976

GENEVA
1977

PARTICLE ACCELERATION
AND DETECTION

W. Blum
W. Riegler
L. Rolandi

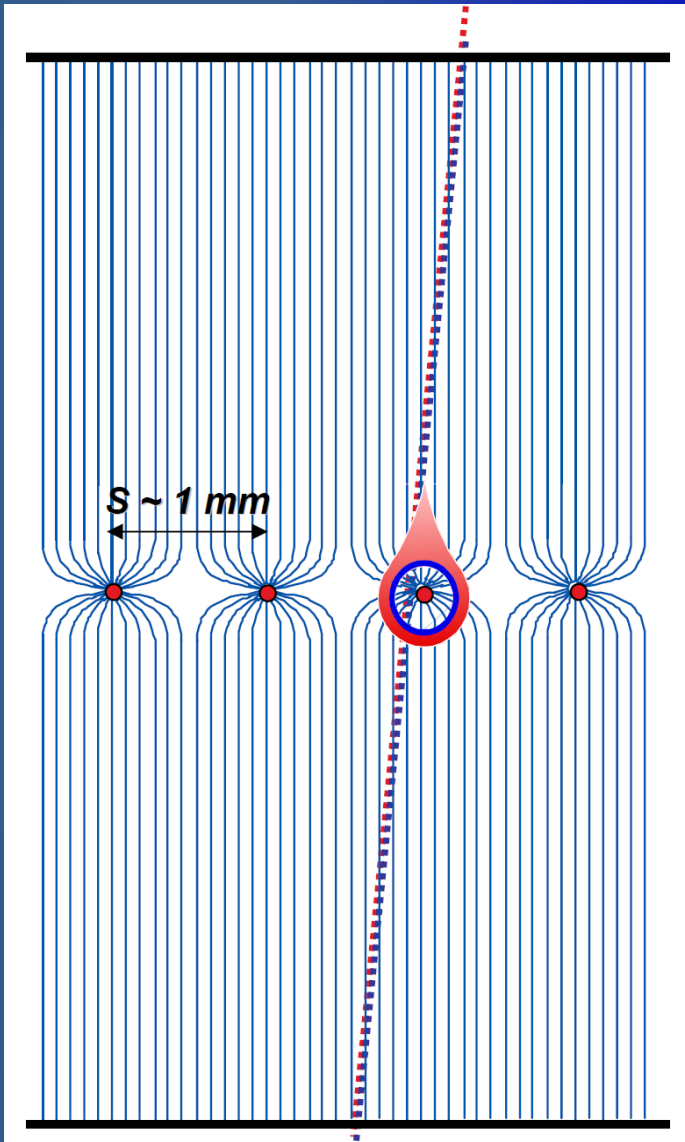
Particle Detection with Drift Chambers

Second Edition

 Springer

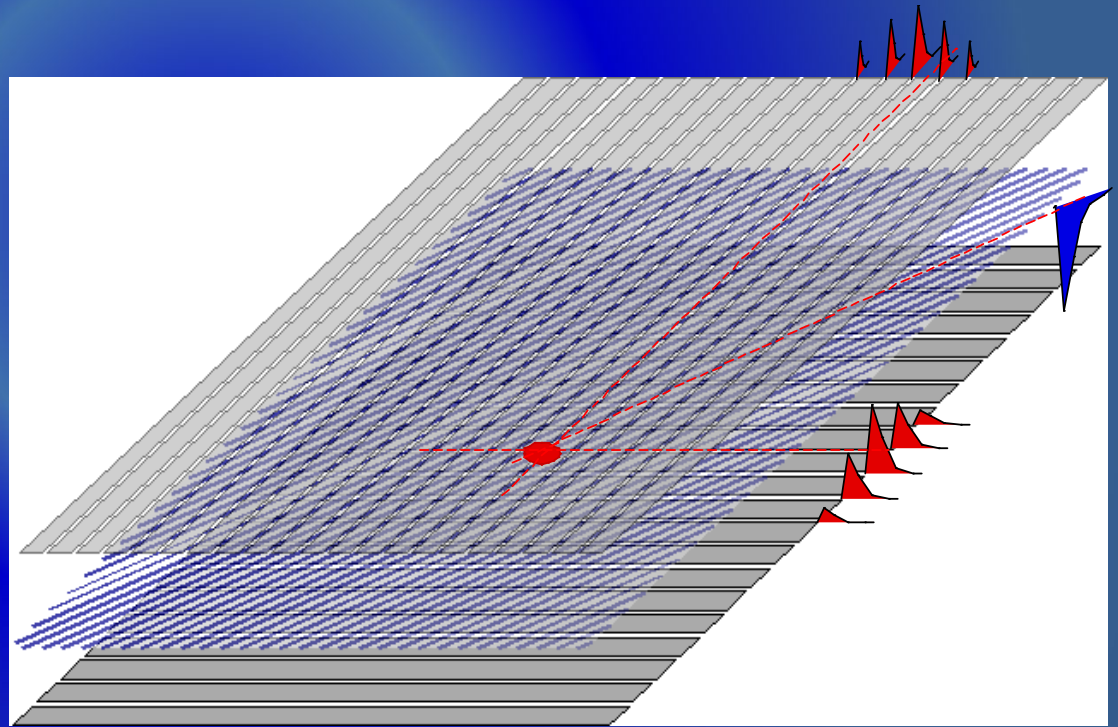
Multi-Wire Proportional Chamber (MWPC)

Simple idea to multiply SWPC cell → First electronic device allowing high statistics experiments !!



High-rate MWPC with digital readout:
Spatial resolution is limited to $s_x \sim s/\sqrt{12} \sim 300 \mu\text{m}$

TWO-DIMENSIONAL MWPC READOUT CATHODE
INDUCED CHARGE (Charpak and Sauli, 1973)



Spatial resolution determined by: Signal / Noise Ratio
Typical (i.e. 'very good') values: $S \sim 20000 e$; noise $\sim 1000e$
Space resolution $< 100 \mu\text{m}$

MWPC: First Presentation and First Large Experiment

*colloque
international
sur
l'électronique
nucléaire*

First presentation:

VERSAILLES, *international
symposium*
10-13 September 1968 *on
nuclear
electronics*

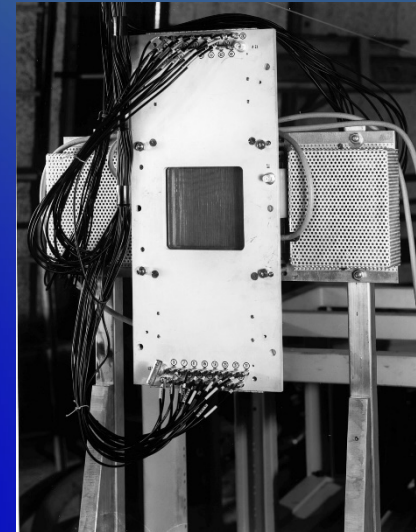
Chambres à Etincelles Spark chambers

**Rapporteur
Reporter**

M. CHARPAK
CERN - GENEVE (Suisse)

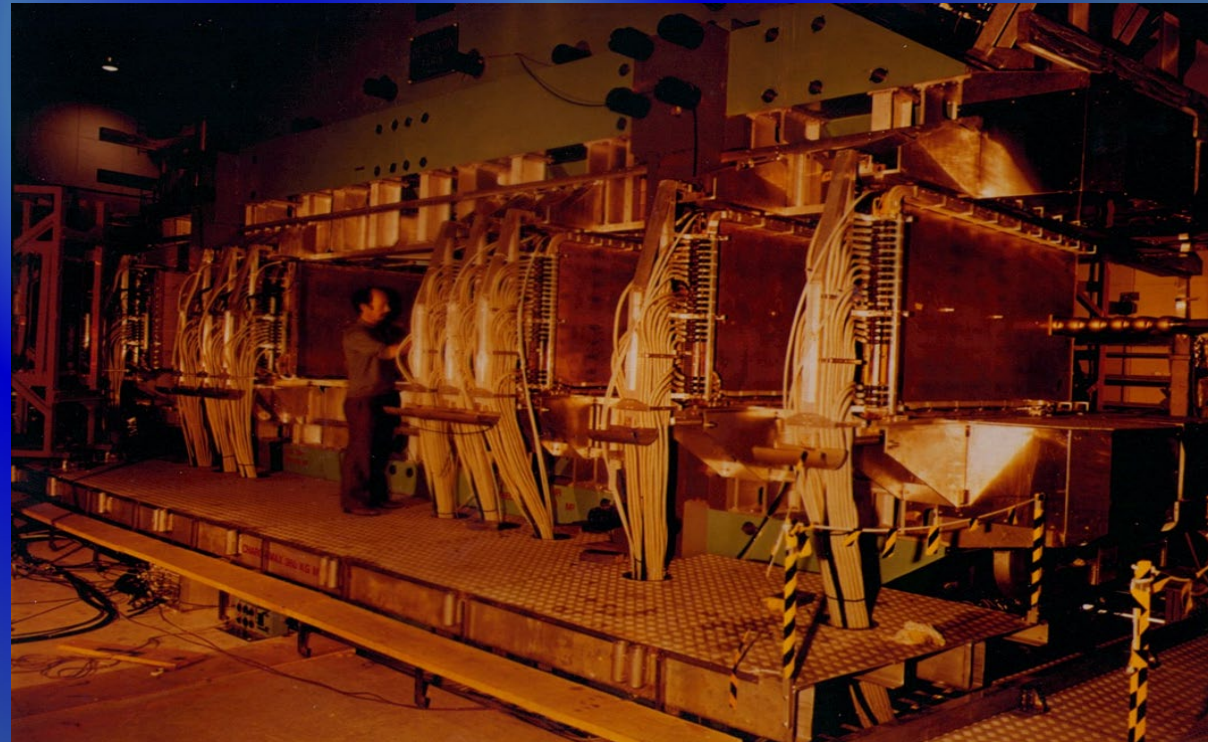
**Secrétaire
scientifique
Scientific
Secretary**

M. FEUVRIS
Faculté des Sciences - Lyon
(France)



First Large Experiment:

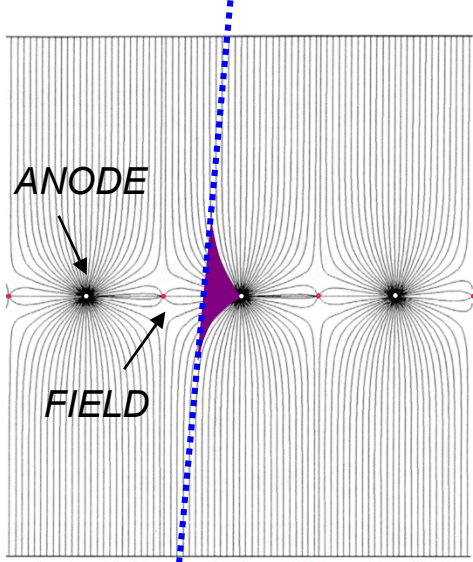
**1972-1983:
SPLIT FIELD MAGNET
DETECTOR: ~ 40 LARGE
AREA MWPCs @ CERN ISR**



Drift Chambers

FIRST DRIFT CHAMBER OPERATION (H. WALENTA ~ 1971);
HIGH ACCURACY DRIFT CHAMBERS (Charpak-Breskin-Sauli ~ 1973-75)

THE ELECTRONS DRIFT TIME PROVIDES THE DISTANCE OF THE TRACK FROM THE ANODE:



Choose drift gases with little dependence $v_D(E) \rightarrow$ linear space - time relation $r(t)$

Measure drift time t_D
[need to know t_0 ; fast scintillator, beam timing]

Determine location of original ionization:

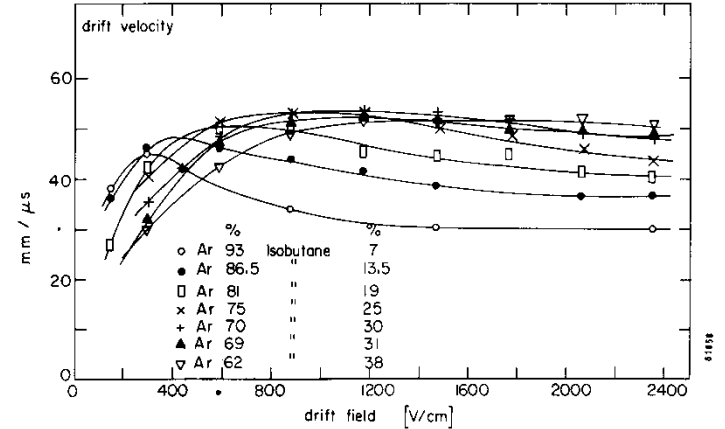
$$x = x_0 \pm v_D \cdot t_D$$

$$y = y_0 \pm v_D \cdot t_D$$

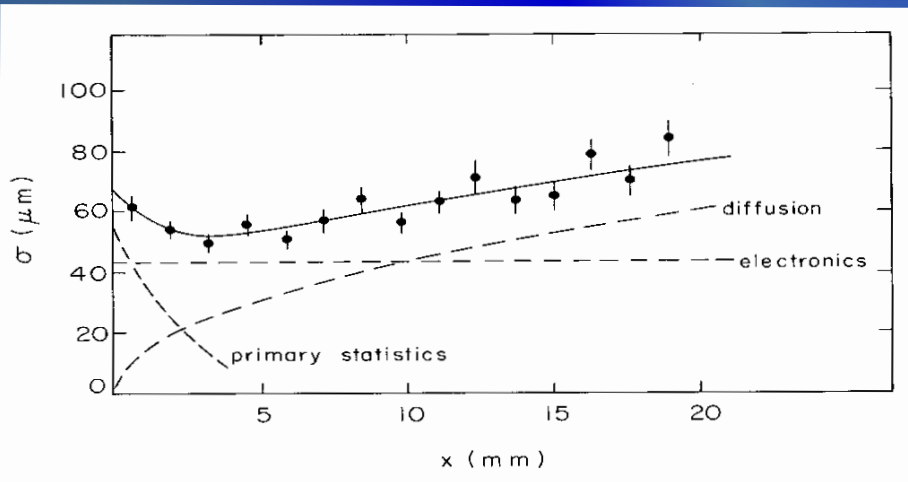
If drift velocity changes along path:

$$x = \int_0^{t_D} v_D dt$$

In any case:
Need well-defined drift field ...



The spatial resolution is not limited to the cell size :



$$\sigma_x^2 = \underbrace{\left(\frac{1}{64N^2}\right) \cdot \frac{1}{x^2}}_{1^{st} \text{ ionization statistics}} + \underbrace{\frac{2D}{v_d} \cdot x}_{\text{diffusion}} + \underbrace{\sigma_{\text{const}}^2}_{\text{electronics } \delta\text{-electrons}}$$

Typical single point resolutions of drift chambers:
50...150 μm depends on length of the drift path

- ✓ **primary ionization statistics:** how many ion pairs, ionization fluctuations dominates close to the wire
- ✓ **diffusion of electrons in gas:** dominates for large drift length
- ✓ **electronics:** noise, shaping characteristics constant contribution (drift length independent)

Wire & Drift Chambers: Wide-Spread Tool in HEP for > 40 Years



Interior of OPAL drift chamber
Length: 4 m; R = 185 cm; 159 measurements per track

[$\sigma_{r\phi} = 135 \mu\text{m}$, $\sigma_z = 60 \text{ mm}$]

Original Gaseous Detectors (mostly wires/straws and RPC) in LHC Experiments

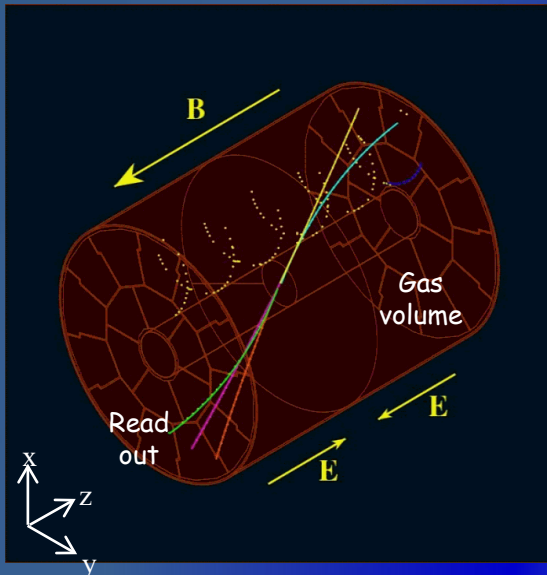
ALICE: TPC (tracker), TRD (transition rad.), TOF (MRPC), HMPID (RICH-pad chamber), Muon tracking (pad chamber), Muon trigger (RPC)

ATLAS: TRD (straw tubes), MDT (muon drift tubes), Muon trigger (RPC, thin gap chambers)

CMS: Muon detector (drift tubes, CSC), RPC (muon trigger)

LHCb: Tracker (straw tubes), Muon detector (MWPC, GEM)

ALICE Time Projection Chamber (TPC)

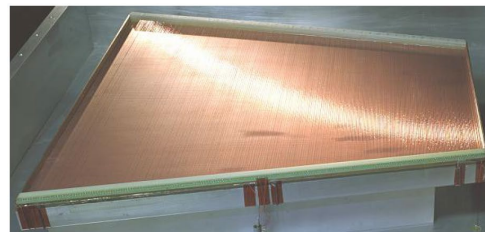
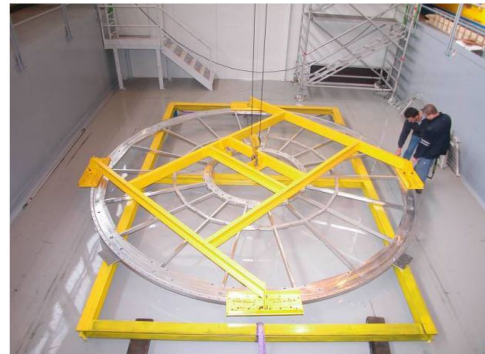


- Largest TPC:
 - Length 5m
 - Diameter 5m
 - Volume 88m³
 - Detector area 32m²
 - Channels ~570 000
- High Voltage:
 - Cathode -100kV
- Material X₀
 - Cylinder from composite materials from airplane industry (X₀ = ~3%)

- **Track point recorded in 3-D**
 (2-D channels in x-y) x (1-D channel in z = v_{drift} × t_{drift})
- **Particle identification by dE/dx**
 long ionization track, segmented in 100-200 measurements

Precision in z: 250μm

End plates 250μm

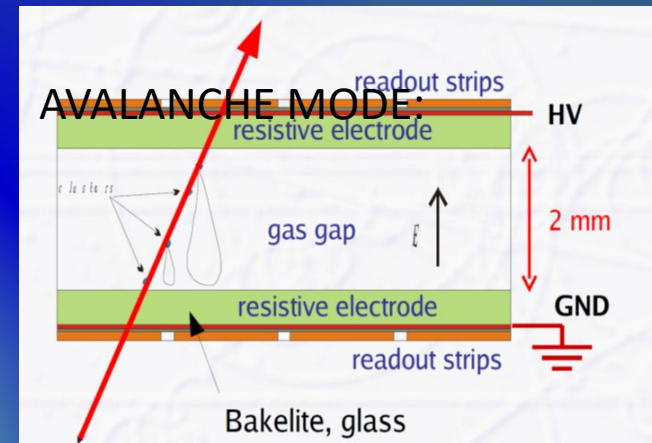


Wire chamber: 40μm

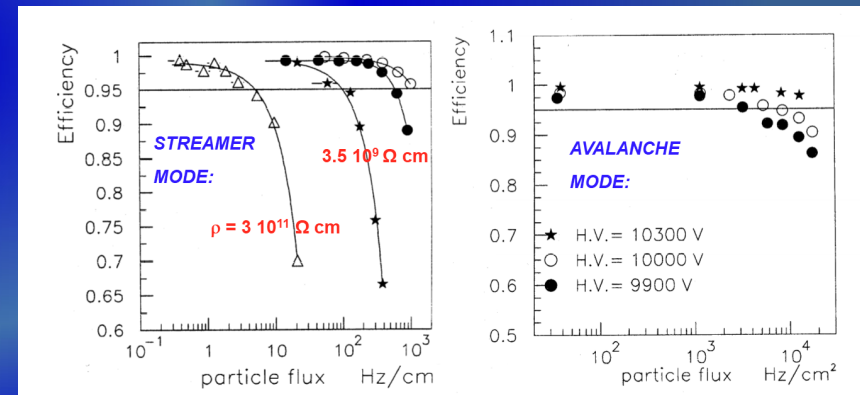
	STAR	ALICE	ILC
Inner radius (cm)	50	85	32
Outer radius (cm)	200	250	170
Length (cm)	2 * 210	2 * 250	2 * 250
Charge collection	wire	wire	MPGD
Pad size (mm)	2.8 * 11.5 6.2 * 19.5	4 * 7.5 6*10(15)	2 * 6
Total # pads	140000	560000	1200000
Magnetic field [T]	0.5	0.5	4
Gas Mixture	Ar/CH4 (90:10)	Ne/CO2 (90:10)	Ar/CH4/CO2 (93:5:2)
Drift Field [V/cm]	135	400	230
Total drift time (μs)	38	88	50
Diffusion σ _T (μm/√cm)	230	220	70
Diffusion σ _L (μm/√cm)	360	220	300
Resolution in rφ (μm)	500-2000	300-2000	70-150
Resolution in rz (μm)	1000-3000	600-2000	500-800
dE/dx resolution [%]	7	7	< 5
Tracking efficiency[%]	80	95	98

Muon Systems: Resistive Plate Chambers (RPC)

- two resistive plates ($\sim 10^9 \Omega \text{ cm}$) with a small gas gap (2 mm) and large high voltage (12 kV) on outside electrodes
- strong E-field: operation in “streamer mode”
 - gas avalanche starting in gas gap (no wires involved)
 - developing of avalanche or “streamers” (blob with lots of charge)
 - signal on external read-out strips via influence (segmented for position resolution)
 - streamer/discharge is “self-quenching”: stops when near-by resistive electrodes are locally discharged (E-field breaks down)



Experiment	Electrodes material & resistivity	Gas mixture	Operation mode; charge/track	Particle rates; Accumulated charge
L3	Oiled bakelite $2 \times 10^{11} \Omega \text{ cm}$	Ar/iC ₄ H ₁₀ /C ₂ H ₂ F ₄ (57:37:6)	Streamer	Consistent with cosmic rays
Belle	Float glass $10^{12} - 10^{13} \Omega \text{ cm}$	Ar/iC ₄ H ₁₀ /C ₂ H ₂ F ₄ (30:8:62)	Streamer	$\sim 10\text{-}20 \text{ Hz/cm}^2$;
BaBar	Oiled bakelite $10^{11} - 10^{12} \Omega \text{ cm}$	Ar/iC ₄ H ₁₀ /C ₂ H ₂ F ₄ (60.6:4.7:34.7)	Streamer 1000pC/track	$\sim 10\text{-}20 \text{ Hz/cm}^2$; <10 C/cm ² (in 2010)
ATLAS	Oiled bakelite $2 \times 10^{10} \Omega \text{ cm}$	C ₂ H ₂ F ₄ /iC ₄ H ₁₀ /SF ₆ (96.7:3:0.3)	Avalanche 30 pC/track	<0.1 kHz/cm ² ; <0.3 C/cm ²
CMS barrel	Oiled bakelite: $10^{10} \Omega \text{ cm}$	C ₂ H ₂ F ₄ /iC ₄ H ₁₀ /SF ₆ (96:3.5:0.5)	Avalanche 30 pC/track	<0.1 kHz/cm ² ; <0.3 C/cm ²
ALICE	Oiled bakelite $3 \times 10^9 \Omega \text{ cm}$	Ar/iC ₄ H ₁₀ /C ₂ H ₂ F ₄ /SF ₆ (49:40:7:1)	Streamer	<0.1 kHz/cm ² ; <0.2 C/cm ²
LHC-b	Oiled bakelite $9 \times 10^9 \Omega \text{ cm}$	C ₂ H ₂ F ₄ /iC ₄ H ₁₀ /SF ₆ (95:4:1)	Avalanche 30 pC/track	0.25-0.75 kHz/cm ² 0.35-1.1 C/cm ²



Advantages:

- simple device, good to cover large areas,
- used as trigger devices in LHC experiments, BX trigger (25 ns)

Disadvantages:

- Choice of resistive material + surface quality crucial, affects “dark” trigger rate

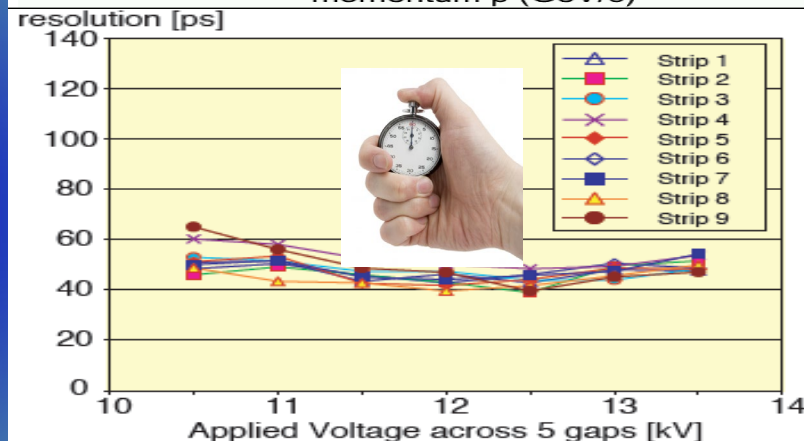
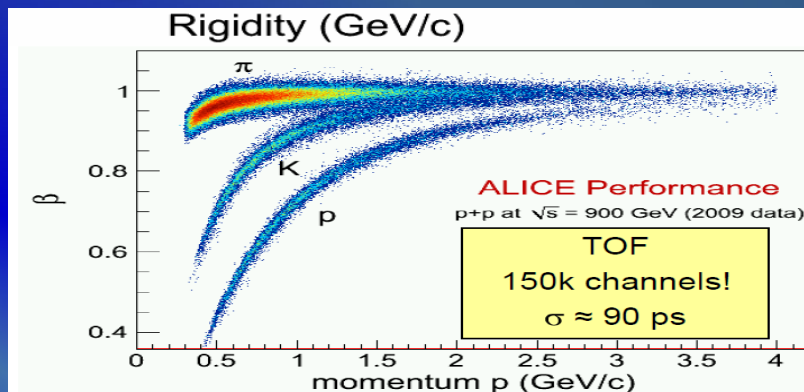
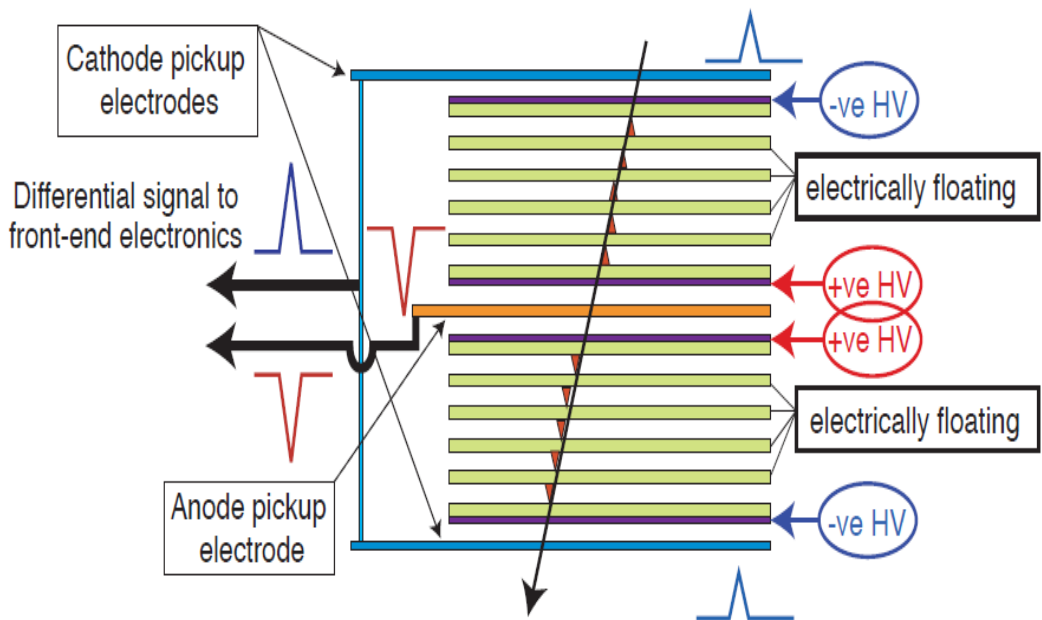
ALICE Multi-Gap RPC: Timing Resolution

- Relevant scale in HEP: $t \sim L(m)/c \sim o(ns)$

$$T_1 - T_2 = \frac{L}{c} \left(\frac{1}{\beta_1} - \frac{1}{\beta_2} \right) = \frac{L}{c} \left(\sqrt{1 + m_1^2/p^2} - \sqrt{1 + m_2^2/p^2} \right) \cong (m_1^2 - m_2^2)L / 2cp^2$$

- Traditional technique:
 - Scintillator + PMT $\sim o(100 \text{ psec})$
- Breakthrough with a spark discharge in gas
 - Pestov counter \rightarrow ALICE MRPC $\sim 60 \text{ psec}$

ALICE-TOF has 10 gaps (two stacks of 5 gas gaps); each gap is 250 micron wide



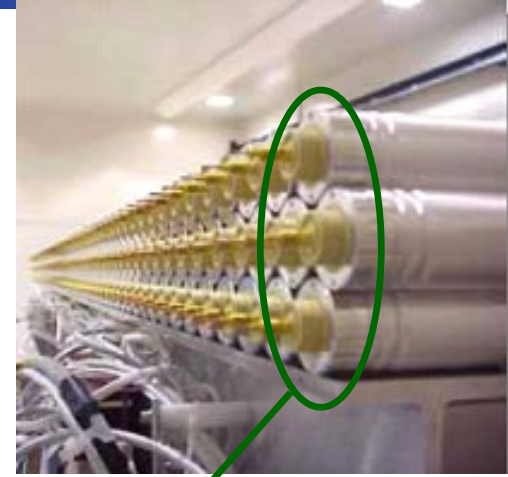
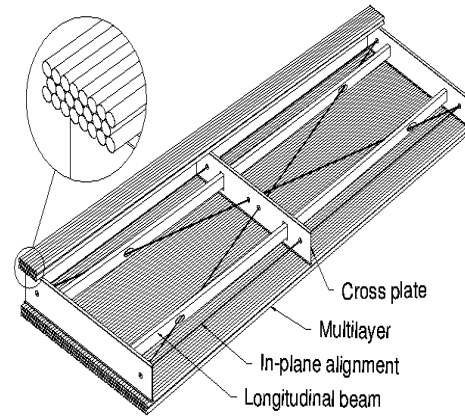
Technology	Time resolution
• Pestov Counter	30-50 ps
• RPC	$\sim 1-5 \text{ ns}$ (MIP)
• MultiGap RPC	$\sim 50 \text{ ps}$ (MIP)
• GEM	$\sim 1-2 \text{ ns}$ (UV) $\sim 5-10 \text{ ns}$ (MIP)
• Micromegas	$\sim 700 \text{ ps}$ (UV) $\sim 5-10 \text{ ns}$ (MIP)

ALICE MDT: Resolution Limits of High-Rate Wire Chambers

L3 Muon Spectrometer (LEP):
 ~ 40000 chan. ; σ (chamber) < 200 μm

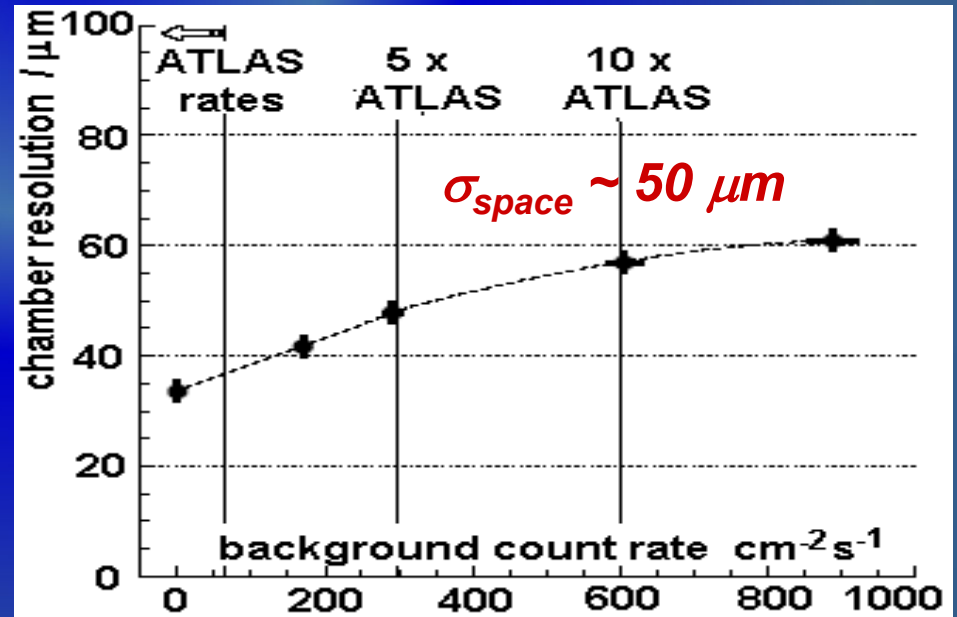
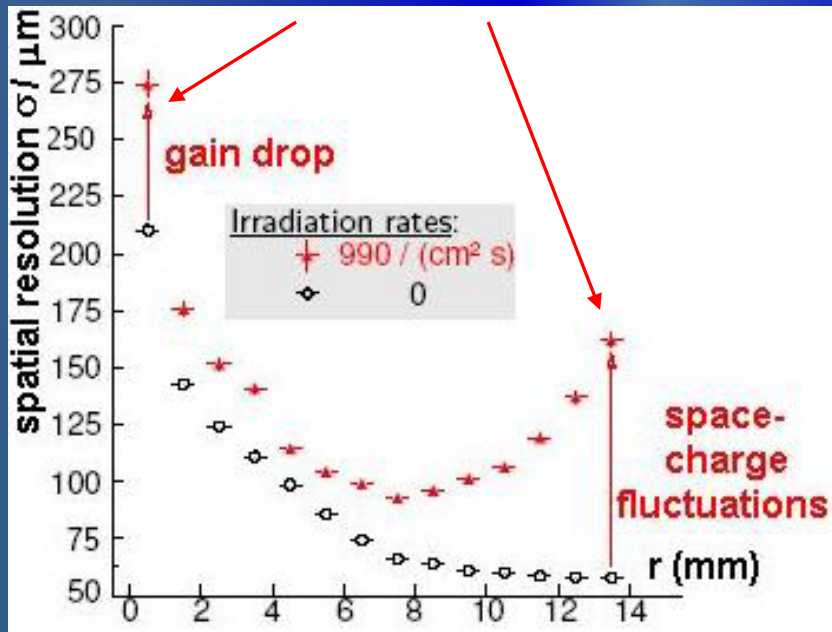
ATLAS Muon Drift Tubes (LHC):
 ~ 1200 chambers, σ (chamber) ~ 50 μm

- 370000 tubes, 740000 end-plugs
- 12000 CCD for optical alignment

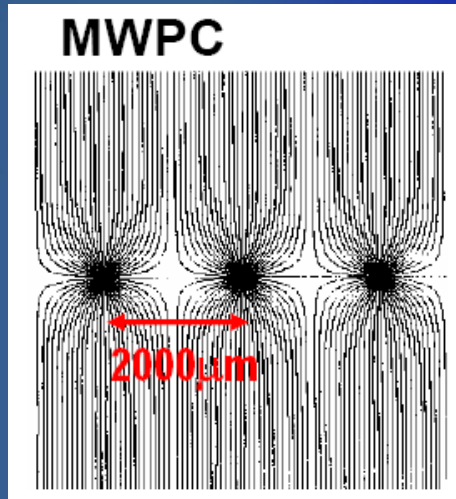


Intrinsic limitation of wire chambers:
 (resolution degradation at high rates):

1 chamber \rightarrow 2 layers of 3 drift tubes
 Spatial resolution /chamber (2 layers of 3 drift tubes)



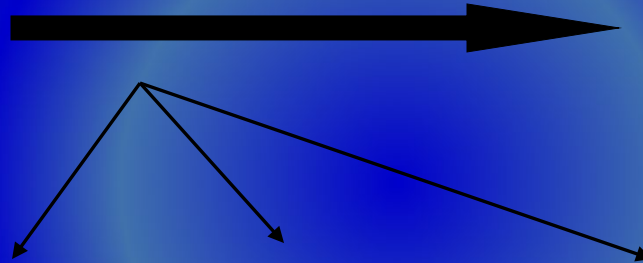
Micro-Pattern Gaseous Detectors: Bridging the Gap for Tracking between Wire Chambers and Silicon-based Devices



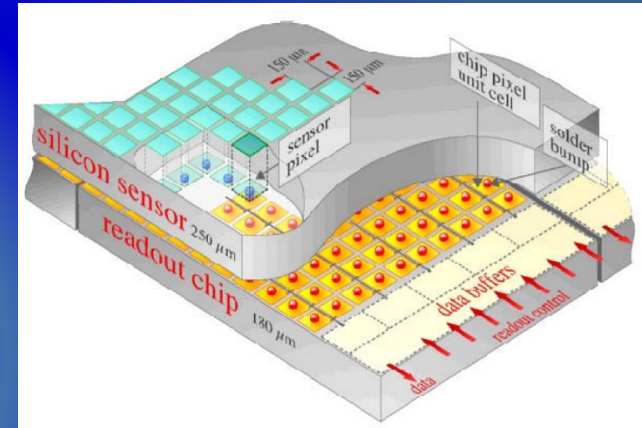
$\sigma \sim 100 \mu\text{m}$



$\sigma < 10 \mu\text{m}$



Pixel System:



Advantages of gas detectors:

- low radiation length
- large areas at low price
- flexible geometry
- spatial, energy resolution ...

Problem:

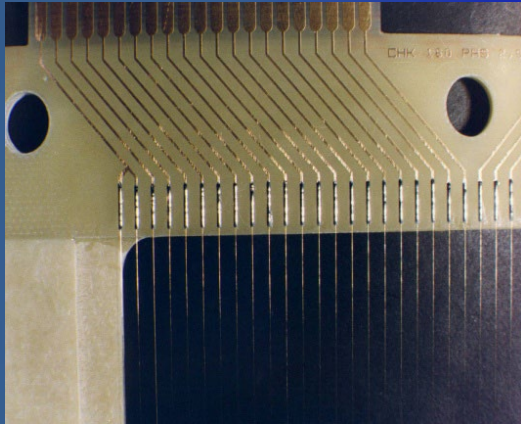
- ✓ rate capability limited by space charge defined by the time of evacuation of positive ions

Solution:

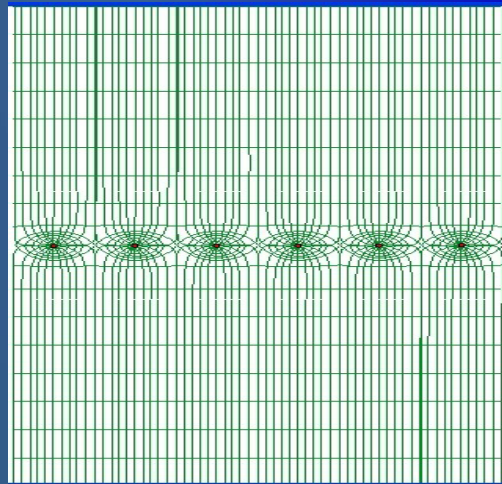
- ✓ reduction of the size of the detecting cell (limitation of the length of the ion path) using chemical etching and photo-lithographic techniques developed for microelectronics and keeping at same time similar field shape.

Micro-Strip Gas Chamber (MSGC): An Early MPGD

Multi-Wire Proportional Chamber (MWPC)

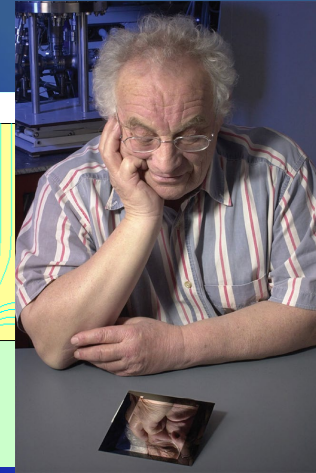
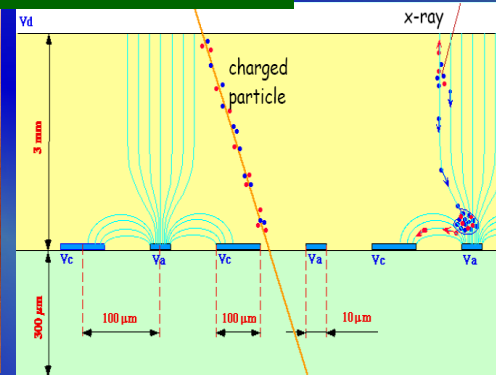
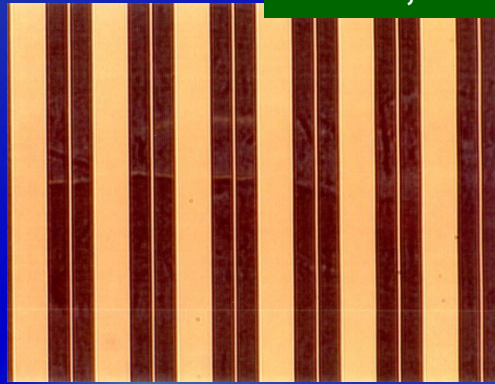


Typical distance between wires limited to ~ 1 mm due to mechanical and electrostatic forces



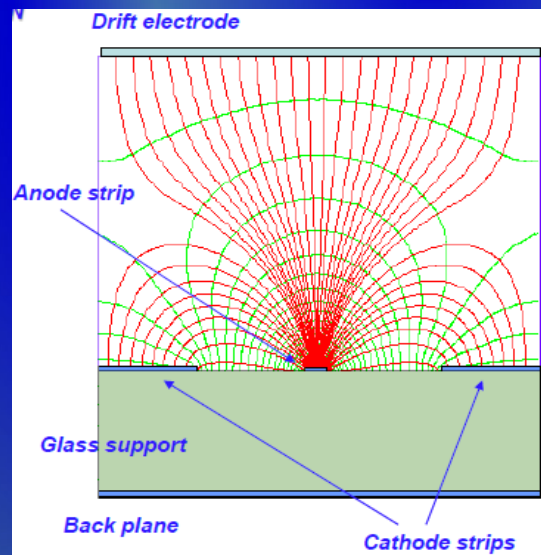
Micro-Strip Gas Chamber (MSGC)

A. Oed, NIMA263 (1988) 351

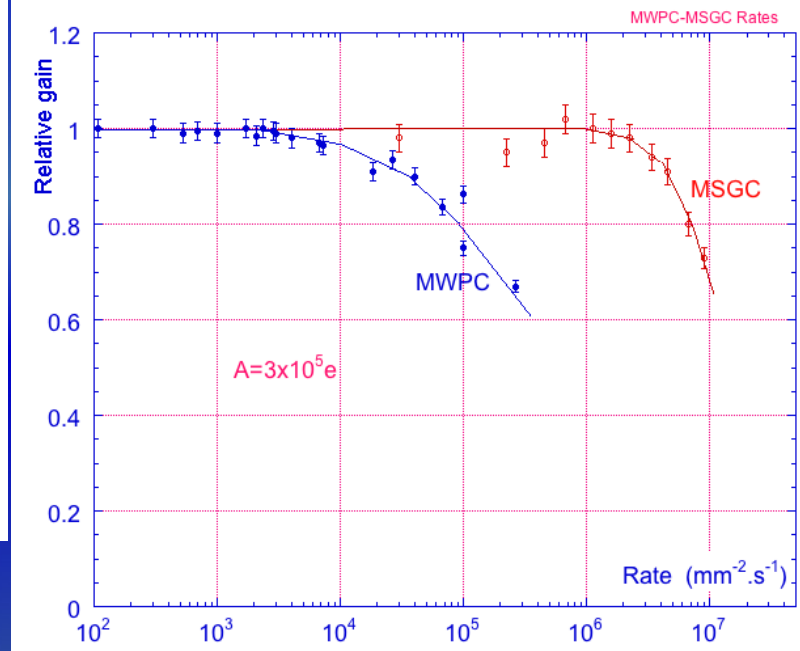


Excellent spatial resolution

MSGC significantly improves rate capability due to fast removal of positive ions



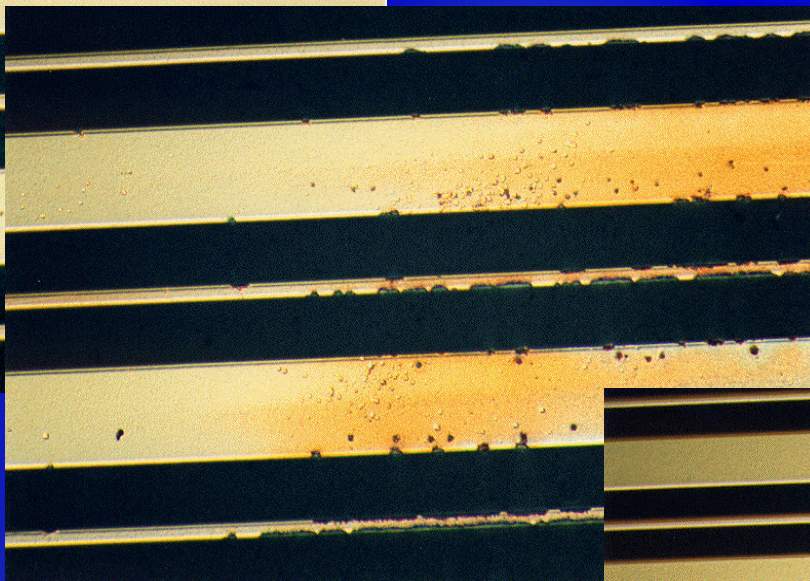
Typical distance between electrodes ~ 100 μm



MSGC Discharge Problems

Excellent spatial resolution, but poor resistance to discharges

*Discharge is very fast (~ns)
Difficult to predict or prevent*



MICRODISCHARGES

*Owing to very small distance between anode and cathode the transition from proportional mode to streamer can be followed by spark, discharge, if the avalanche size exceeds RAETHER'S LIMIT
 $Q \sim 10^7 - 10^8$ electrons*



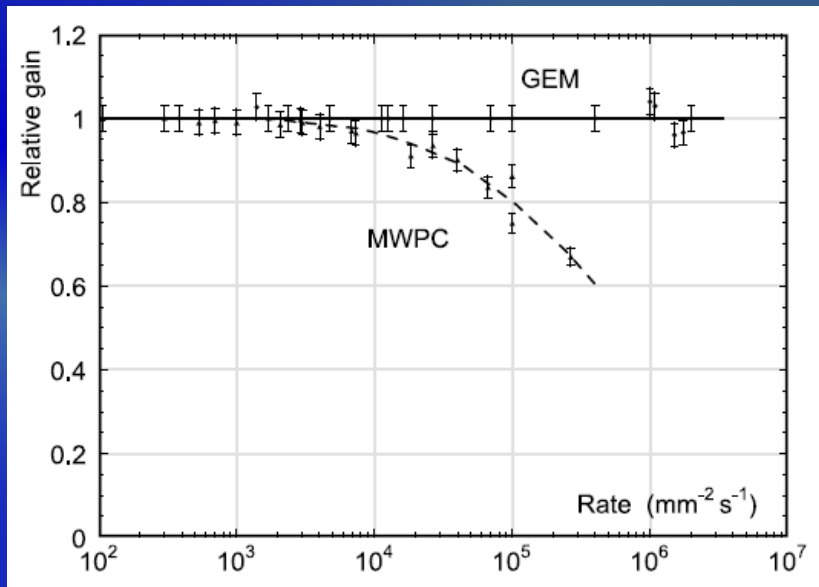
FULL BREAKDOWN

Micro-Pattern Gaseous Detector Technologies (MPGD)

Rate Capability: MWPC vs GEM:

- ✓ Micromegas
- ✓ Gas Electron Multiplier (GEM)
- ✓ Thick-GEM (LEM), Hole-Type & RETGEM
- ✓ MPDG with CMOS pixel ASICs ("GridPix")

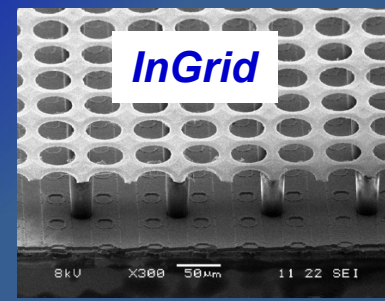
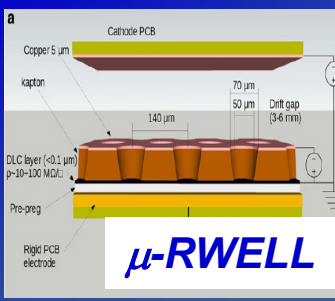
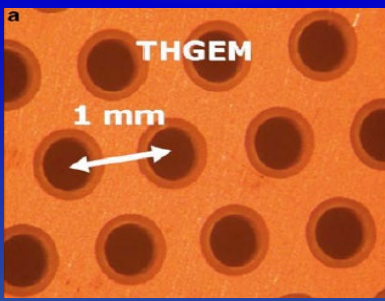
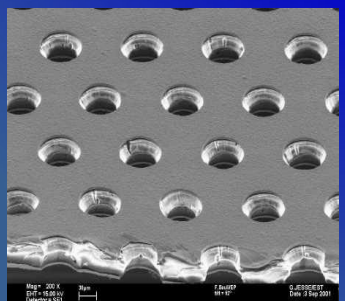
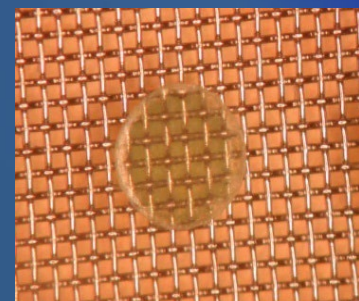
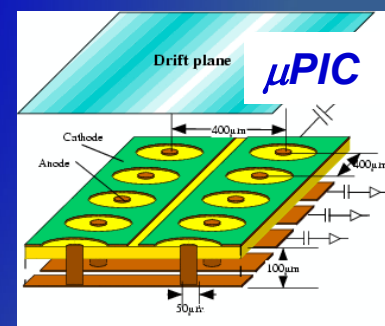
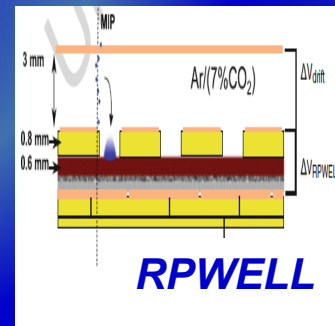
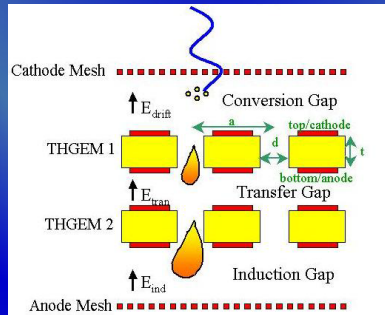
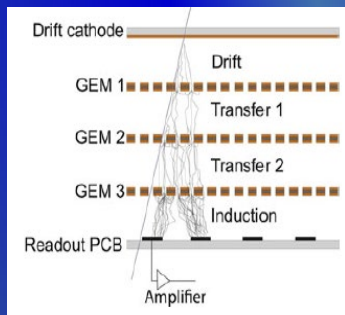
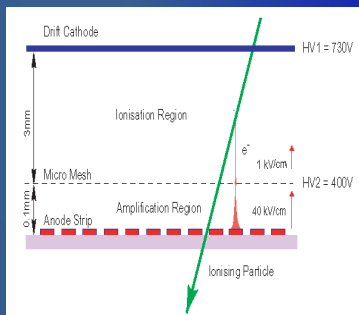
- ✓ Micro-Pixel Chamber (μ -PIC)
- ✓ μ -Resistive WELL (μ -RWELL)
- ✓ Resistive-Plate WELL (RPWELL)



Micromegas

GEM

THGEM

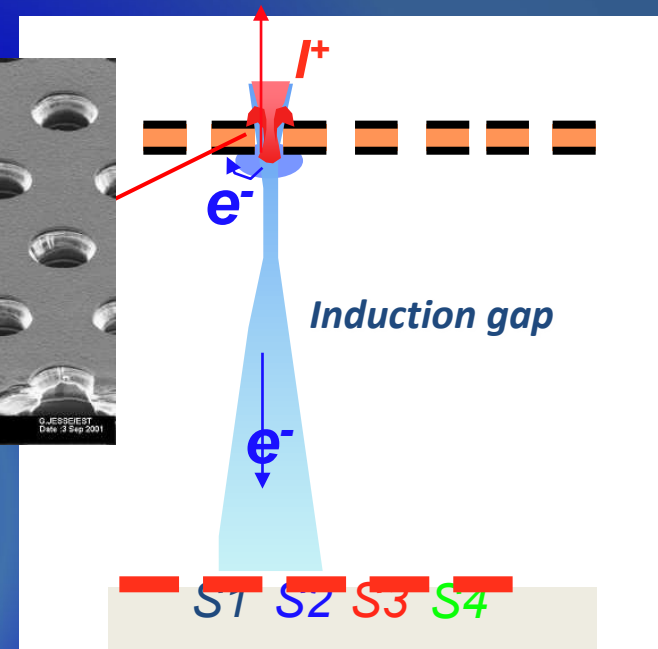
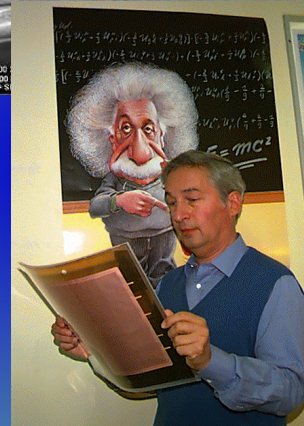
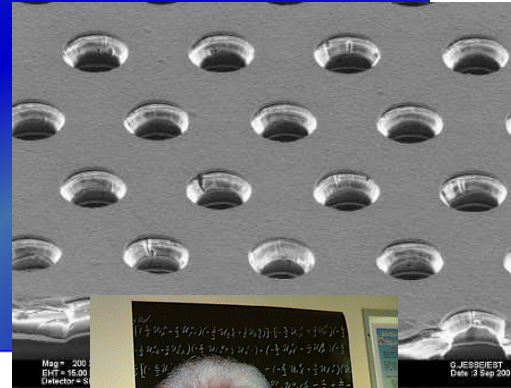
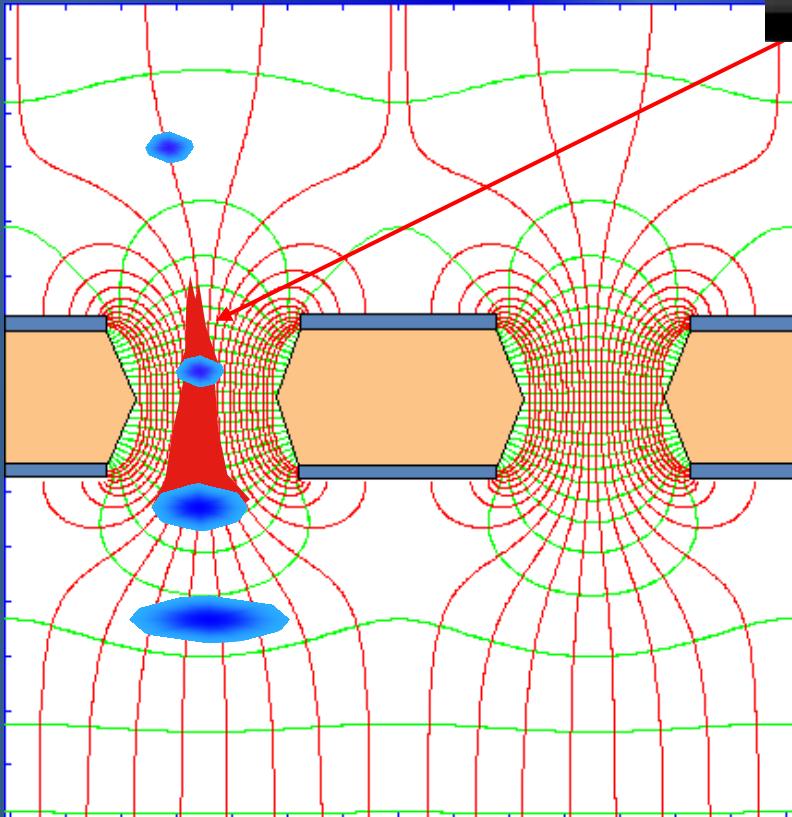


Gas Electron Multiplier (GEM)

Thin metal-coated polymer foil chemically pierced by a high density of holes

A difference of potentials of $\sim 500\text{V}$ is applied between the two GEM electrodes.

→ the primary electrons released by the ionizing particle, drift towards the holes where the high electric field triggers the electron multiplication process.



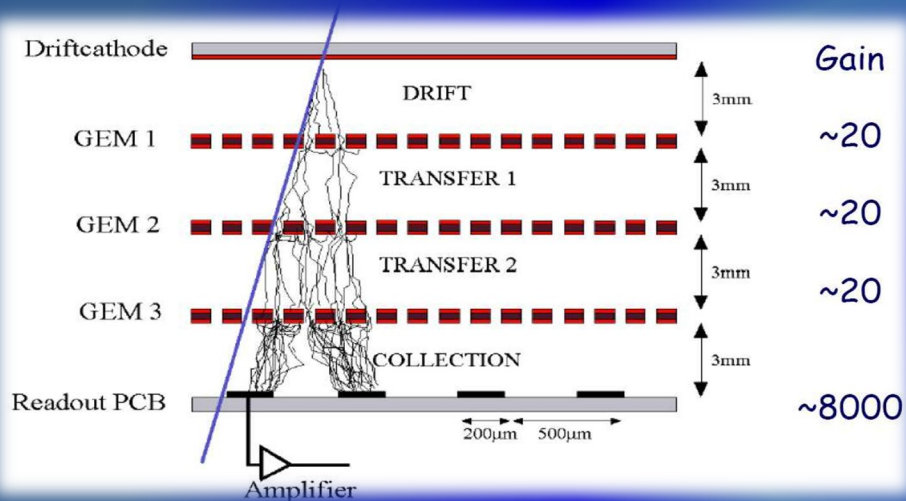
F. Sauli, NIMA386 (1997) 531

- ✓ Electrons are collected on patterned readout board.
- ✓ A fast signal can be detected on the lower GEM electrode for triggering or energy discrimination.
- ✓ All readout electrodes are at ground potential.
- ✓ Positive ions partially collected on GEM electrodes

Avalanche Simulation in GEM & Triple-GEM Structures

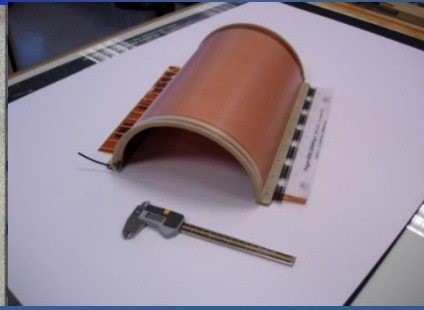
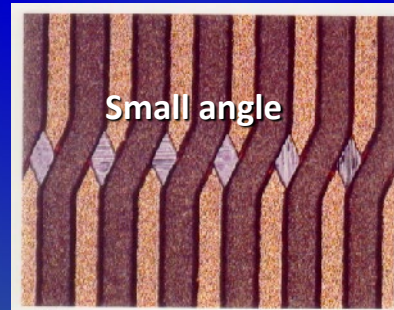
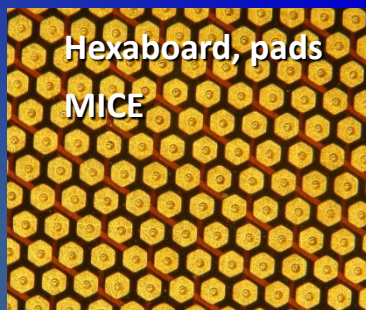
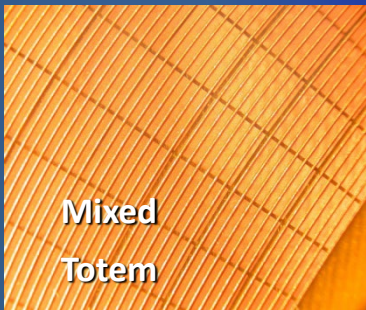
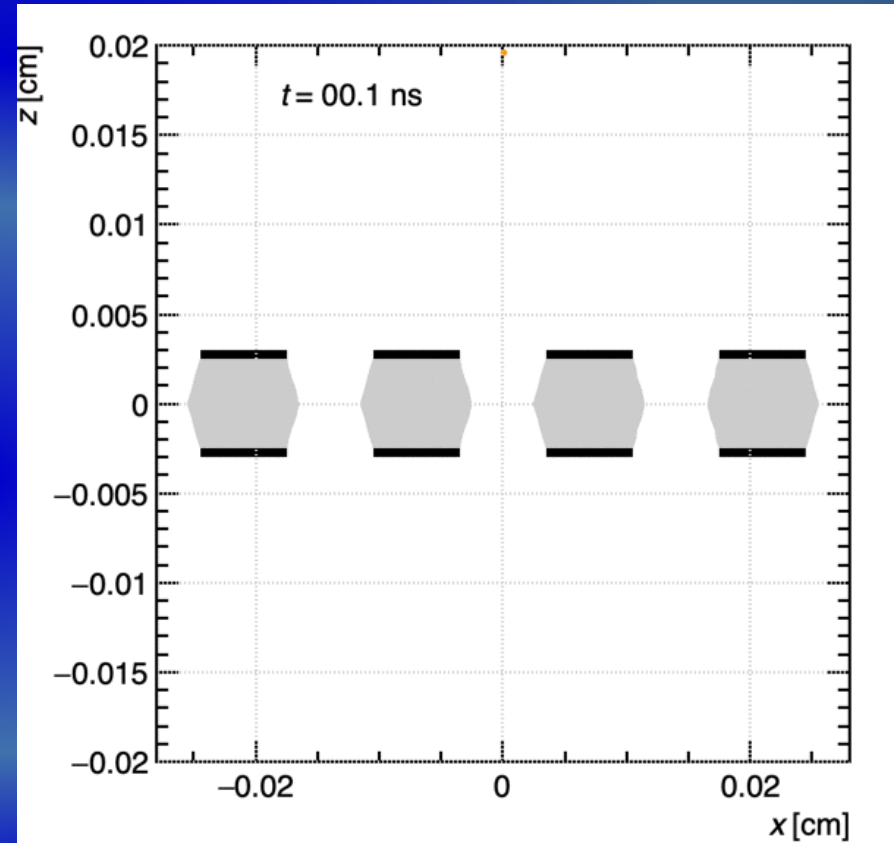
Animation of the avalanche process (Garfield++): monitor in ns-time electron/ion drifting and multiplication in GEM

Full decoupling of amplification stage (GEM) and readout stage (PCB, anode)



Amplification and readout structures can be optimized independently !

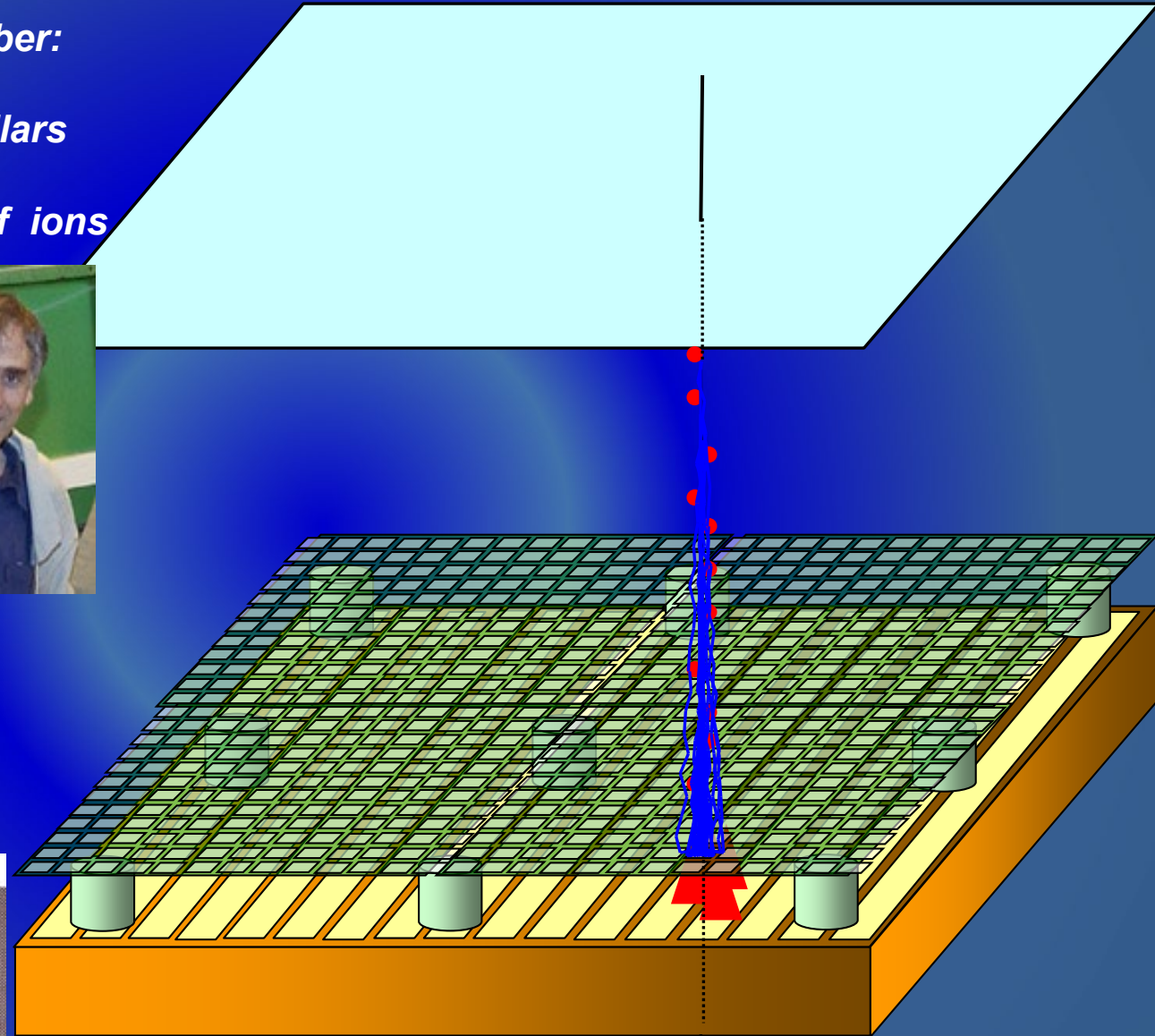
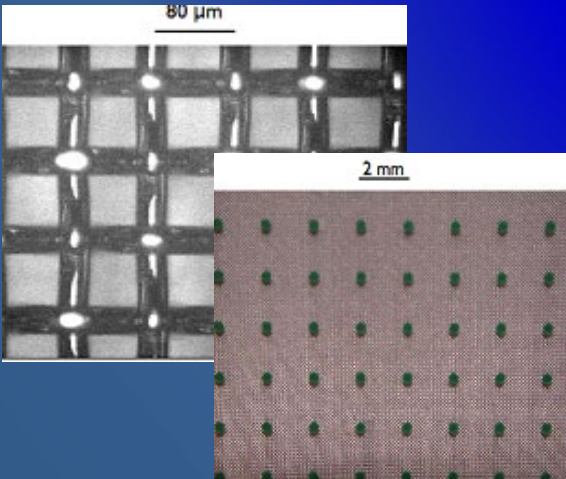
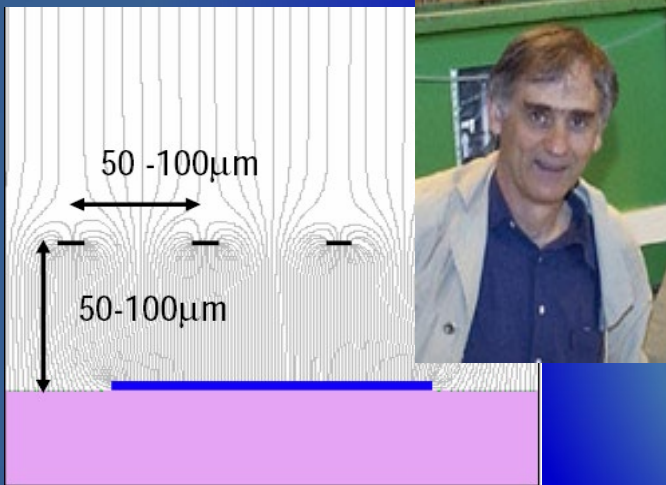
<http://cern.ch/garfieldpp/examples/gemgain>



Micro Mesh Gaseous Structure (MICROME GAS)

*Micromesh Gaseous Chamber:
micromesh supported
by 50-100 mm insulating pillars*

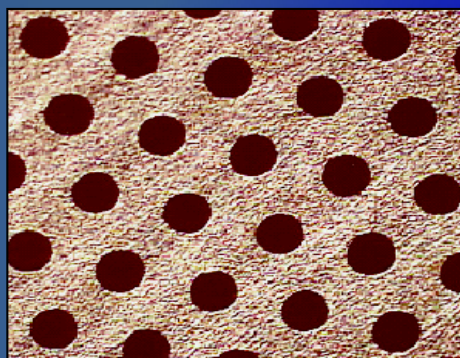
Small gap: fast collection of ions



Other MPGDs Concepts: THGEM, μ RWELL, RPWELL

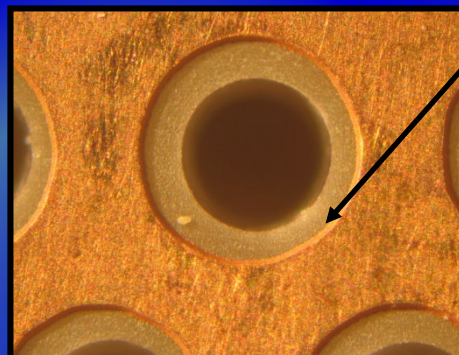
THGEM Manufactured by standard PCB techniques of precise drilling in G-10 (and other materials) and Cu etching

STANDARD GEM



1 mm

THGEM



0.1 mm rim
to prevent
discharges

L. Periale, NIMA478 (2002) 377
LEM!: P. Jeanneret,
PhD thesis, 2001

μ RWELL and RPWELL

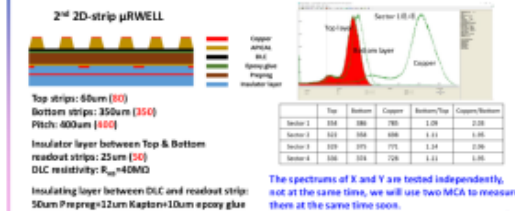
High-rate μ RWELL prototypes
made by new techniques



https://indico.cern.ch/event/889389/contributions/4020068/attachments/2115302/3560690/RD51_collaboration_meeting_Youxi.pptx

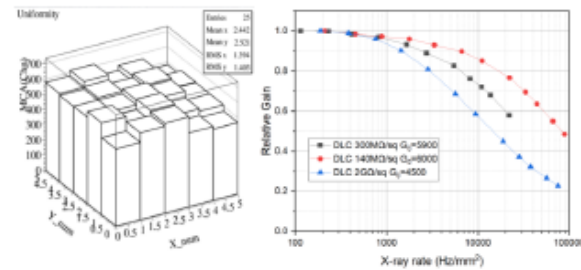
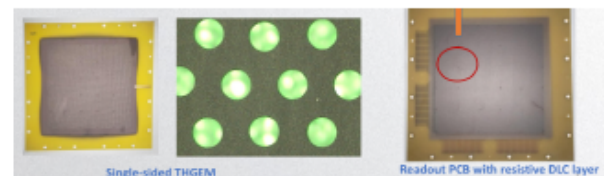
μ RWELL with 2D-Strip
Readout – For RD51 Tracker

Optimization of the geometry of the readout strips



https://indico.cern.ch/event/1040996/contributions/4404219/attachments/2266859/3849374/2021-06-18_RD51-Collaboration%20Meeting-ZhouYi-Final.pdf

Development of RWELL
detectors for large area & high
rate applications



<https://indico.cern.ch/event/889389/contributions/4020068/attachments/2115585/3559628/RD51CollaborationMeeting-egf.pdf>

Simulation Tools and Modelling of MPGDs

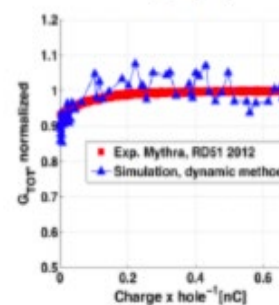
MPGDs and the mean free path

- ▶ Recall:
 - ▶ Mean free path of electrons in Ar: $2.5 \mu\text{m}$,
- ▶ Compare with:
 - ▶ Micromegas mesh pitch: $63.5 \mu\text{m}$
 - ▶ GEM polyimide thickness: $50 \mu\text{m}$
 - ▶ Micromegas wire thickness: $18 \mu\text{m}$
 - ▶ GEM conductor thickness: $5 \mu\text{m}$
- ▶ Hence:
 - ▶ mean free path approaches small structural elements;
 - ▶ such devices should be treated at a molecular level.
- ▶ In addition, MPGDs usually have structures for which no nearly-exact (e.g. 3d structures) fields are known.

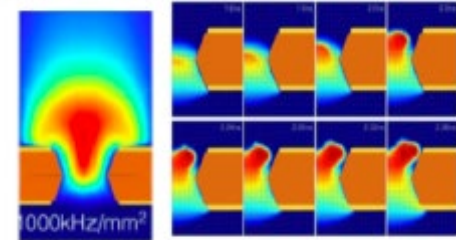
Modelling and simulation are crucial for *detailed understanding of detector physics* and for developing and exploiting *novel MPGD technologies*

- **Resistive detectors:** modelling of signal induction, understand protection schemes and rate capabilities
- **Ion physics:** minimise ion backflow, understand ion-induced damages and feedback processes, ion species/clustering and mobility
- **Modelling of scintillation** processes for optical readout: light production, quenching, timing of light production processes

GEM charging up



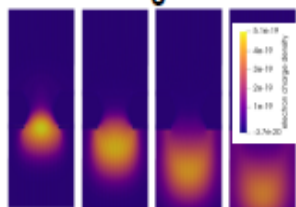
Ion backflow & Discharge formation density in GEMs



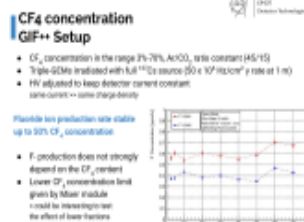
S. Franchino et al., IEEE (2015)

Gas mixture studies

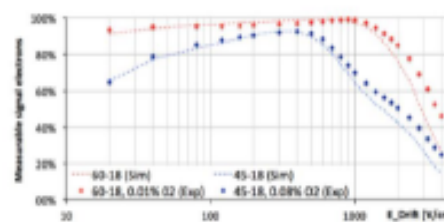
Gain simulations in MPGDs Including space charge effect using Elmer



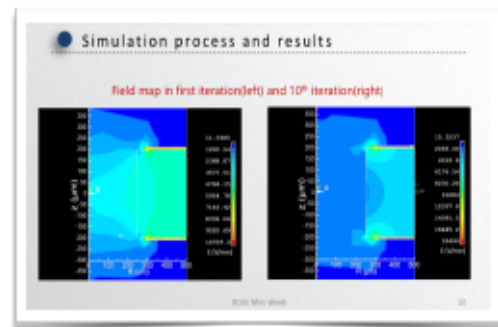
F impurities with CF4-based gas mixtures



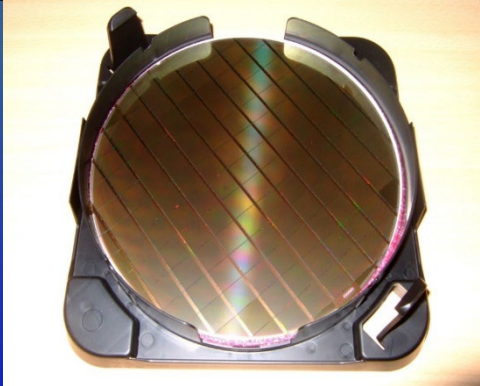
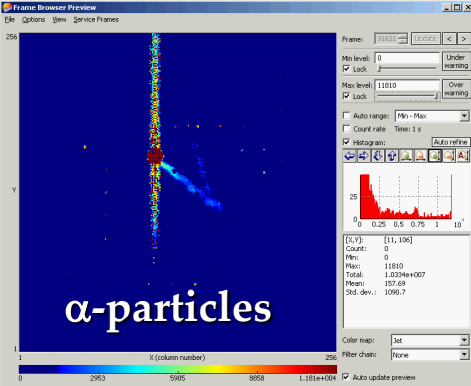
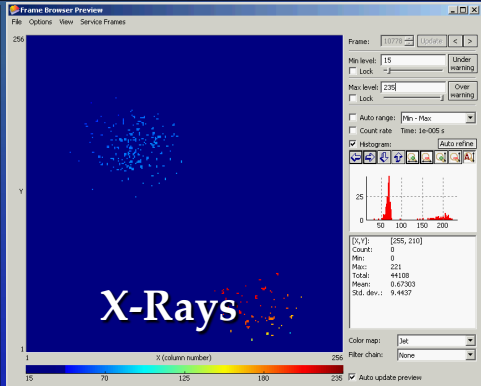
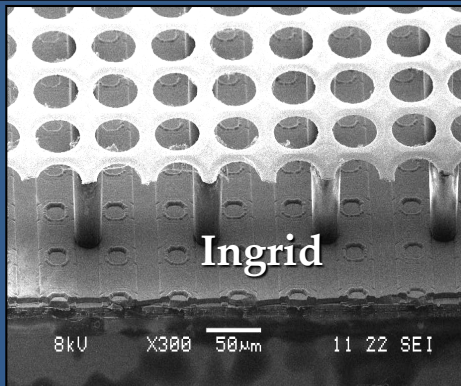
ATLAS NSW Micromegas mesh transparency



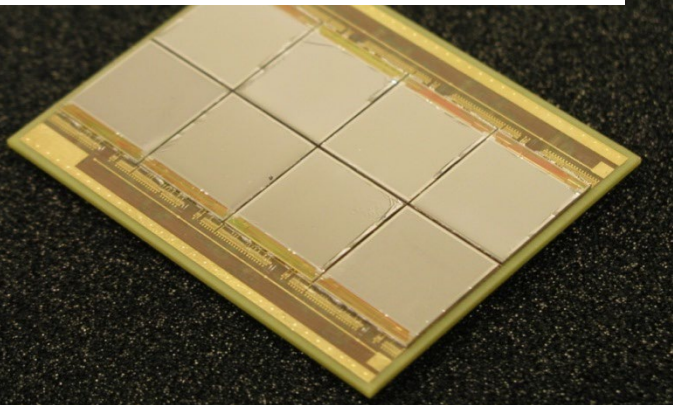
A fast simulation method for THGEM charging-up study



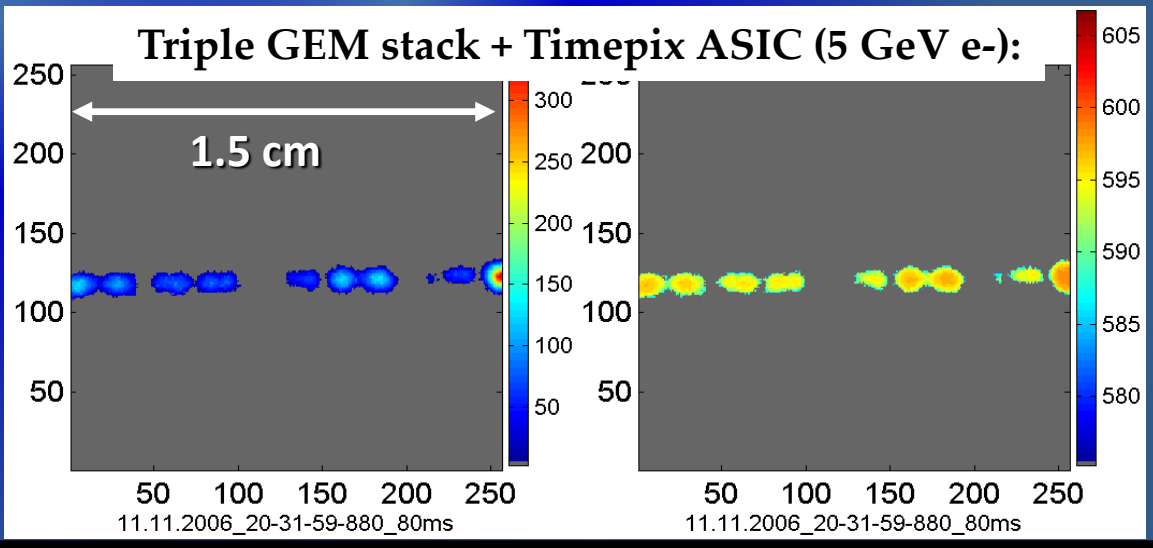
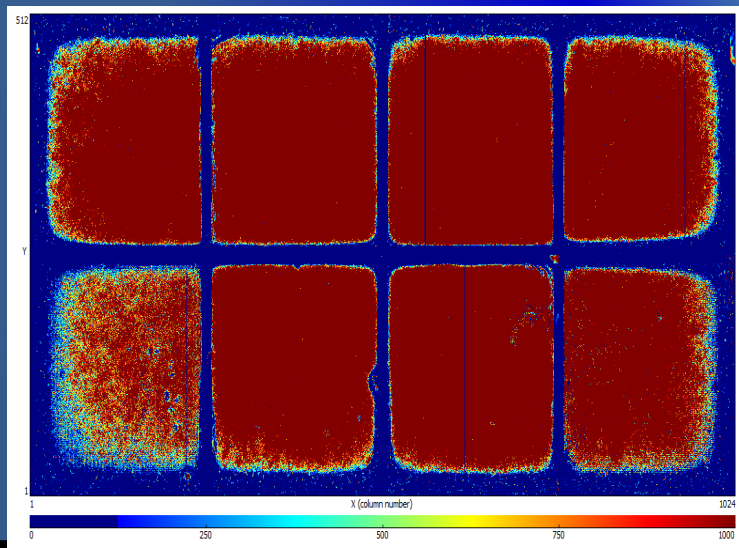
https://indico.cern.ch/event/989368/contributions/4039491/attachments/211515/3558765/APellecchia_Elmer_RD51_Oct2020.pdf



“Octopuce” (8 Timepix ASICs):



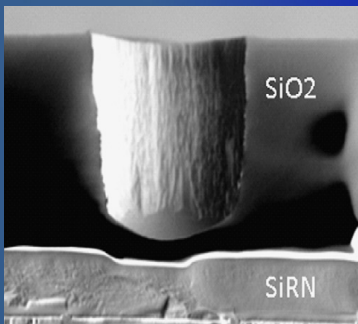
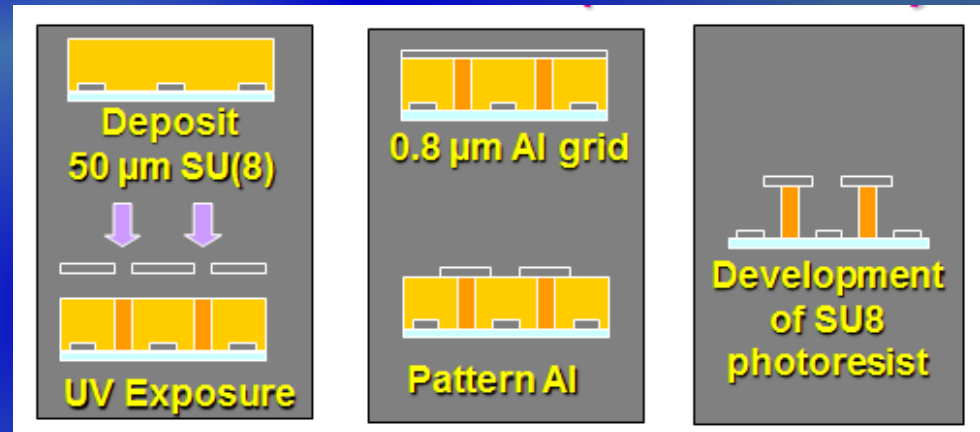
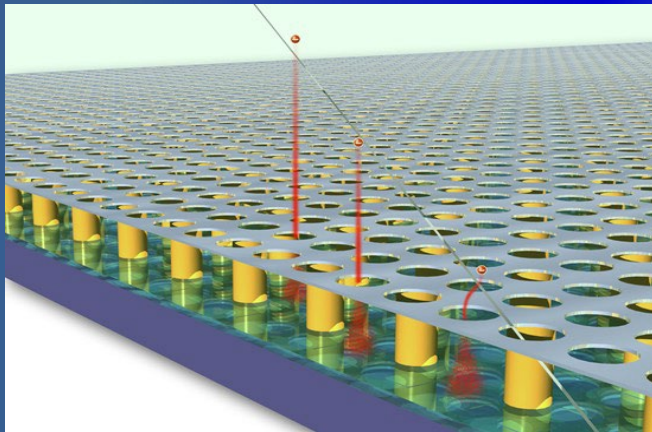
ULTIMATE INTEGRATION OF GASEOUS and SILICON DETECTORS – PIXEL READOUT of MICRO-PATTERN GASEOUS DETECTORS



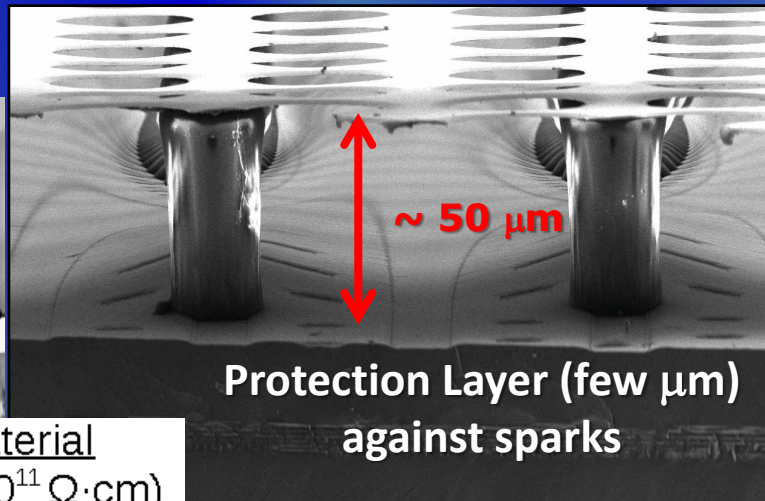
Pixel Readout of MPGDs: "GridPix" Concept

"InGrid" Concept: By means of advanced wafer processing-technology **INTEGRATE** **MICROMEAS** amplification grid directly **on top of CMOS ("Timepix") ASIC**

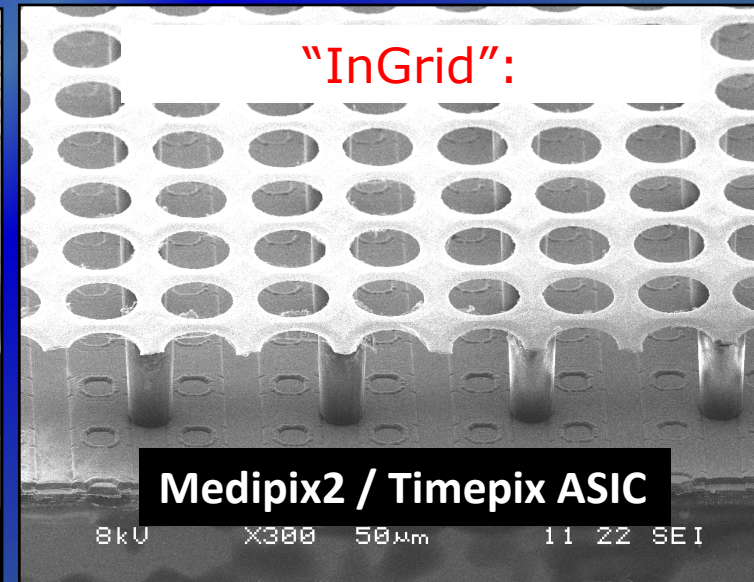
3D Gaseous Pixel Detector → 2D (pixel dimensions) x 1D (drift time)



high resistive material
15 μm aSi:H (~10¹¹ Ω·cm)
8 μm Si_xN_y (~10¹⁴ Ω·cm)



X600 20 μm 19 21 SEI



8kV X300 50 μm 11 22 SEI

Towards Large-Scale Pixel "GridPix" TPC

Testbeams with GridPixes:

160 GridPixes (Timepix) & 32 GridPixes (Timepix3)



NIM A956 (2020) 163331

(Octopuce)	(TimePix1)	TPX3 chip	Quad	Module
	(2007-14)	2017	2018	2019

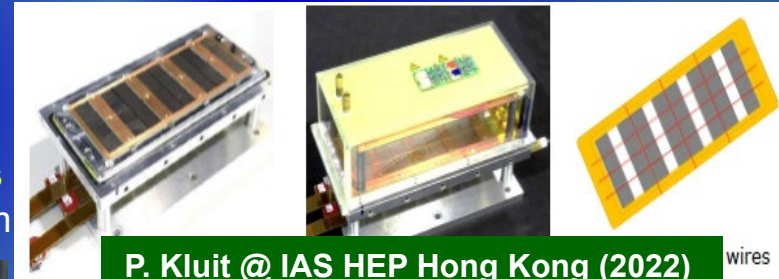
A PIXEL TPC IS REALISTIC!

Physics properties of pixel TPC:

- Improved dE/dx by cluster counting
- Improved meas. of low angle tracks
- Excellent double track separation
- Lower occupancy @ high rates
- Fully digital read out (TOT)

Quad board (Timepix3) as a building block

→ 8-quad detector (32 GridpPixs) with a field cage at test-beam @ DESY in June 2021:



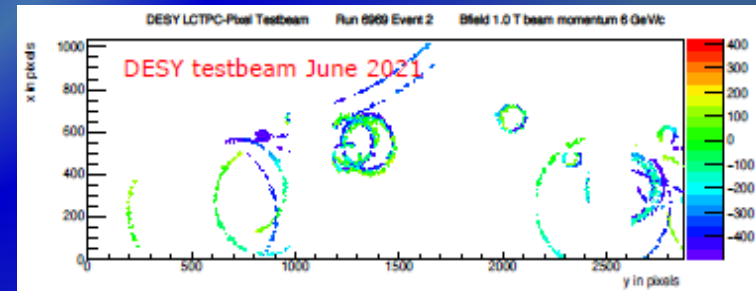
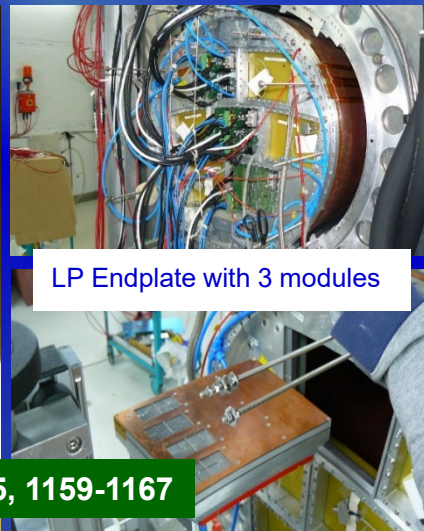
P. Kluit @ IAS HEP Hong Kong (2022)

wires

3 modules for LP TPC @ DESY: 160 (1 x 96 & 2 x 32) GridPixs
 320 cm² active area, 10,5 M. channels, new SRS Readout system



IEEE TNS 64 (2017)5, 1159-1167

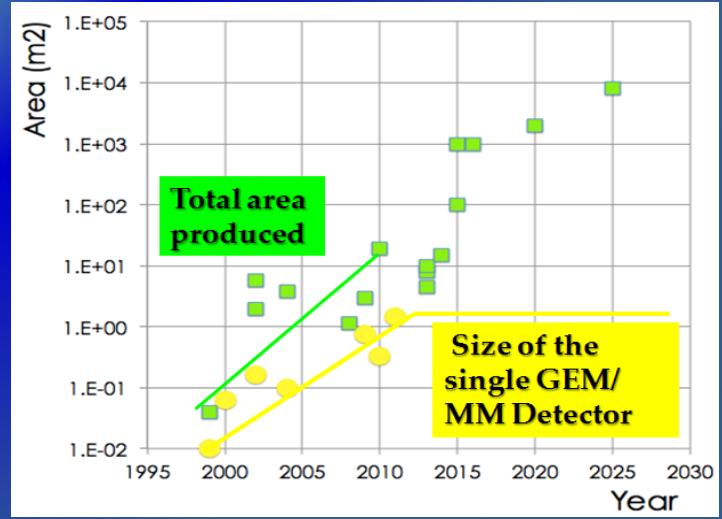
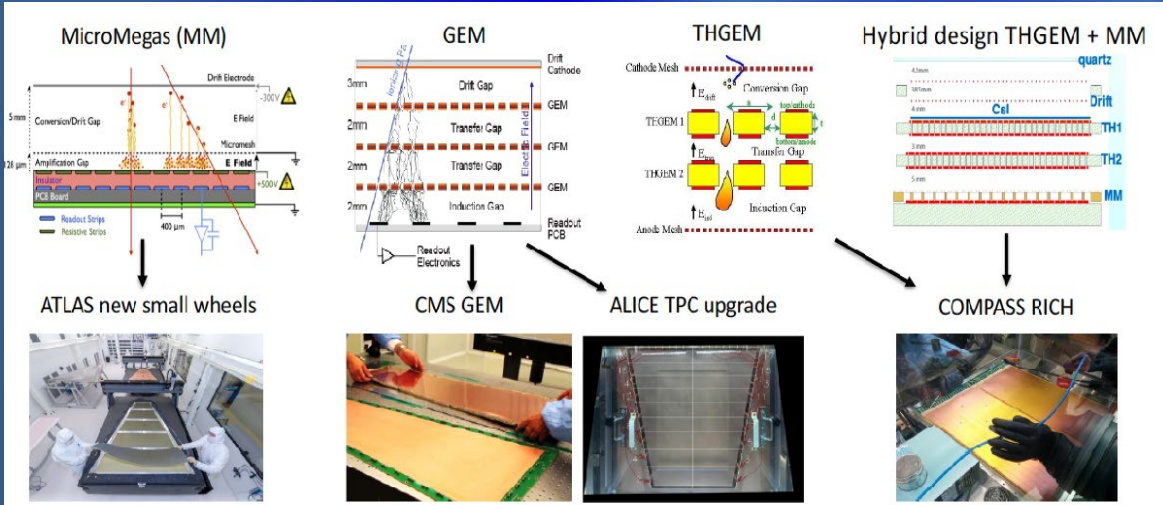


- ✓ ion back flow can be further reduced by applying a double grid.
- ✓ Protection layer resistivity to be reduced
- ✓ New Timepix4 developments

MPGD Technologies @ CERN Experiments

- The integration of MPGDs in large experiments was not rapid, despite of the first large-scale application in COMPASS at SPS in the 2000's
- Scaling up MPGD detectors, while preserving the typical properties of small prototypes, allowed their use in the LHC upgrades
 - Many emerged from the R&D studies within the CERN-RD51 Collaboration

Experiment / Timescale	Application Domain	MPGD Technology	Total detector size / Single module size	Operation Characteristics / Performance	Special Requirements / Remarks
COMPASS TRACKING > 2002	Fixed Target Experiment (Tracking)	3-GEM Micromegas w/ GEM preampl.	Total area: 2.6 m ² Single unit detect: 0.31x0.31 m ² Total area: ~ 2 m ² Single unit detect: 0.4x0.4 m ²	Max.rate: ~100kHz/mm ² Spatial res.: ~70-100µm (strip), ~120µm (pixel) Time res.: ~ 8 ns Rad. Hard.: 2500 mC/cm ²	Required beam tracking (pixelized central / beam area)
TOTEM TRACKING: > 2009	Hadron Collider / Forward Physics (5.3 ≤ η ≤ 6.5)	3-GEM (semicircular shape)	Total area: ~ 4 m ² Single unit detect: up to 0.03m ²	Max.rate: 20 kHz/cm ² Spatial res.: ~120µm Time res.: ~ 12 ns Rad. Hard.: ~ mC/cm ²	Operation in pp, pA and AA collisions.
LHCb MUON DETECTOR > 2010	Hadron Collider / B-physics (triggering)	3-GEM	Total area: ~ 0.6 m ² Single unit detect: 20-24 cm ²	Max.rate: 500 kHz/cm ² Spatial res.: ~ cm Time res.: ~ 3 ns Rad. Hard.: ~ C/cm ²	Redundant triggering
COMPASS RICH UPGRADE > 2016	Fixed Target Experiment (RICH - detection of single VUV photons)	Hybrid (THGEM + CsI and MM)	Total area: ~ 1.4 m ² Single unit detect: ~ 0.6 x 0.6 m ²	Max.rate: 100 Hz/cm ² Spatial res.: < 2.5 mm Time res.: ~ 10 ns	Production of large area THGEM of sufficient quality
ATLAS MUON UPGRADE CERN LS2	Hadron Collider (Tracking/Triggering)	Resistive Micromegas	Total area: 1200 m ² Single unit detect: (2.2x1.4m ²) ~ 2-3 m ²	Max. rate: 15 kHz/cm ² Spatial res.: < 100µm Time res.: ~ 10 ns Rad. Hard.: ~ 0.5C/cm ²	Redundant tracking and triggering; Challenging constr. in mechanical precision
CMS MUON UPGRADE CERN LS2	Hadron Collider (Tracking/Triggering)	3-GEM	Total area: ~ 143 m ² Single unit detect: 0.3-0.4m ²	Max. rate: 10 kHz/cm ² Spatial res.: ~100µm Time res.: ~ 5-7 ns Rad. Hard.: ~ 0.5 C/cm ²	Redundant tracking and triggering
ALICE TPC UPGRADE CERN LS2	Heavy-Ion Physics (Tracking + dE/dx)	4-GEM / TPC	Total area: ~ 32 m ² Single unit detect: up to 0.3m ²	Max.rate: 100 kHz/cm ² Spatial res.: ~300µm Time res.: ~ 100 ns dE/dx: 11 % Rad. Hard.: 50 mC/cm ²	- 50 kHz Pb-Pb rate; - Continues TPC readout - Low IBF and good energy resolution



CERN Detector Seminars in 2022: LS2 Upgrades

Major MPGDs developments for ATLAS, CMS, ALICE upgrades, towards establishing technology goals and technical requirements, and addressing engineering and integration challenges ... and first results from Run 3 !!!

"The New Small Wheel project of ATLAS"

by Theodoros Vafeiadis (17 Jun 2022)

<https://indico.cern.ch/event/1168778/>

"Continuous data taking with the upgraded ALICE GEM-TPC"

by Robert Helmut Munzer (24 Jun 2022),

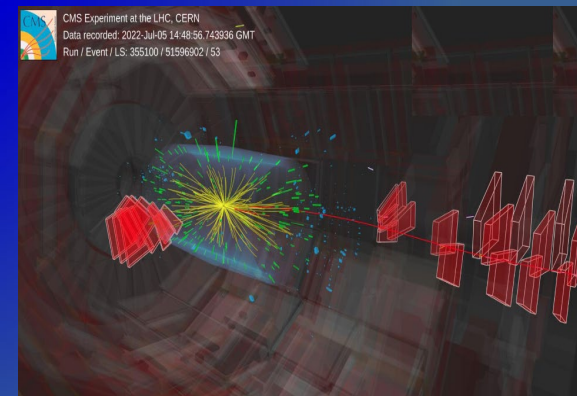
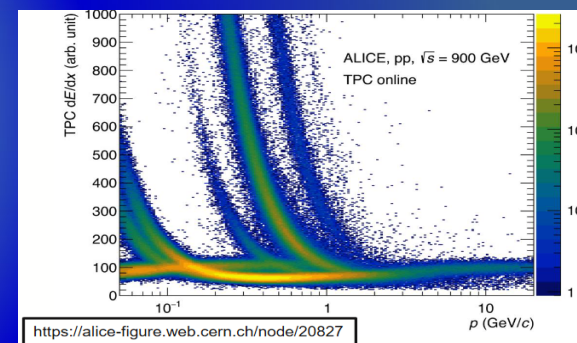
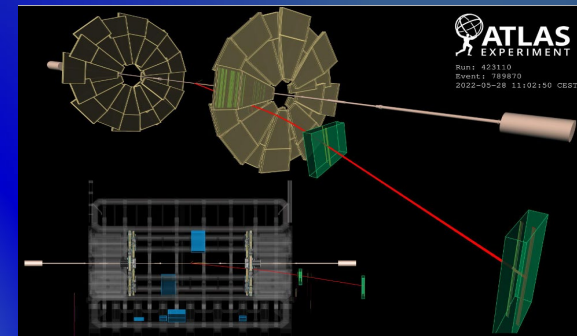
<https://indico.cern.ch/event/1172978/>

"The GEM detectors within the CMS Experiment"

Michele Bianco (08 Jul 2022)

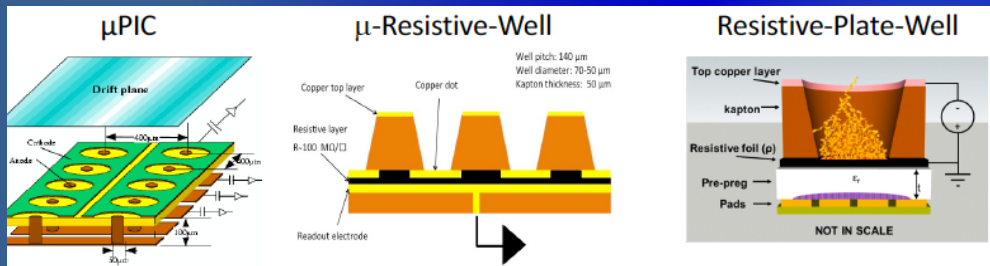
<https://indico.cern.ch/event/1175363/>

All three major LHC upgrades, incorporating MPGDs, started their R&D in close contact with RD51, using dedicated setups at GDD-RD51 Laboratory



MPGD Technologies @ Future R&D Trends

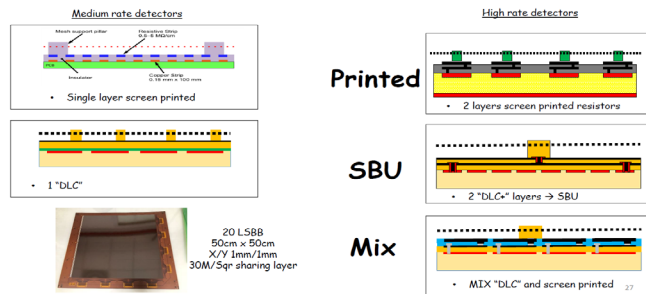
- ✓ **RESISTIVE MATERIALS** and related detector architectures for **single-stage designs** (μ PIC, μ -RWELL, RPWELL, resistive MM)
 - improves detector stability; single-stage is advantage for assembly, mass production & cost.



- **Diamond-like carbon (DLC) resistive layers**
 - Solutions to improve high-rate capability (\geq MHz)

Resistive
DLC
Collaboration

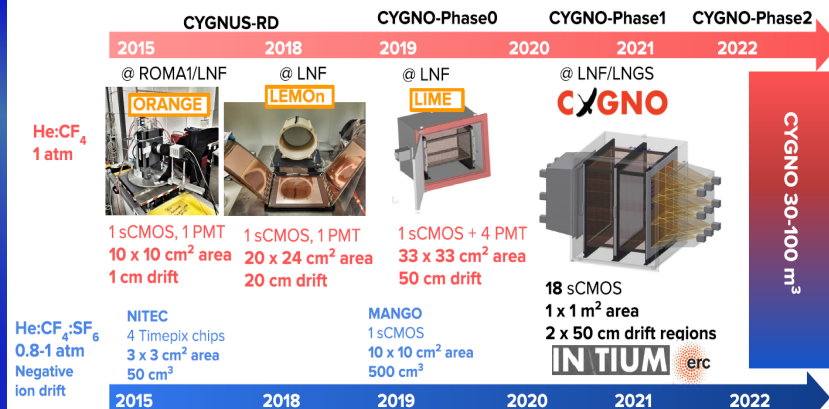
Different Resistive protection approach with Micro-Megas



- ✓ **Picosecond Timing Detector (RD51 PICOSEC Collaboration)** – MM device with radiator and radiation-hard PC

- **OPTICAL READOUT:** hybrid approaches combining gaseous with non-gaseous in a single device (e.g. CYGNUS- TPC project):

CYGNUS roadmap and synergy with INITIUM



- **New manufacturing techniques & structures:**

- Solid-state photon and neutron converters, **INNOVATIVE NANOTECHNOLOGY COMPONENTS (graphene layers);**

- Material studies (low out-gassing, radiation hardness, radio-purity, converter robustness and eco-friendly gases).

- Emerging technologies related to novel PCs, MicroElectroMechanical Systems (MEMS), sputtering, 3-D printing of amplifying structures and cooling circuits

Towards Large Area in Fast Timing GASEOUS DETECTORS

Multi-Gap Resistive Plate Chambers (MRPC):

- ✓ ALICE TOF detector (160m²) achieved time res. ~ 60 ps
- ✓ New studies with MRPC with 20 gas gaps using a low-resistivity 400 μm-thick glass → down to 20 ps time resolution

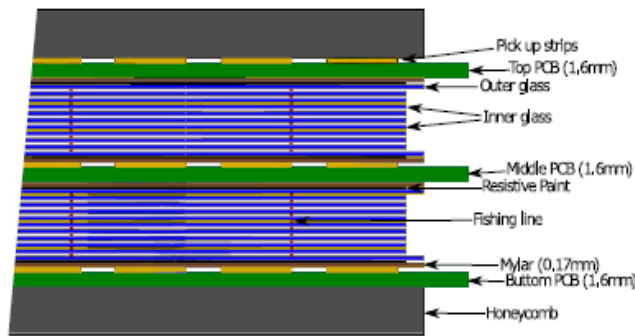
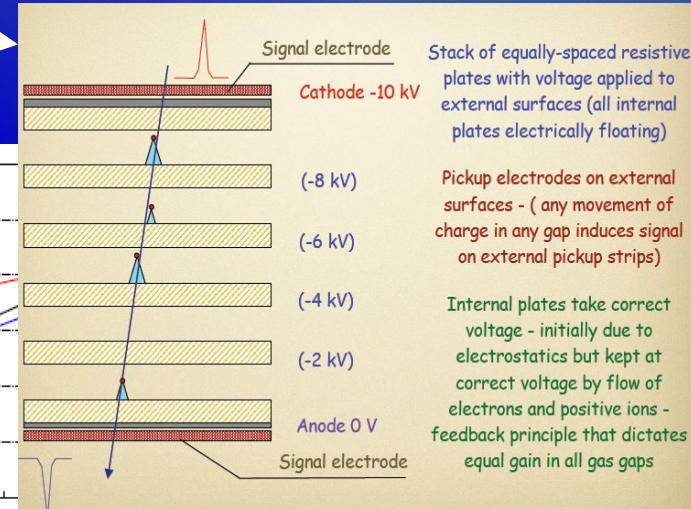
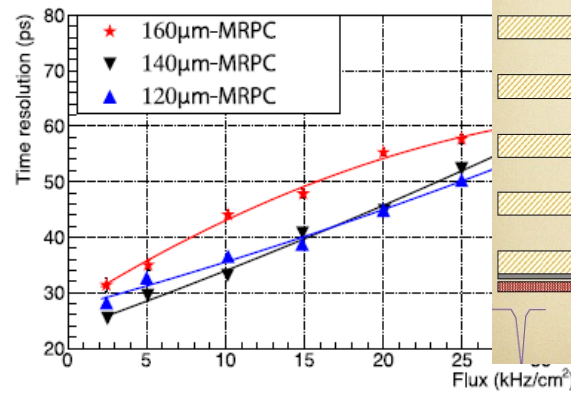


Fig. 1. Cross section of the double stack 20-gap MRPC.

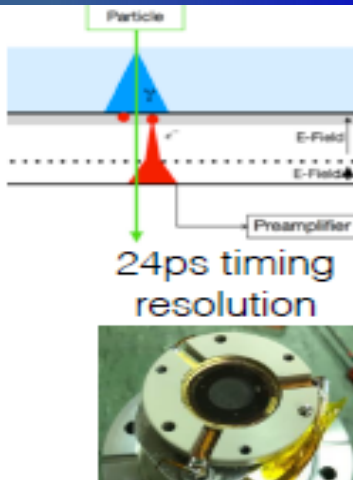


Gaseous Detectors: Micromegas with Timing (RD51 Picosec Collaboration)

$\sigma \sim 25$ ps timing resolution (per track)

Cherenkov radiator + Photocathode + Micromegas

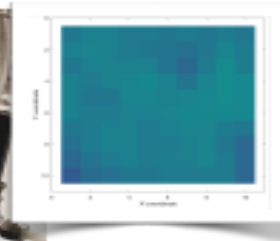
Tested in RD51 testbeam July 2021



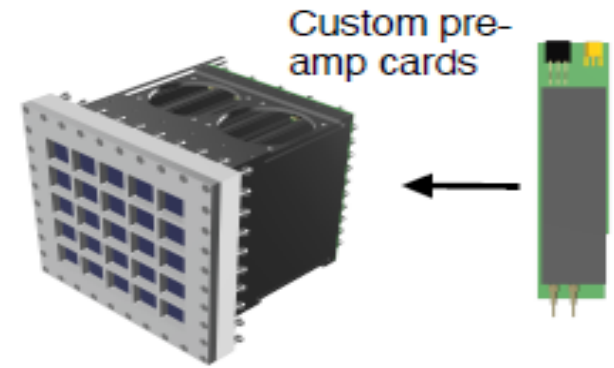
Single pad (2016)
ø1 cm



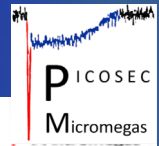
10x10 module
□ 1 cm



Planarity
< 10μm



<https://indico.cern.ch/event/1040998/contributions/4398412/attachments/2265036/3845651/PICOSEC-update-final.pdf>

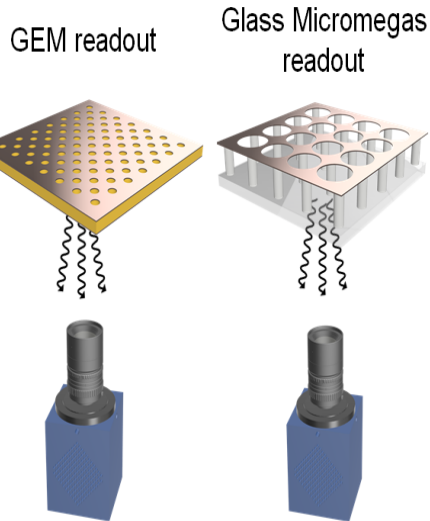


Optical Readout for Micro-Pattern Gaseous Detectors

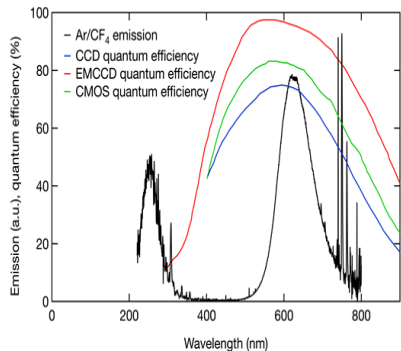
Courtesy CERN GDD group

Concept

Scintillation light emitted during amplification processes in MPGDs can be read out with CCD or CMOS cameras.



Emission spectrum of Ar / CF₄ gas mixture with UV and visible scintillation

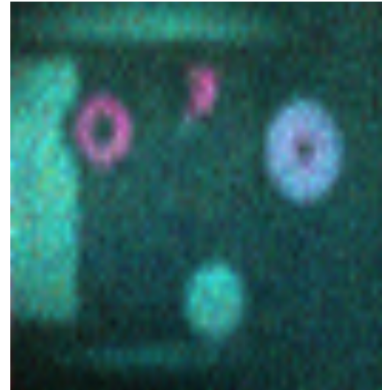


Examples and applications

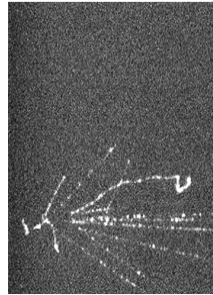
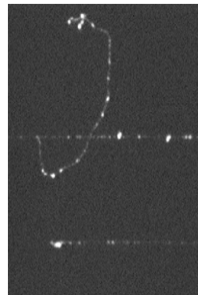
X-ray radiography



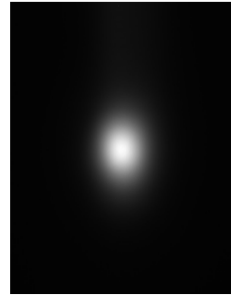
Energy-resolved imaging



Track reconstruction



Beam monitoring

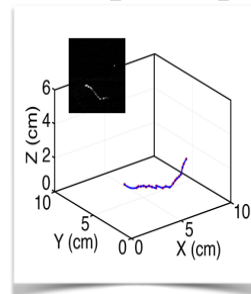
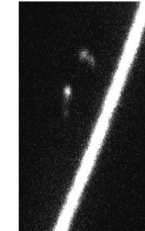
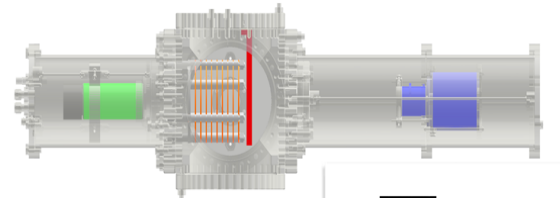


Rapid X-ray imaging (fluoroscopy) with sub-ms exposure per frame



R&D and current projects

Low-pressure optical TPC to resolve events with wide dynamic range (low energy X-rays in presence of alpha particle or nuclear recoils)



Use of high-speed cameras for 3D track reconstruction resolving drift time differences



Graphene-based Functional Structures and Nanostructures for novel MPGD Concepts

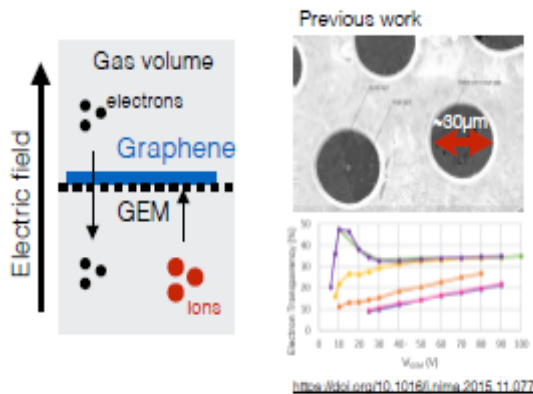
Graphene layers for: ion-backflow suppression, protection of photocathodes, solid conversion layers

PhD project of Giorgio Orlandini (FAU Erlangen-Nürnberg) in EP-DT-DD Gaseous Detector Development lab

The unique properties of two-dimensional materials such as graphene as well as carbon-based nanostructures offer new perspectives for novel gaseous radiation detectors. This may include performance improvements for detectors for HEP experiments as well as new application fields combining wideband sensitivity of advanced materials with high gain factors and granularity offered by Micro Pattern Gaseous Detectors.

Application 1:

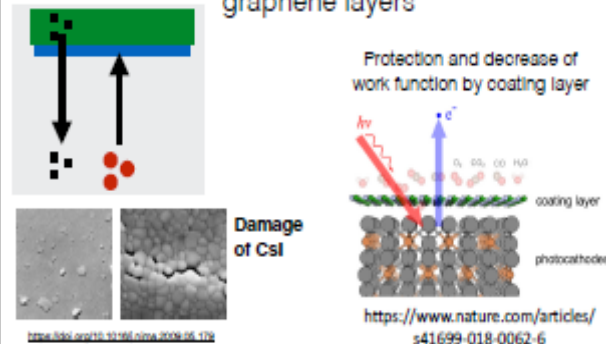
Suspended graphene for ion back-flow suppression and gas separation



Suppressing ion back flow can significantly improve high-rate capabilities and reduced electric field distortions in Time Projection Chambers.

Application 2:

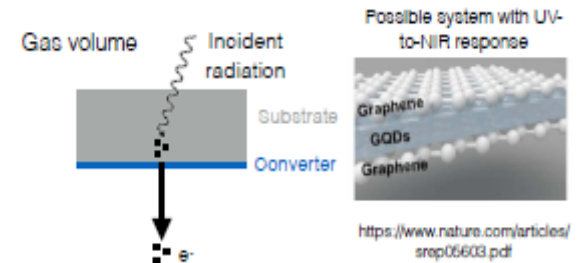
Protection of photocathodes with graphene layers



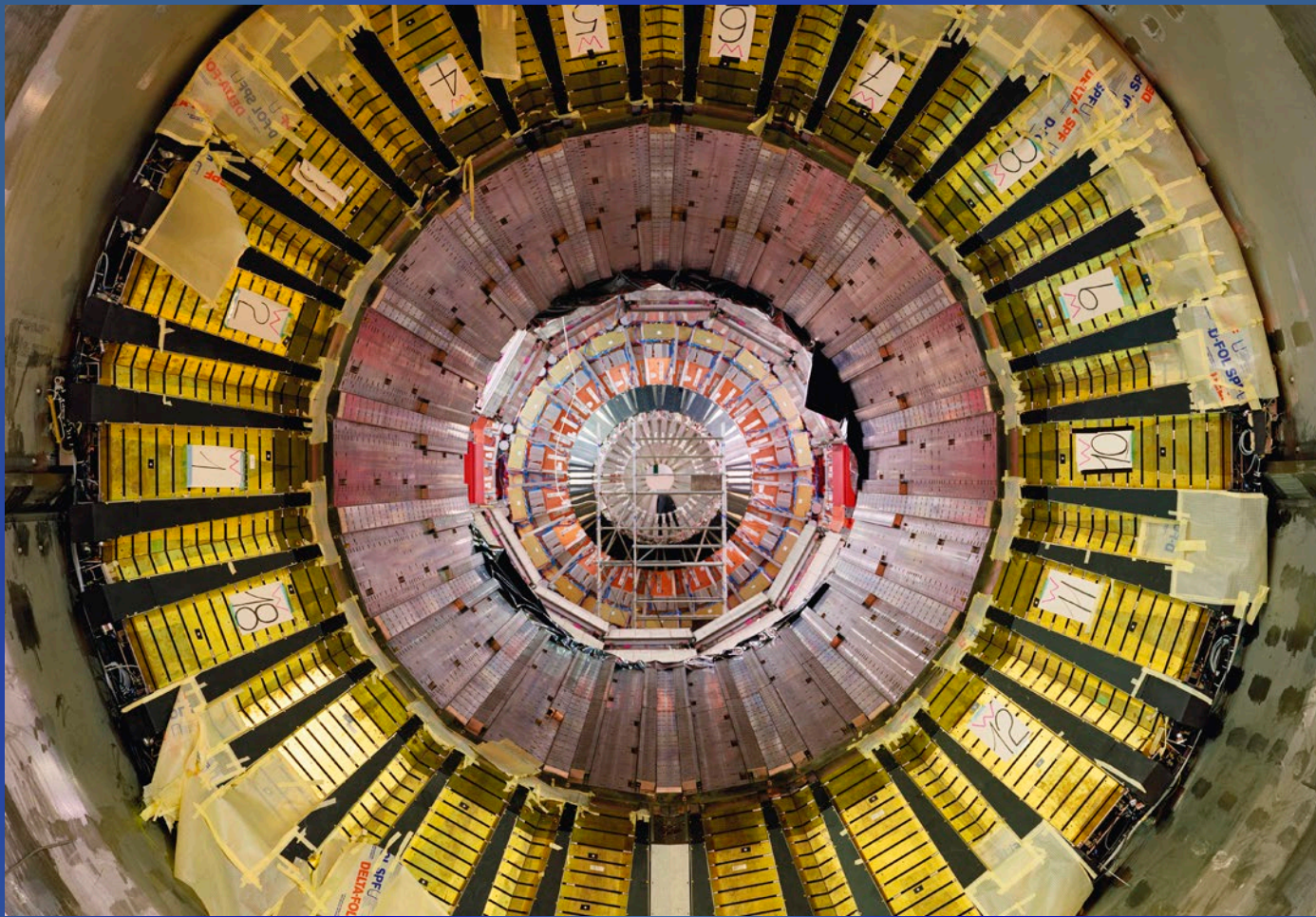
Atomically thin coating layers could protect sensitive photocathodes such as CsI against environmental factors and ion bombardment, which is important for preserving specifications of precise timing detector in harsh ion-back flow conditions. Additionally, modifications of the work functions of converter layers can be used to increase QE.

Application 3:

Graphene and nanostructures for photoconversion and as solid converters



Graphene quantum dots (GQD), carbon nanotubes and graphene have been shown to exhibit broadband sensitivity and could be used as versatile conversion layers. Utilising solid conversion layers enables high detection efficiencies and can be used for precise timing with gaseous radiation detectors.



*Knowledge is limited. Whereas the Imagination
embraces the entire world...* Albert Einstein

Bridge the gap between science and society ...

***The Role of Big High Energy Physics Laboratories:
– innovate, discover, publish, share***

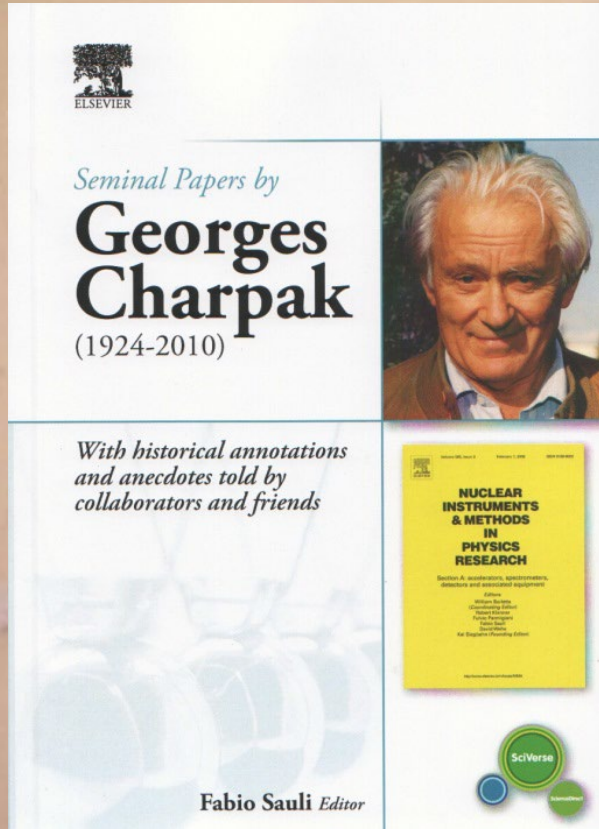


... and bring the world closer together

A scenic landscape featuring snow-capped mountains in the background, a dense forest of evergreen trees in the middle ground, and a calm lake in the foreground that perfectly reflects the scene. The sky is a mix of blue and yellow, suggesting a sunrise or sunset. The text "BACK-UP SLIDES" is overlaid in a bold, yellow, italicized font across the center of the image.

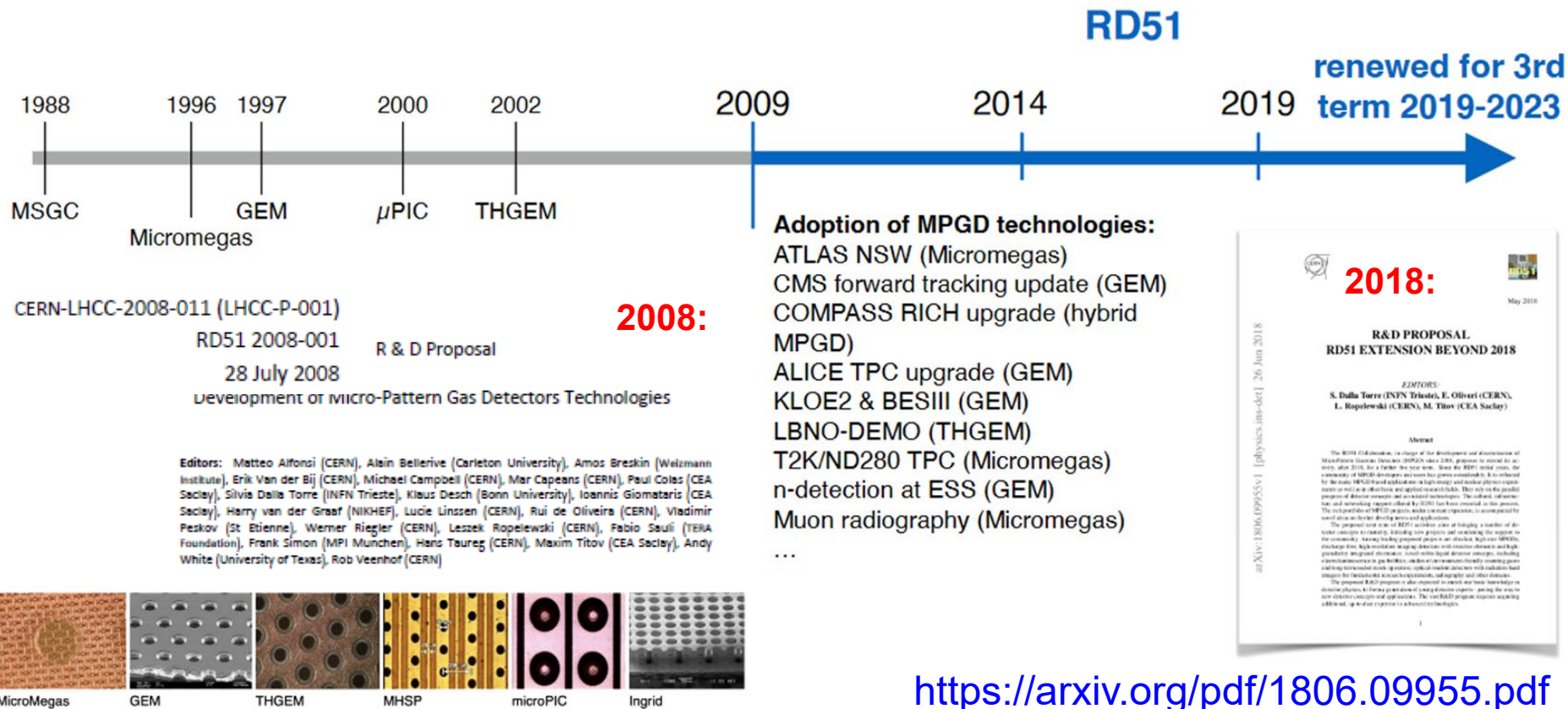
BACK-UP SLIDES

Georges Charpak with Friends



CERN-RD51 Collaboration & MPGD Technology Advances

RD51 CERN-based “TECHNOLOGY - DRIVEN R&D COLLABORATION” was established to advance MPGD concepts and associated electronics readout systems



- Renewed by the CERN Research Board for the 3rd term 2019 – 2023
- Beyond 2023, RD51 will serve as a nuclei of the new DRD1 (“all gas detectors”) collaboration, anchored at CERN, as part of the ECFA Detector R&D Roadmap implementation

RD51 and the rise of micro-pattern gas detectors

Since its foundation, the RD51 collaboration has provided important stimulus for the development of MPGDs.

Improvements in detector technology often come from capitalizing on industrial progress. Over the past two decades, advances in photolithography, microelectronics and printed circuits have opened the way for the production of micro-structured gas-amplification devices. By 2008, interest in the development and use of the novel micro-pattern gaseous detector (MPGD) technologies led to the establishment at CERN of the RD51 collaboration. Organized for a five-year term, RD51 was later prolonged for several years beyond 2013. While many of the MPGD technologies introduced before RD51 were founded (figure 1), new techniques becoming available or affordable, new ones still being introduced, and existing ones are still being improved.

In the late 1980s, the development of the multi-layered MSGC (MSGC) created great interest because of its high rate capability, which was orders of magnitude higher than in wire chambers, and its position resolution of a few tens of micrometres at particle fluxes exceeding about 1 MHz/mm². Developed for projects at high-luminosity colliders, MSGCs promised to fill a gap between the high-performance but expensive solid-state detectors, and cheap but rate-limited traditional wire chambers. However, detailed studies of their long-term behaviour at high rates and in hadron beams revealed two possible weaknesses of the MSGC technology: the formation of deposits on the electrodes, affecting gain and performance (“ageing effects”), and spark-induced damage to electrodes in the presence of highly ionizing particles.

These initial ideas have since led to more robust MPGD structures, in general using modern photolithographic processes on thin insulating supports. In particular, ease of manufacturing, operational stability and superior performances for charged-particle tracking, muon detection and triggering have given rise to two main designs: the gas electron-multiplier (GEM) and the micro-mesh gaseous structure (Micromegas). By using a pitch size of a few hundred micrometres, both devices exhibit intrinsic high-rate capability (> 1 MHz/mm²), excellent spatial and multi-track resolution (around 30 µm and 500 µm, respectively), and time resolution for single photoelectrons in the sub-nanosecond range.

Coupling the microelectronics industry and advanced PCB technology has been important for the development of gas detectors with increasingly smaller pitch size. An elegant example is the use of a CMOS pixel ASIC, assembled directly below the GEM or Micromegas amplification structure. Modern “wafer post-processing technology” allows for the integration of a Micromegas grid directly on top of a Medipix or Timepix chip, thus forming

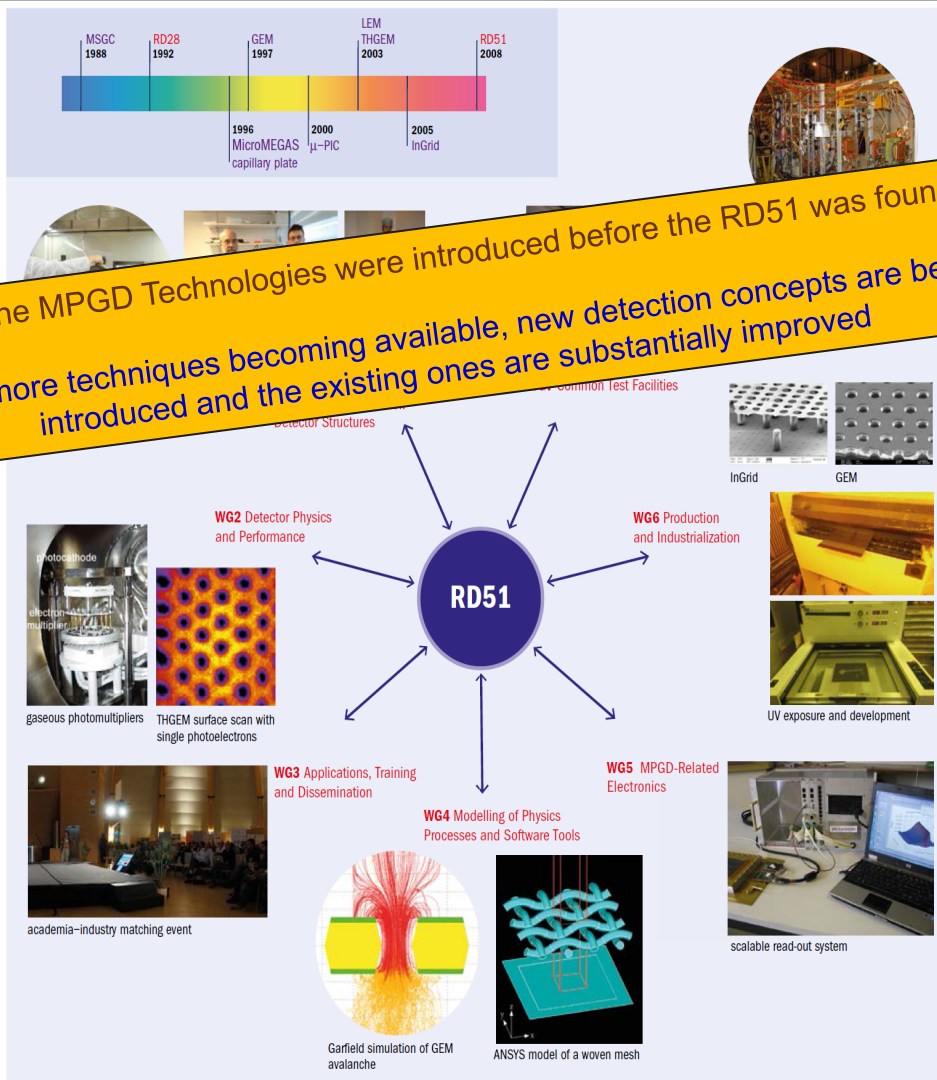


Fig.1. The seven working groups of RD51, with illustrations of just a few examples of the different kinds of work involved. Top left: the 20-year pre-history of RD51. (Image credits: RD51 Collaboration.)

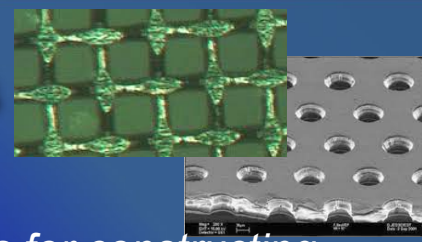
integrated read-out of a gaseous detector (InGrid). Using this approach, MPGD-based detectors can reach the level of integration and resolving power typical of solid-state pixel detectors for applications requiring imaging detectors with large area and moderate spatial resolution (e.g. ring-imaging CHIC counters), coarser macro-patterned structures offering an interesting economic solution with relatively low mass and power consumption – thanks to the intrinsic robustness of the structures. Such detectors are the thick GEM (THGEM), the electron multiplier (LEM), patterned resistive thick GEM (RETGEM) and the resistive-plate WELL (RPWELL).

RD51 and its working groups

The main objective of RD51 is to advance the technological development and application of MPGDs. While a number of activities have emerged related to the LHC upgrade, most importantly, RD51 serves as an access point to MPGD “know-how” for the worldwide community – a platform for sharing information, results and experience – and optimizes the cost of R&D through the sharing of resources and the creation of common projects and infrastructure. All partners are already pursuing either basic- or application-oriented R&D involving MPGD concepts. Figure 1 shows the organization of seven Working Groups (WG) that cover all of the relevant aspects of MPGD-related R&D.

WG1 Technological Aspects and Development of New Detector Structures. The objectives of WG1 are to improve the performance of existing detector structures, optimize fabrication methods, and develop new multiplier geometries and techniques. One of the most prominent activities is the development of large-area GEM, Micromegas and THGEM detectors. Only one decade ago, the largest MPGDs were around 40 × 40 cm², limited by existing tools and materials. A big step towards the industrial manufacturing of MPGDs with a size around a square metre came with new fabrication methods – the single-mask GEM, “bulk” Micromegas, and the novel Micromegas construction scheme with a “floating mesh”. While in “bulk” Micromegas, the metallic mesh is integrated into the PCB read-out, in the “floating-mesh” scheme it is integrated in the panel containing drift electrodes and placed on pillars when the chamber is closed. The single-mask GEM technique overcomes the cumbersome practice of alignment of two masks between top and bottom films, which limits the achievable lateral size to 50 cm. This technology, together with the novel “self-stretching technique” for assembling GEMs without glue and spacers, simplifies the fabrication process to such an extent that, especially for large-volume production, the cost per unit area drops by orders of magnitude. ▶

2022: MPGDs for High Luminosity LHC Upgrades

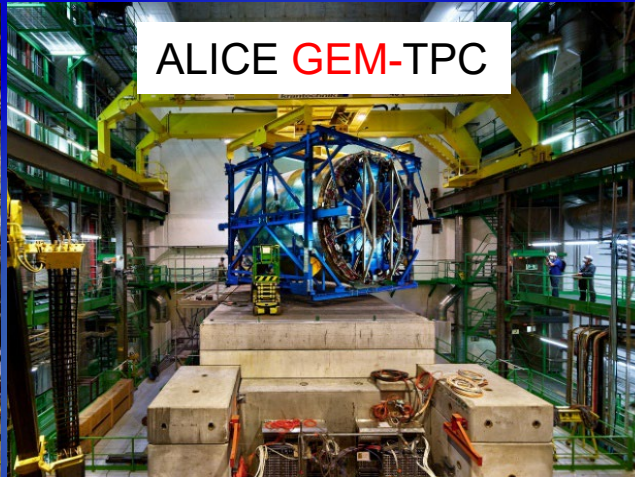


The successful implementation of MPGDs for relevant upgrades of CERN experiments indicates the degree of maturity of given detector technologies for constructing large-size detectors, the level of dissemination within the HEP community and their reliability

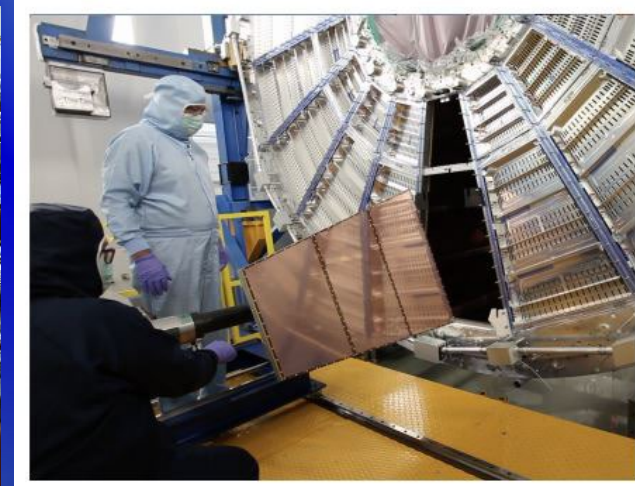
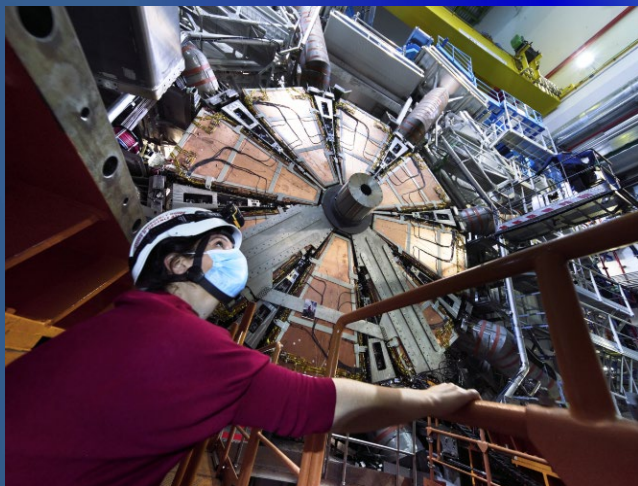
ATLAS NSW **MicroMegas**



ALICE **GEM-TPC**



CMS **GEM** muon endcaps



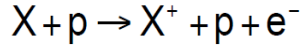
<https://ep-news.web.cern.ch/content/atlas-new-small-wheel-upgrade-advances-0>

<https://ep-news.web.cern.ch/upgraded-alice-tpc>

<https://ep-news.web.cern.ch/content/demonstrating-capabilities-new-gem>

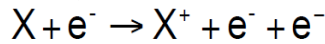
Gaseous Detectors: Ionization Statistics (II)

Primary ionization



p = charge particle traversing the gas
 X = gas atom
 e^- = delta-electron (δ)

Secondary ionization



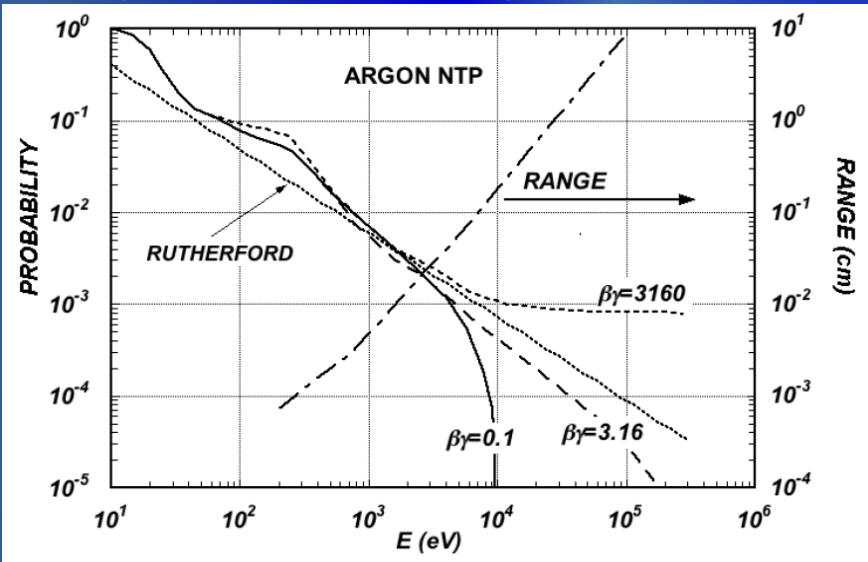
if E_δ is high enough ($E_\delta > E_i$)

Relevant Parameters
for gas detectors

Ionization energy	:	E_i	$\langle n_T \rangle = \frac{L \cdot \langle \frac{dE}{dx} \rangle_i}{W_i}$ [about 2-6 times n_p] [L: layer thickness]
Average energy/ion pair	:	W_i	
Average number of primary ion pairs [per cm]	:	n_p	
Average number of ion pairs [per cm]	:	n_T	

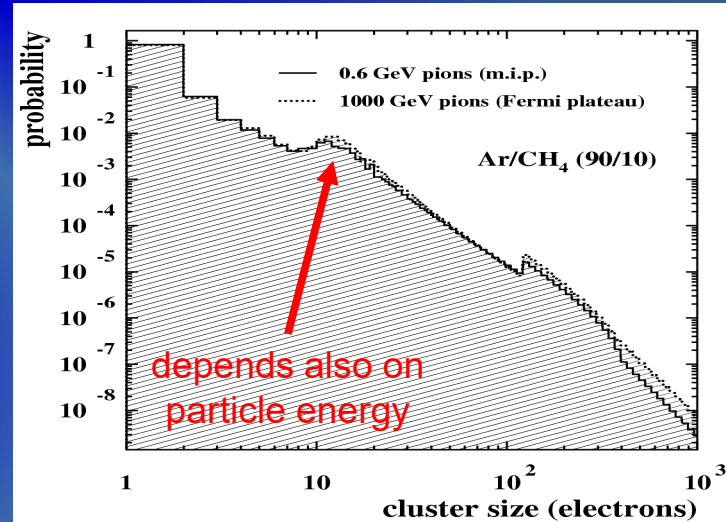
Differences
due to δ -electrons

About 0.6% of released electrons in Ar have > 1keV energy \rightarrow
 practical range is 70 μ m, contributing to coordinate meas. error



Total Ionization/Cluster Size Distribution:

Probabilities (%) to create N_{el} electrons
 (electrons are not evenly spaced,
 not even exponentially):



	N_{el}	Ar	He
single el. \rightarrow	1	65.6	76.6
multi el. cluster \rightarrow	2	15.0	12.5
	3	6.4	4.6
	4	3.5	2.0
	5	2.25	1.2
	6	1.55	0.75
	7	1.05	0.50
	8	0.81	0.36
	9	0.61	0.25
	10	0.49	0.19



less multi-electron clusters at Helium (better!)

Ionization Statistics: Importance of PAI Model

- Every ionization process is a **quantum mechanical transition** initiated by the Coulomb field of the particle and the field created by neighbouring polarizable atoms; the average energy losses are described by the **Bethe-Bloch formula with Sternheimer's density effect corrections**;
- The fluctuations caused by **Rutherford scattering** on quasi-free electrons follow a Landau distribution and **the influence of atomic shells is described by the photoabsorption ionization (PAI) model**, which allows simulation of each energy transfer, with relaxation cascades and simulation of delta-electrons;
- **Heed: a photo-absorption & ionization model:**

Energy loss fluctuations
2 GeV protons on an (only !) 5 cm thick Ar gas layer:

Core formulae PAI model

▶ Key: photo-absorption cross section $\sigma_y(E)$

$$\frac{\beta^2 \pi}{\alpha} \frac{d\sigma}{dE} = \frac{\sigma_y(E)}{E} \log \left(\frac{1}{\sqrt{(1-\beta^2 \epsilon_1)^2 + \beta^4 \epsilon_2^2}} \right) + \text{Relativistic rise}$$

$$\frac{1}{N \hbar c} \left(\beta^2 - \frac{\epsilon_1}{|\epsilon|^2} \right) \theta + \text{Черенков radiation}$$

$$\frac{\sigma_y(E)}{E} \log \left(\frac{2m_e c^2 \beta^2}{E} \right) + \text{Resonance region}$$

$$\frac{1}{E^2} \int_0^E \sigma_y(E_1) dE_1 \quad \text{Rutherford scattering}$$


With:

$$\epsilon_2(E) = \frac{N_e \hbar c}{EZ} \sigma_y(E)$$

$$\epsilon_1(E) = 1 + \frac{2}{\pi} P \int_0^{\infty} \frac{x \epsilon_2(x)}{x^2 - E^2} dx$$

$$\theta = \arg(1 - \epsilon_1 \beta^2 + i \epsilon_2 \beta^2) = \frac{\pi}{2} - \arctan \frac{1 - \epsilon_1 \beta^2}{\epsilon_2 \beta^2}$$

Heed



▶ PAI model or absorption of real photons:

Atom + $\pi^- \rightarrow \text{Ion}^{++} + \pi^- + e^-$ (photo-electric effect, real or virtual photon)
 Atom + $\gamma \rightarrow \text{Ion}^{++} + e^-$

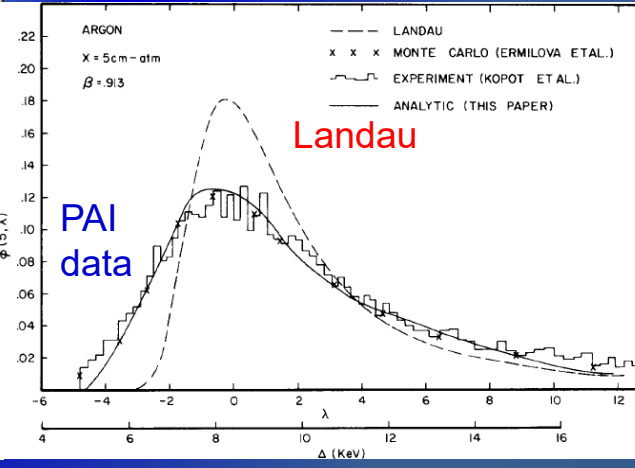
▶ Decay of excited states:

$\text{Ion}^{++} \rightarrow \text{Ion}^{++} + e^-$ (Auger)
 $\text{Ion}^{++} \rightarrow \text{Ion}^+ + \gamma$ (fluorescence)
 $\text{Ion}^{++} \rightarrow \text{Ion}^+$ (Coster-Kronig)

▶ Processing of electrons:

- ▶ below ionisation energy transport
- ▶ photo- & Auger-electrons (clusters, "delta-electrons"):

$e^- + \text{Atom} \rightarrow \text{Ion}^+ + 2 e^-$ (absorption of high-energy electrons)



- ✓ Importance of PAI model (all terms in formula are important):
- All electron orbitals (shells) participate:**
 - outer shells: frequent interactions, few electrons;
 - inner shells: few interactions, many electrons.

Transport of Electrons in Gases: Drift Velocity

Electron transport theory =

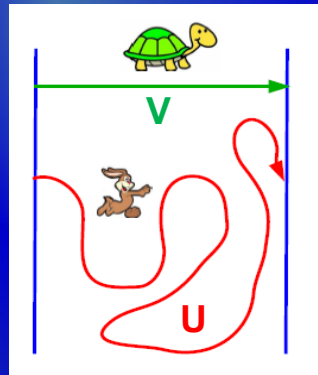
BALANCE BETWEEN ENERGY ACQUIRED FROM THE FIELD AND COLLISION LOSSES

Electrons are completely 'randomized' in each collision. The actual drift velocity v along the electric field is quite different from the average velocity u of the electrons i.e. \rightarrow about 100 times smaller.

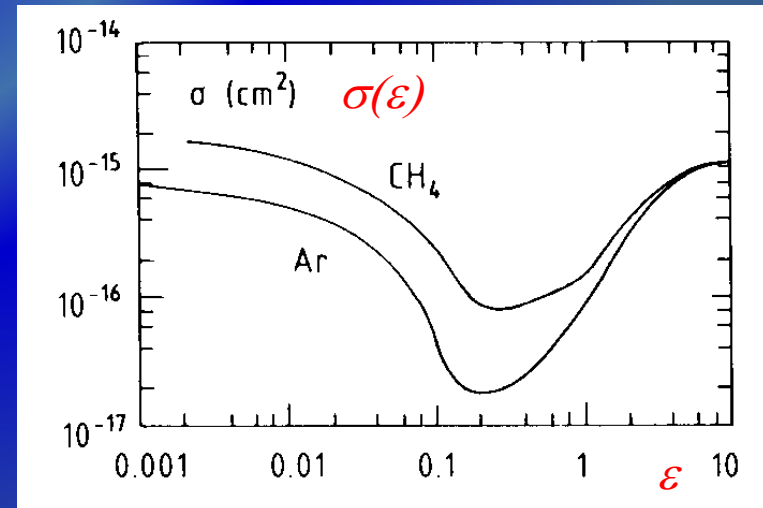
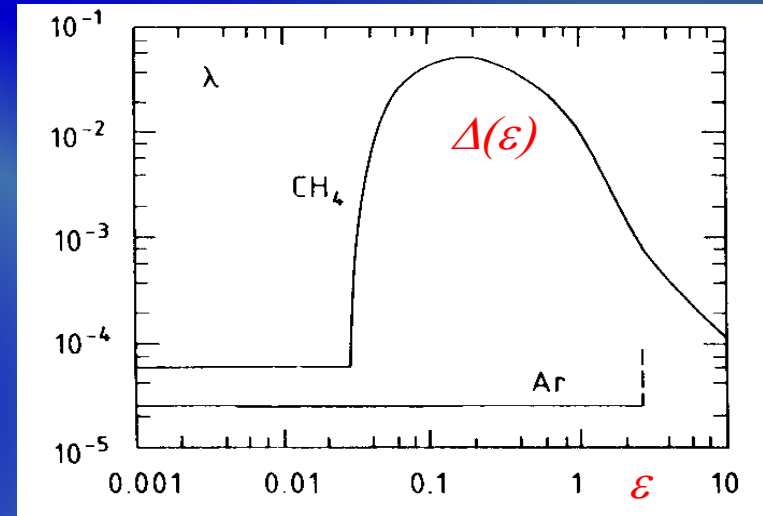
The velocities v and u are determined by the atomic cross section $\sigma(\epsilon)$ and the fractional energy loss $\Delta(\epsilon)$ per collision (N is the gas density i.e. number of gas atoms/m³, m is the electron mass.):

$$v = \sqrt{\frac{eE}{mN\sigma}} \sqrt{\frac{\Delta}{2}}$$

$$u = \sqrt{\frac{eE}{mN\sigma}} \sqrt{\frac{2}{\Delta}}$$



Because $\sigma(\epsilon)$ and $\Delta(\epsilon)$ show a strong dependence on the electron energy in the typical electric fields, the electron drift velocity v shows a strong and complex variation with the applied electric field.



Electron Drift in Presence of Electric and Magnetic Fields

Equation of motion of free charge carriers in presence of E and B fields:

$$m \frac{d\vec{v}}{dt} = e\vec{E} + e(\vec{v} \times \vec{B}) + \vec{Q}(t) \quad \text{where } \vec{Q}(t) \text{ stochastic force resulting from collisions}$$

Time averaged solutions with assumptions: $\vec{v}_D = \langle \vec{v} \rangle = \text{const.}$ $\langle \vec{Q}(t) \rangle = \frac{m}{\tau} \vec{v}_D$ friction force

$$\left\langle \frac{d\vec{v}}{dt} \right\rangle = 0 = e\vec{E} + e(\vec{v}_D \times \vec{B}) - \frac{m}{\tau} \vec{v}_D \quad \tau \text{ mean time between collisions}$$

$$\vec{v}_D = \frac{\mu |\vec{E}|}{1 + \omega^2 \tau^2} \left[\hat{E} + \omega \tau (\hat{E} \times \hat{B}) + \omega^2 \tau^2 (\hat{E} \cdot \hat{B}) \hat{B} \right]$$

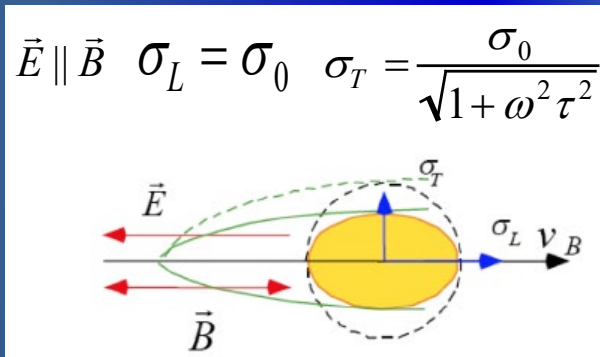
$$\mu = \frac{e\tau}{m}$$

mobility

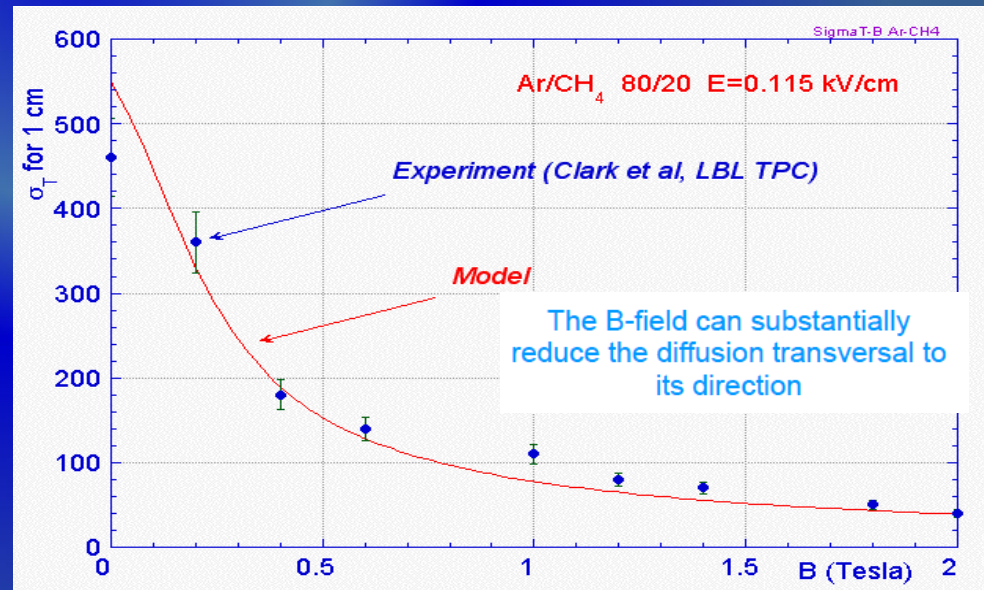
$$\omega = \frac{eB}{m}$$

cyclotron frequency

More precise calculation is available in Magboltz, which computes drift velocity by tracing electrons at the microscopic level through numerous collisions with gas molecules



This reduction is exploited to substantially improve spatial resolution in the Drift and TPC Chambers



E.g.: $\omega\tau \sim 20$ for Ar/CF₄/iC₄H₁₀ (95:3:2)

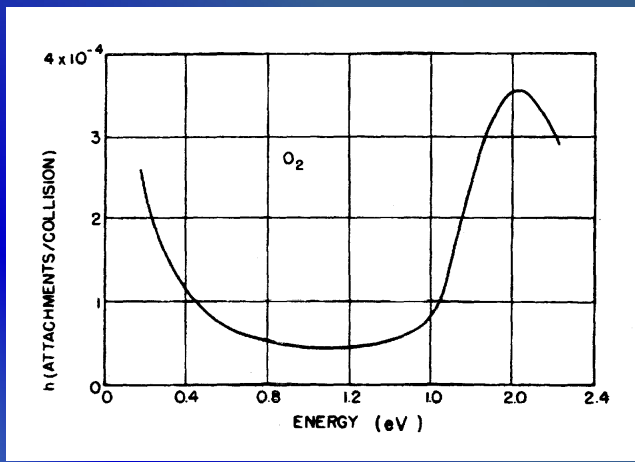
Electron Capture Losses for Electronegative Gases (Attachment)

- ✓ Some quencher gases can attach electrons
- ✓ Energy-momentum conservation: **3-body or dissociation**
- ✓ **The attachment cross section is energy-dependent**, therefore strongly depends on the gas composition and electric field

Examples:

- ▶ O_2 : mostly 3-body O_2^- and at higher ϵ 2-body dissociative;
- ▶ H_2O : $[H_2O]_n$ has positive electron affinity, H_2O probably not;
- ▶ CF_4 : mostly dissociative $F^- + CF_3$, $F + CF_3^-$ (below 10 eV);
- ▶ SF_6 : $SF_6^* < 0.1$ eV, $\sigma = 10^{-18}$ cm², then $F^- + SF_n^-$ (n=3, 4, 5)
- ▶ CS_2 : negative ion TPC;
- ▶ CO_2 : O^- , $[CO_2]_n^-$ but no CO_2^- (4 eV and 8.2 eV).

Attachmant coefficient of oxygen:

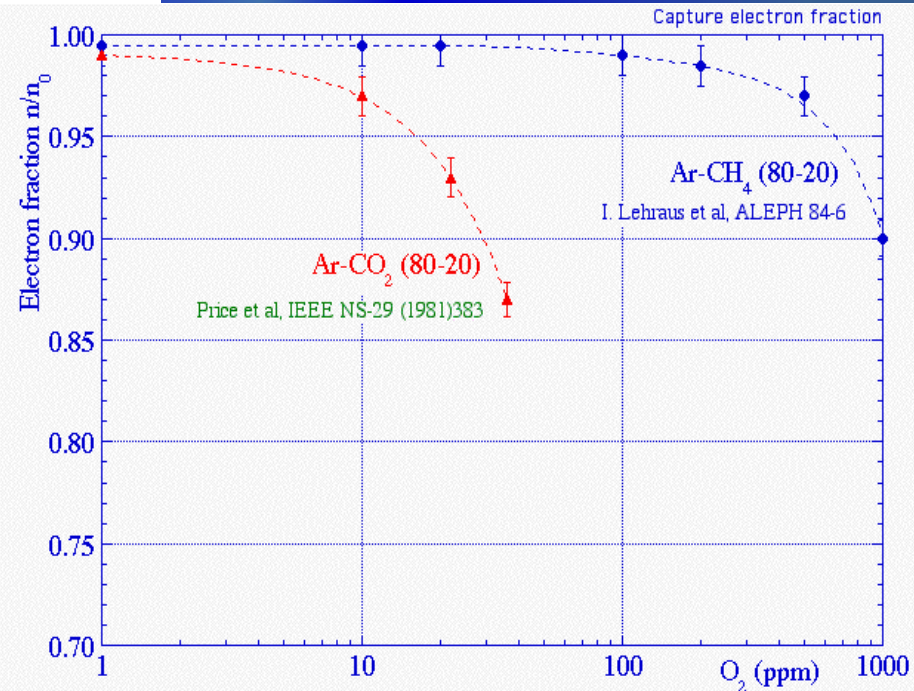
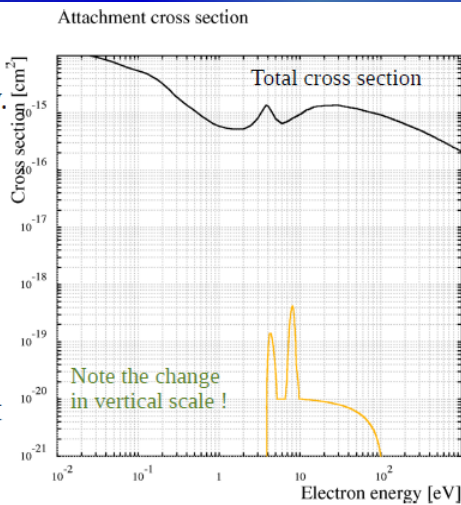


Electrons surviving after 20 cm drift (E = 200 V/cm):

Certain quenchers as CO2 can significantly enhance the effect of oxygen → large increase in attachment

- ▶ CO_2 has a tiny attachment cross section at low energy.
- ▶ The 4 eV peak is linked to a short-lived $^2\Pi_u$ shape resonance which decays $e^- CO_2 \rightarrow CO + O^-$;
- ▶ The 8.2 eV peak is thought to be a Feshbach resonance.

[A. Moradmand et al. (2013) 10.1103/PhysRevA.88.032703]



Transport of Ions in Gases: Drift and Diffusion

Signals in Wire Chambers, Micromegas are generated by ion movement

Drift velocity of ions

is almost linear function of E $v_D^{ion} = \mu^{ion} E$

Mobility: $\mu^{ion} = \frac{e\tau}{m}$ is

constant for given gas at fixed P and T, direct consequence of the fact that average energy of ion is unchanged up to very high E fields.

Diffusion of ions

IONS DIFFUSION (Einstein's law):

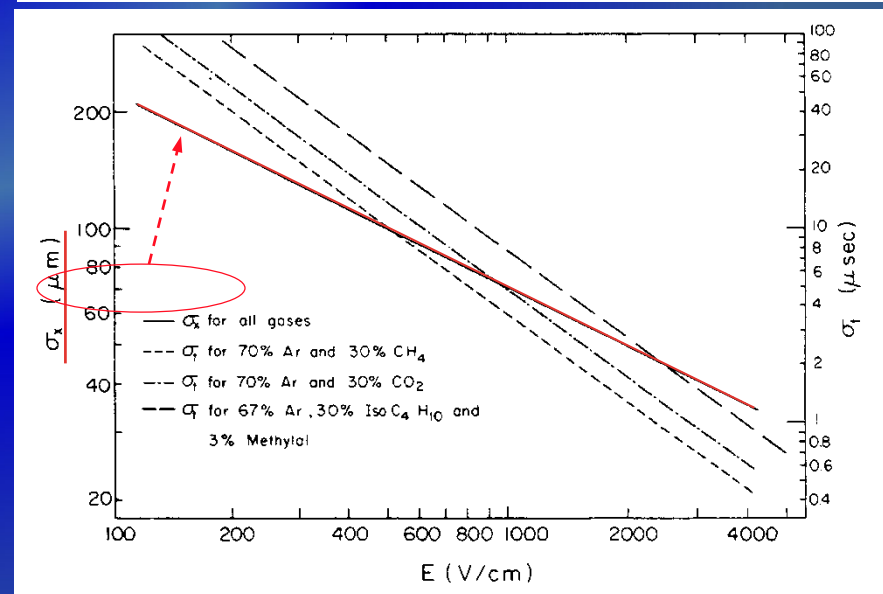
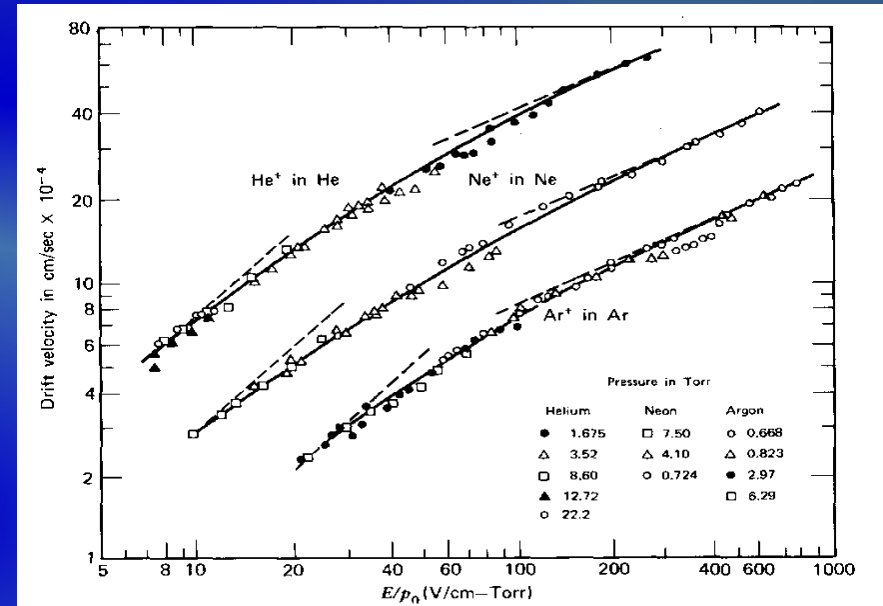
$$\frac{D}{\mu} = \frac{KT}{e}$$

$$\sigma_x = \sqrt{2Dt}$$

$$\sigma_x = \sqrt{\frac{2KT x}{e E}}$$

Linear diffusion is independent of the nature of ions and gas → thermal limit (same for all gases)

It has been historically assumed that, due to a very effective charge transfer mechanism, only ions with the lowest ionization potential survive after a short path in the mixture → NOT TRUE !!!



Transport of Ions in Gases: Drift and Diffusion

Recent experimental data suggests that the signal ions, in e.g. CO₂-quenched mixtures of Ar and Ne are **CO₂⁺ · (CO₂)_n cluster ions, and not CO₂⁺ or noble gas ions**

Principal reactions involving CO₂

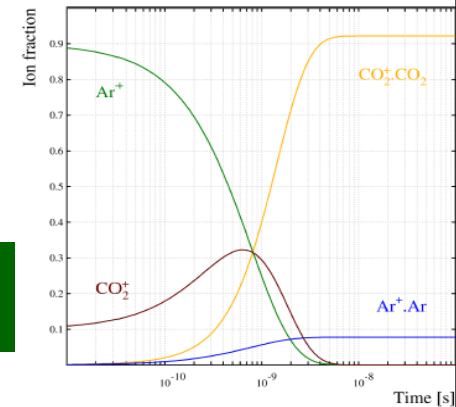
- ▶ Ar⁺: charge exchange, $\tau \approx 0.85$ ns
 - ▶ $\text{Ar}^+ + \text{CO}_2 \rightarrow \text{Ar} + \text{CO}_2^+$
- ▶ Ne⁺: charge transfer in 2-steps, $\tau \approx 8$ ns
 - ▶ $\text{Ne}^+ + \text{CO}_2 \rightarrow \text{Ne} + \text{CO}^+ + \text{O}$
 - ▶ $\text{CO}^+ + \text{CO}_2 \rightarrow \text{CO} + \text{CO}_2^+$

- ▶ CO₂: 3-body association, 7-20 ps
 - ▶ $\text{CO}_2^+ + 2\text{CO}_2 \rightarrow \text{CO}_2^+ \cdot \text{CO}_2 + \text{CO}_2$

*R. Veenhof, private communications
Y. Kalkan, JINST 10, 07, P07004 (2015)*

Reaction dynamics in Ar CO₂

- ▶ Reactions:
 - ▶ $\text{Ar}^+ + \text{CO}_2 \rightarrow \text{Ar} + \text{CO}_2^+$
 - ▶ $\text{CO}_2^+ + 2\text{CO}_2 \rightarrow \text{CO}_2^+ \cdot \text{CO}_2 + \text{CO}_2$
 - ▶ $\text{Ar}^+ + 2\text{Ar} \rightarrow \text{Ar}^+ \cdot \text{Ar} + \text{Ar}$
- ▶ Parameters:
 - ▶ $p = 1$ bar
 - ▶ mix: 90 % Ar + 10 % CO₂



Life cycle of CO₂⁺·(CO₂)_n

- ▶ CO₂⁺·CO₂ has a dissociation energy of 0.6 eV
 - ▶ far above thermal energies at 1 bar (35 meV);
 - ▶ it is a long-lived cluster – calculated lifetime = 5 ns.
[B.M. Smimov, “Cluster Ions and Van Der Waals Molecules,” CRC press]
- ▶ This is much longer than the formation time $\tau = 7$ -20 ps via 3-body association in 10 % CO₂ with Ar + CO₂ as “helpers”.
- ▶ Hence, any isolated CO₂⁺ rapidly binds again.
- ▶ CO₂⁺·(CO₂)_n probably lives shorter but will recombine. The cluster size n will therefore fluctuate at the ns time scale.

Summary ions

- ▶ Avalanches ionise the constituent gases, and the initial ions undergo a staggering sequence of reactions.
 - ▶ In Ar-CO₂ and Ne-CO₂ mixtures, the signal ions are CO₂⁺·(CO₂)_n clusters, which are slower than CO₂⁺;
 - ▶ water forms larger clusters, further reducing the mobility;
 - ▶ pure noble gases form dimers, Ar₂⁺, Ne₂⁺ which are faster than Ar⁺ and Ne⁺ due to resonant charge exchange;
 - ▶ Xe forms dimers, trimers and probably bigger objects;
 - ▶ alkanes combine to form heavier molecules.

Since the cluster ions are slower than the initial ions, the signals induced by ion motion in Micromegas or TPC might be altered (also lead to larger space-charge effect in gas volume)

Electric Fields: (nearly) Exact Boundary Element Method

, **neBEM** Field Solver (that solves the Poisson equation to obtain electric field throughout the device volume) is an integrated part of device simulation. One such Green function based solver (nearly exact Boundary Element Method), is integrated to GARFIELD since 2009.

Merits of neBEM:

- Analytic integration of influence of charge distributed over small rectangular / triangular boundary elements (new formulation). Very precise potential and electric field values are obtained for any 2D / 3D geometry.
- Competitively accurate w.r.t any other commercial FEM / BEM package.
- Primitive geometry modeling.
- Parallelized using OpenMP.
- Field maps and reduced order modeling crudely implemented.
- Preliminary implementation of space charge and charging up simulations.

<http://nebem.web.cern.ch/nebem>
(Supratik Mukhopadhyay, Nayana Majumdar)

Maintained and updated by SINP (independent release till 05 Mar 2019, version 1.9.04; Since 2019, released along with Garfield++)

Future projects for neBEM:

- Orders of magnitude improvement in speed is possible:
 - FMM / GMRES or similar algorithms.
 - Better parallelization (OpenMP, GPU)
 - Smaller data storage and faster flow.
- Improvements in geometry modeler, surface mesh generation, adaptive mesh.
- Space charge and charging up simulation to be improved significantly. Charge transport through dielectrics is another important area to be explored.
- Graphical user interface.

RD51-NOTE-2009-001

RD51 Note-2009-001

NIMA, vol. 566, issue 2, p489

neBEM: a Field Solver

Supratik Mukhopadhyay, Nayana Majumdar, Sudeb Bhattacharya

INO Section, Saha Institute of Nuclear Physics
1/AF, Sector 1, Bidhannagar, Kolkata 700064, WB, India
supratik.mukhopadhyay@saha.ac.in, nayana.majumdar@saha.ac.in,
sudeb.bhattacharya@saha.ac.in

Signal Formation in Detectors with Resistive Elements

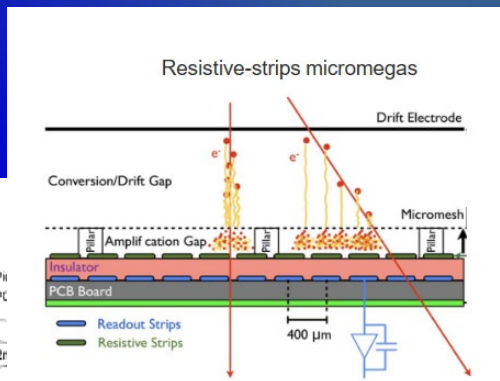
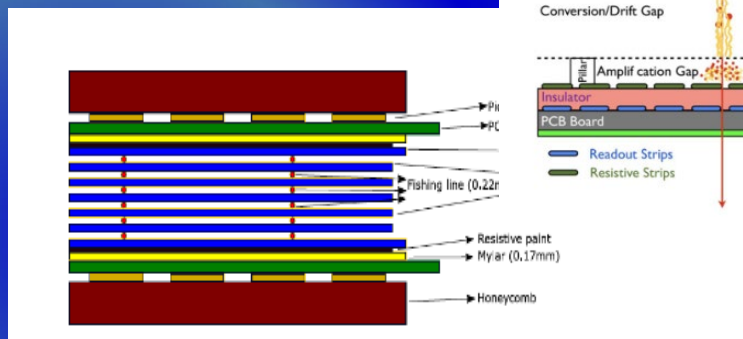
RD51 supports ongoing efforts on **interfacing between different modeling tools** – to address properly involved processes at the microscopic level - **extending present simulation framework to other gaseous & Si-detectors**

EP R&D SEMINAR, Signal formation in detectors with resistive elements by **Djunes Janssens**:

https://indico.cern.ch/event/1167590/contributions/4903447/attachments/2460899/4219187/EPSeminar_DjunesJanssens.pdf

Garfield++ and COMSOL to model the signal formation in detectors with resistive elements by applying an extended form of the Ramo-Shockley theorem

Gaseous (MPGD, RPC,..)



Solid State (Silicon, Diamond,..)

Ramo-Shockley theorem extension for conducting media

The time-dependent weighting potential is comprised of a static **prompt** and a dynamic **delayed** component:

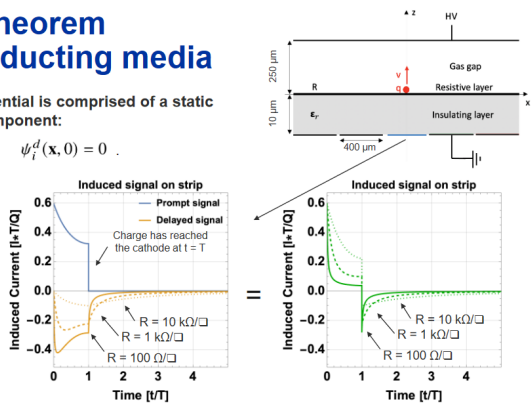
$$\psi_i(\mathbf{x}, t) \doteq \psi_i^p(\mathbf{x}) + \psi_i^d(\mathbf{x}, t) \quad \text{where} \quad \psi_i^d(\mathbf{x}, 0) = 0$$

The current induced by a point particle q is given by:

$$I_i(t) = -\frac{q}{V_w} \int_0^t dt' \mathbf{H}_i[\mathbf{x}_q(t'), t-t'] \cdot \dot{\mathbf{x}}_q(t')$$

$$\mathbf{H}_i(\mathbf{x}, t) \doteq -\nabla \frac{\partial \psi_i(\mathbf{x}, t)}{\partial t} = -\nabla \psi_i^p(\mathbf{x}) \delta(t) - \nabla \frac{\partial \psi_i^d(\mathbf{x}, t)}{\partial t} \theta(t)$$

Direct induction Reaction from resistive material



Examples of systems of which the weighting potential is **analytically obtainable** see W. Reigler, JINST 11 (2016) no 11, P11002. Further reading: W. Reigler, P. Windschhofer, Nucl. Instrum. Meth. A 980 (2020)

Signal formation in AC-Coupled LGAD

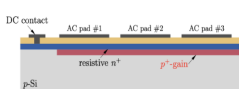
In collaboration with INFN Torino group of N. Cartiglia, we are currently looking at **simulating the currents induced in the AC-Coupled Low Gain Avalanche Diode (LGAD) geometry**.

When successfully benchmarked, it can be used

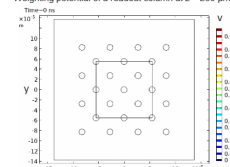
Diamond 3D Pixel Detector

A 3D geometry with thin columnar resistive electrodes orthogonal to the diamond surface, is expected to provide significantly better time resolution with respect to the extensively studied planar diamond sensors.

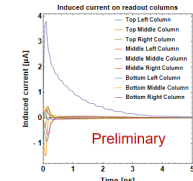
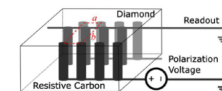
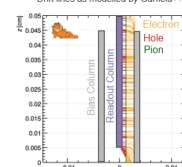
With the team of the INFN TimeSpot project, we are exploring the modelling of signal induction on the readout columns.



Weighting potential of a readout column at z = 250 μm.

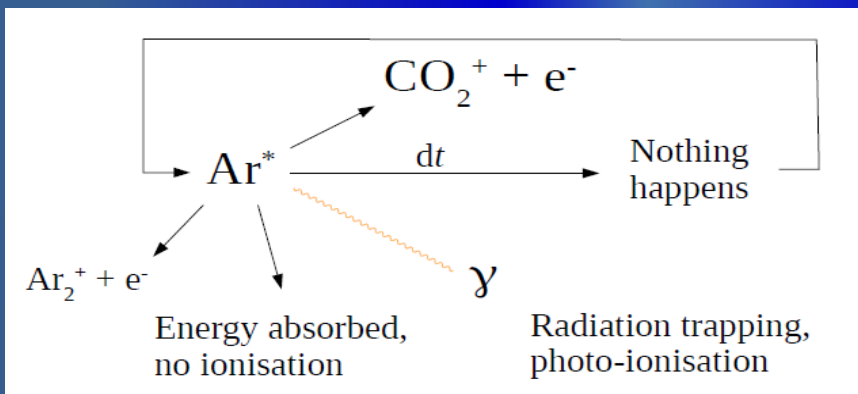


Drift lines as modelled by Garfield++



Ionization Cross Section: Penning Effects

- ✓ Additional ionizing energy transfer mechanisms due to the excited noble gas atoms, called collisional Penning energy transfers, occur when the excitation energy of a noble gas is higher than the ionization potential of an admixture gas.
- ✓ The energy transfer rate, probability that an excited atom ionizes a quenching agent, is a priori not known for a mixture but can be extracted from the fits of the experimental gas gain data using the Magboltz simulations
- ✓ For example, the impact of the Penning effect on gas gain is roughly a factor 10 in Ar-CO₂ mixtures and exceeding a factor of 100 in Ar-C₂H₂ mixtures

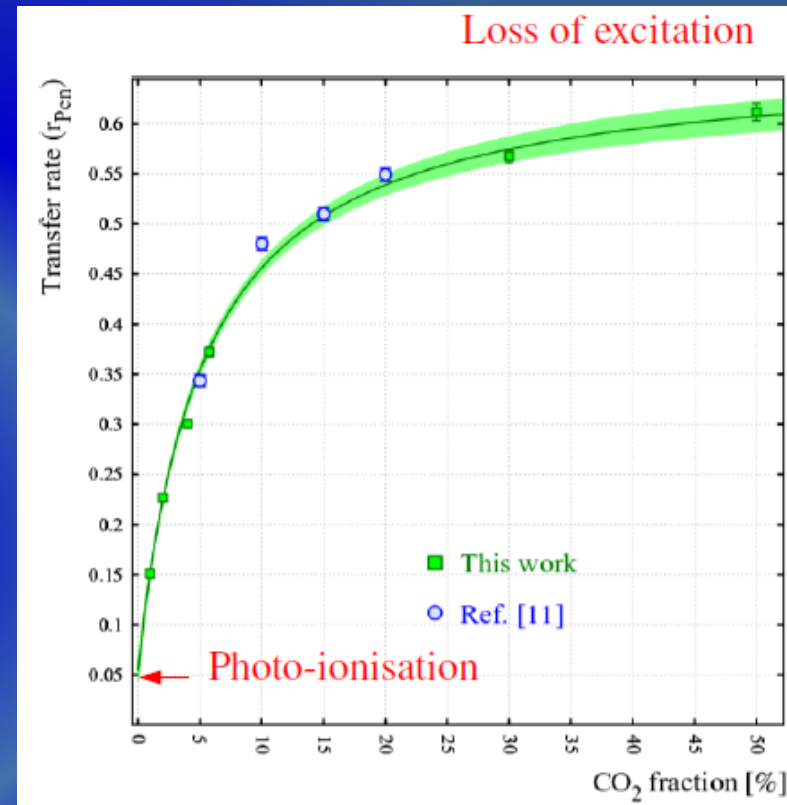


- ▶ The Penning transfer rate r_p is measured by finding the fraction of the excitations to be added to α so that the measured gain is reproduced:

$$G = \exp \int \alpha \left(1 + r_p \frac{v_{exc}}{v_{ion}} \right)$$

- ▶ r_p depends on gas choice, quencher fraction and density.

Ar/CO₂ transfer rates:



- ✓ Collisional energy transfer mostly scales linearly with the gas pressure and the fraction of quenching gas in the mixture, while ionization by photons emitted from excitations is independent of the medium.
- ✓ In addition, collisional Penning transfers of some higher excited states can occur before they decay at atmospheric pressure and are not restricted to metastable states of the excited noble gas.

Multi-Wire Proportional Chamber (MWPC): Wire Displacements

*Resolution of MWPCs limited by wire spacing
better resolution \rightarrow shorter wire spacing \rightarrow more (and more) wires...*

✓ Small wire displacements reduce field quality

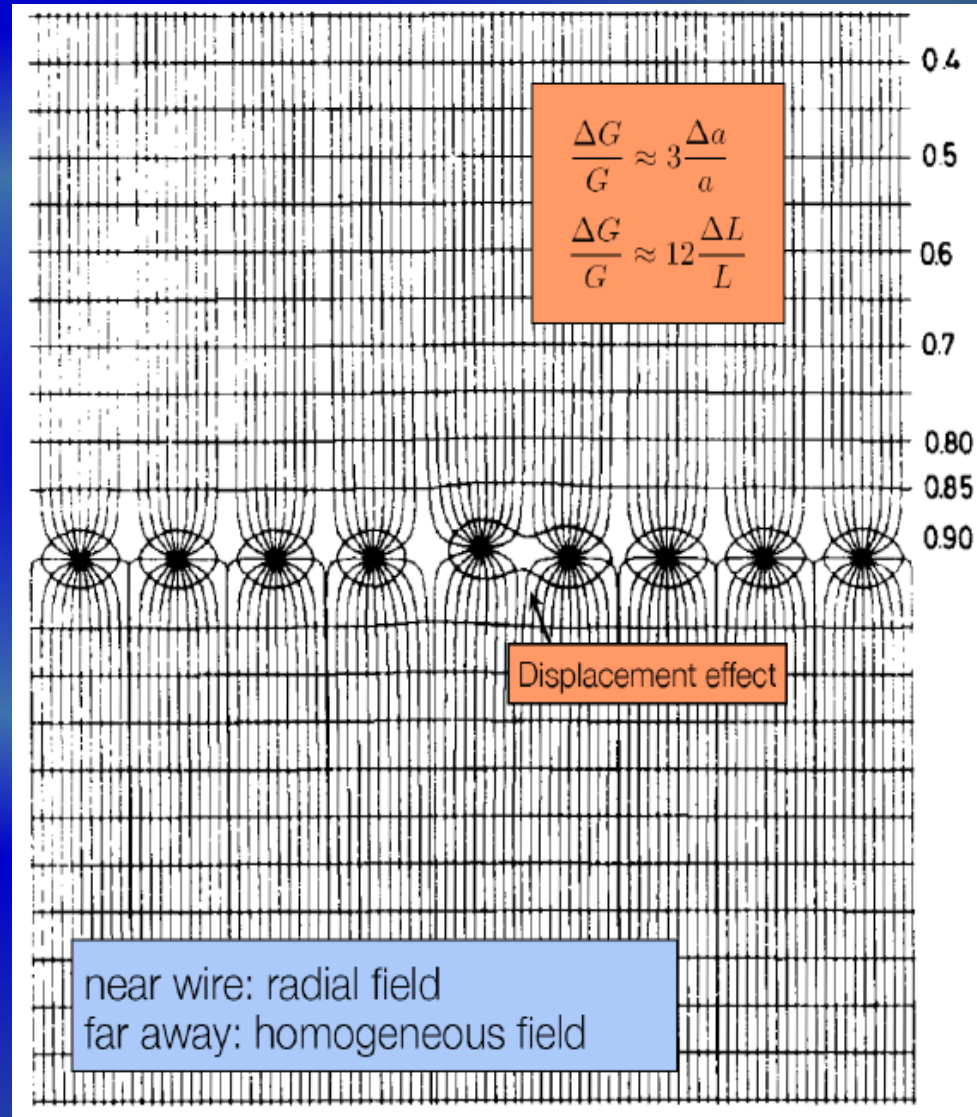
Table 35.1: Maximum tension T_M and stable unsupported length L_M for tungsten wires with spacing s , operated at $V_0 = 5$ kV. No safety factor is included.

Wire diameter (μm)	T_M (newton)	s (mm)	L_M (cm)
10	0.16	1	25
20	0.65	2	85

✓ Need high mechanical precision both for geometry and wire tension ... (electrostatic and gravitation, wire sag ...)

✓ Several simplifying assumptions are made in analytical calculations: electrostatic force acting on the wire does not change during wire movements, or varies linearly with the displacement, the wire shape is parabolic; only one wire moves at a time.

✓ The advantage of numerical integrations using Garfield++ program is to simulate the collective movement of all wires, which are difficult analytically, and to consider all forces acting on a wire: forces between anode wire and other electrodes (wires, cathode) & gravitational force



1968: Multi – Wire Proportional Chamber (MWPC)

NUCLEAR INSTRUMENTS AND METHODS 62 (1968) 262–268; © NORTH-HOLLAND PUBLISHING CO.

THE USE OF MULTIWIRE PROPORTIONAL COUNTERS TO SELECT AND LOCALIZE CHARGED PARTICLES

G. CHARPAK, R. BOUCLIER, T. BRESSANI, J. FAVIER and Č. ZUPANČIČ

CERN, Geneva, Switzerland

Received 27 February 1968

Properties of chambers made of planes of independent wires placed between two plane electrodes have been investigated. A direct voltage is applied to the wires. It has been checked that each wire works as an independent proportional counter down to separations of 0.1 cm between wires.

Counting rates of 10^6 /wire are easily reached; time resolutions

of the order of 100 nsec have been obtained in some gases; it is possible to measure the position of the tracks between the wires using the time delay of the pulses; energy resolution comparable to the one obtained with the best cylindrical chambers is observed; the chambers operate in strong magnetic fields.

1. Introduction

Proportional counters with electrodes consisting of many parallel wires connected in parallel have been used for some years, for special applications. We have investigated the properties of chambers made of planes of independent wires placed between two plane electrodes. Our observations show that such chambers offer properties that can make them more advantageous than wire chambers or scintillation hodoscopes for many applications.

2. Construction

Wires of stainless steel, 4×10^{-3} cm in diameter, are stretched between two planes of stainless-steel mesh, made from wires of 5×10^{-3} cm diameter, 5×10^{-2} cm apart. The distance between the mesh and the wires is 0.75 cm. We studied the properties of chambers with wire separation $a = 0.1, 0.2, 0.3$ and 1.0 cm. A strip of metal placed at 0.1 cm from the wires, at the same potential (fig. 1), plays the same role as the guard rings

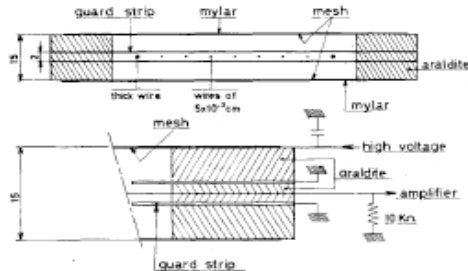


Fig. 1. Some details of the construction of the multiwire chambers.

A copper shield protects the wires at their output from the chamber and contains the solid state amplifiers.

G. Charpak et al., NIMA62 (1968) 262

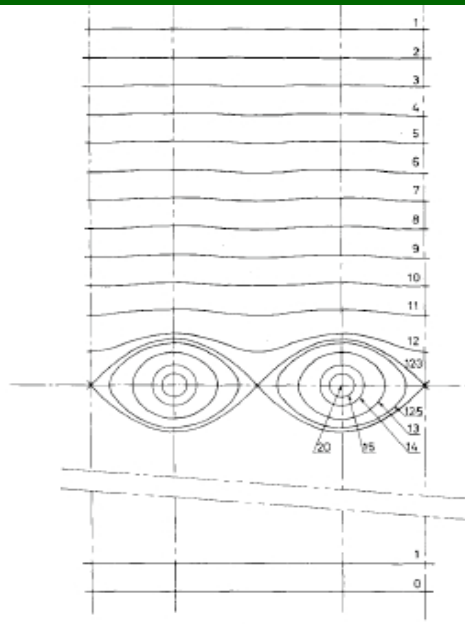
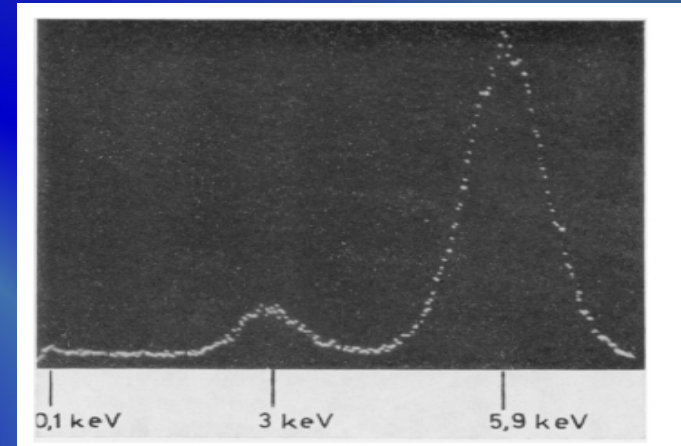
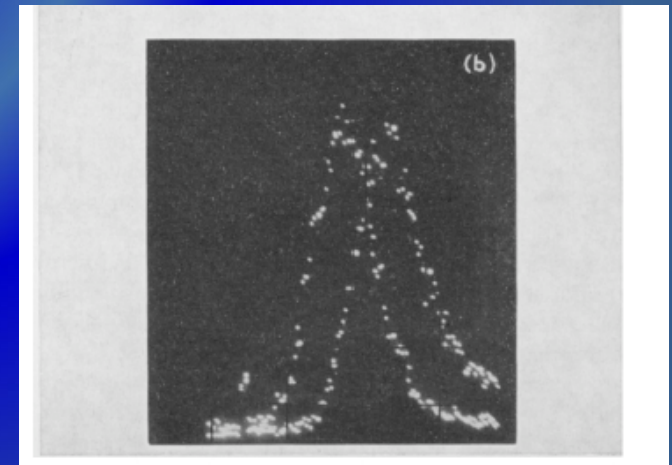


Fig. 2. Equipotentials in a chamber. Wires of 4×10^{-3} cm diameter, 0.3 cm separation, and 1.5 cm total thickness. 20 V applied between the wires and the external mesh. Results from an analogic method.

ENERGY RESOLUTION ON 5.9 KeV:



DEPENDENCE OF COLLECTION TIME FROM TRACK'S DISTANCE:



DRIFT CHAMBERS

The Evolution of Drift Chambers and Future e+e- Colliders

past			present		
SPEAR	MARK2	Drift Chamber	PEP	MARK2	Drift Chamber
	MARK3	Drift Chamber		PEP-4	TPC
DORIS	PLUTO	MWPC		MAC	Drift Chamber
	ARGUS	Drift Chamber		HRS	Drift Chamber
CESR	CLEO1,2,3	Drift Chamber	DELCO	MWPC	
VEPP2/4M	CMD-2	Drift Chamber	BEPC	BES1,2	Drift Chamber
	KEDR	Drift Chamber	LEP	ALEPH	TPC
	NSD	Drift Chamber		DELPHI	TPC
PETRA	CELLO	MWPC + Drift Ch.		L3	Si + TEC
	JADE	Drift Chamber	OPAL	Drift Chamber	
	PLUTO	MWPC	SLC	MARK2	Drift Chamber
	MARK-J	TEC + Drift Ch.		SLD	Drift Chamber
	TASSO	MWPC + Drift Ch.	DAPHNE	KLOE	Drift Chamber
TRISTAN	AMY	Drift Chamber	PEP2	BaBar	Drift Chamber
	VENUS	Drift Chamber	KEKB	Belle	Drift Chamber
	TOPAZ	TPC			

future		
ILC	ILD	TPC
	SiD	Si
CLIC	CLIC	Si
	CLD	Si
FCC-ee	IDEA	Drift Chamber
	Baseline	TPC + Si
CEPC	IDEA	Drift Chamber
SCTF	BINP	Drift Chamber
STCF	HIEPA	Drift Chamber

Lesson #1 - from "open" to "closed" cell

- close
- close
- the tra
- squar
- small
- ... but
- portion
- envelo
- small
- use of
- contrib
- some

Lesson #3 – small cells and He gas

- He radiation length 50× longer than Ar
- slower drift velocity implies smaller Lorenz angle for a given B-field
- He has a smaller cross section for low energy photons than Ar
- small size cells limit the electron diffusion contribution to spatial resolution
- small size cells provide high granularity (improving occupancy) and allow for a larger number of hits per track, improving spatial resolution
- portions of active volume not sampled between the cylindrical envelope of axial wires and the hyperboloid envelope of stereo wires
- accumulation of trapped electrons and ions in a region of very low field
- longitudinal gain variation at boundaries between axial and stereo layers
- spatial resolution dominated by ionization statistics for short drift distances
- adding more quencher to compensate, mitigates the advantage of He

Lesson #4 – full stereo configuration

- no gap
- electro
- consta
- larger
- maxim
- two st
- ... but
- open t
- from th
- consta
- z (radi
- consta

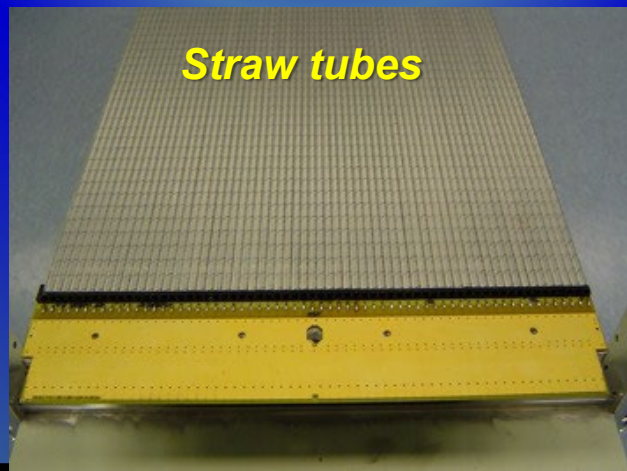
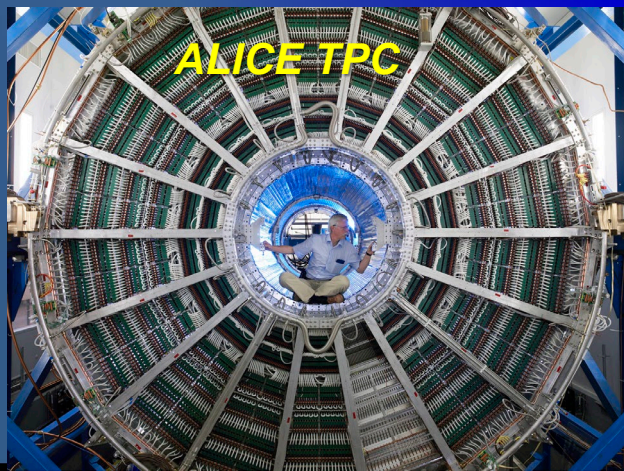
Lesson #5 – summary

- the configuration offering the best performance in terms of **momentum resolution** is one with **small, single sense wire closed cells**, arranged in **contiguous layers of opposite sign stereo angles**, obtained with **constant stereo angle transverse projection**
- the gas mixture is based on helium with a small amount of quencher (**90% He / 10% iC₄H₁₀, KLOE gas**) which, besides low multiple scattering contribution, allows for the exploitation of the **cluster timing** technique, for improved spatial resolution, and of the **cluster counting** technique, for excellent particle identification
- suggested wire material is **Ag coated Al**, but lighter materials are under scrutiny (like **metal coated carbon monofilaments**)

An ultra-light drift chamber (**IDEA concept**) targetted for **FCC-ee** and **CePC (100 km)** was inspired by **DAFNE KLOE Wire Chamber** and by more recent version of it for **MEG2** experiment

Original Gaseous Detectors in LHC Experiments

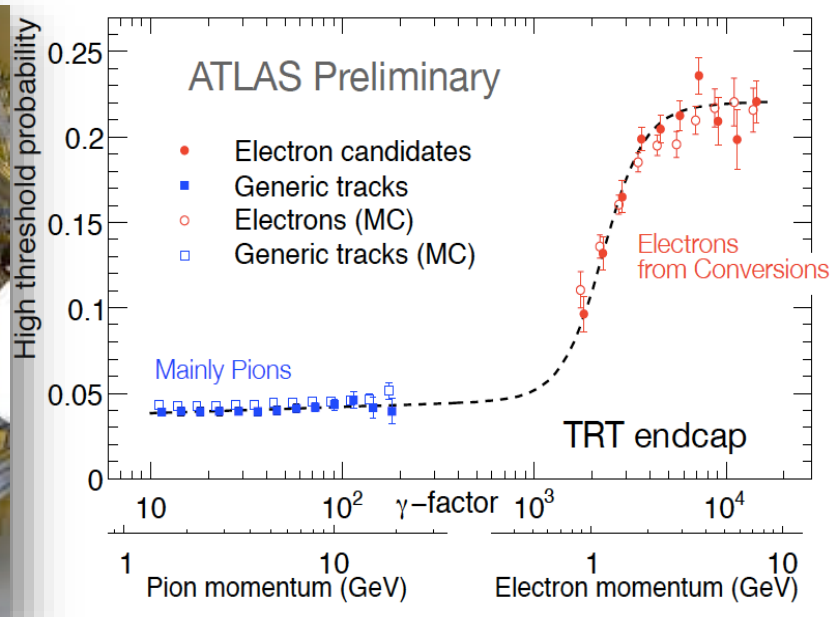
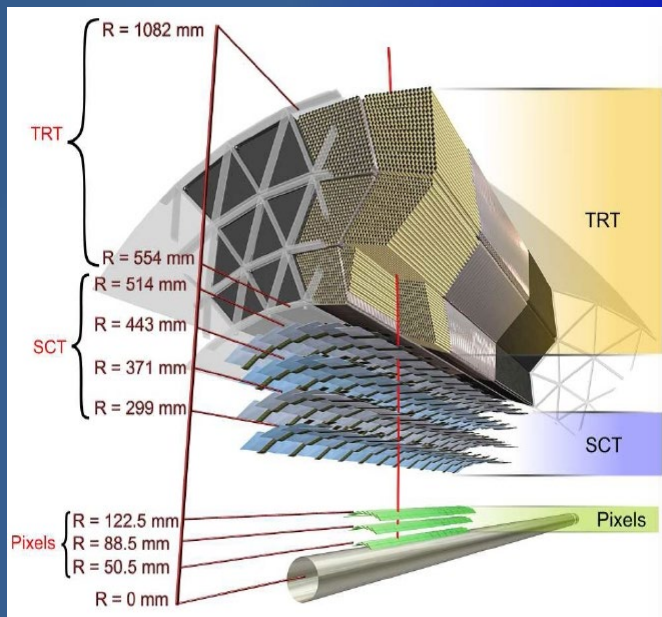
	Vertex	Inner Tracker	PID/ photo- detector	EM CALO	HAD CALO	MUON Track	MUON Trigger
ATLAS	-	TRD (straws)	-	-	-	MDT (drift tubes), CSC	RPC, TGC (thin gap chambers)
CMS	-	-	-	-	-	Drift tubes, CSC	RPC, CSC
TOTEM	-	GEM	-	-	-	-	-
LHCb	-	Straw Tubes	-	-	-	MWPC	MWPC, GEM
ALICE	-	TPC (MWPC)	TOF (MRPC), HPMID (RICH- pad chamber), TRD (MWPC)	-	-	Muon pad chambers	RPC



Gaseous Tracking @ LHC Experiments

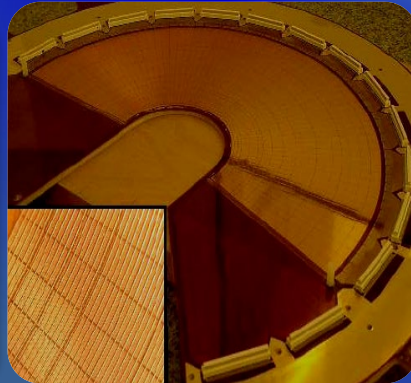
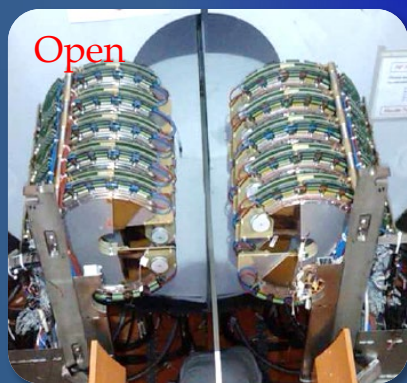
- ✓ Straw tubes (single-wire proportional counters) with xenon-based gas mixture
- ✓ 4 mm in diameter, equipped with a 30 μm diameter gold-plated W-Re wire

ATLAS TRT



- ✓ Stable operation at very high rates up to 12 MHz/cm²
- ✓ Achieved spatial (time) resolution: 135 μm (7 ns) at high intensity $2 \cdot 10^8 \text{ s}^{-1}$

**CMS/TOTEM
GEM**



Muon Detectors: CMS Cathode Strip Chambers (CSC)

Muon detectors **are tracking detectors** (e.g. wire-based tubes):

→ they form the outer shell of the (LHC) detectors

→ they are **not only sensitive to muons** (but to all charged particles)!

→ just by “definition”: if a particle has reached the muon detector (it's considered to be a muon); all other particles should have been absorbed in the calorimeters

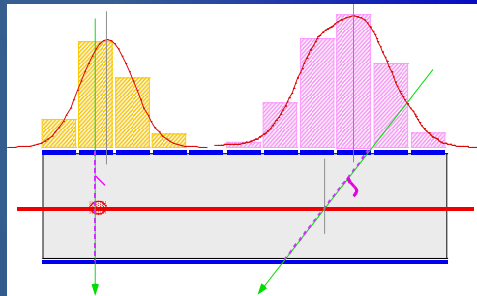
Challenge for muon detectors:

- large surface to cover (outer shell); keep mechanical positioning stable over time
- also good knowledge of (inhomogeneous) magnetic field

CMS CSC: precise measurement of the second coordinate by interpolation of the signal induced on pads.

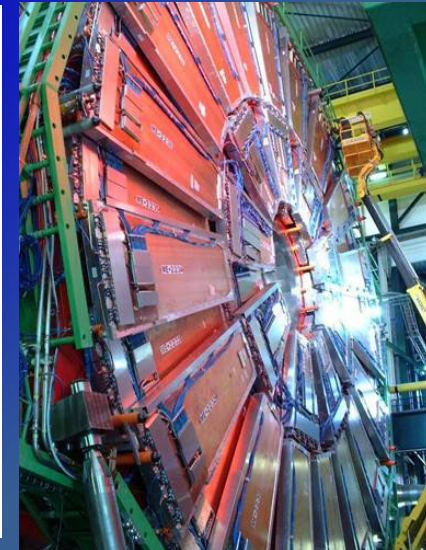
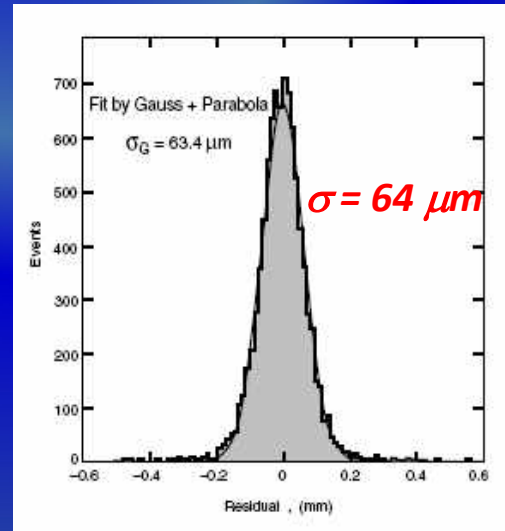
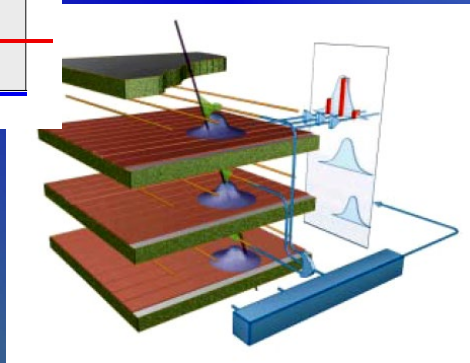
Closely spaced wires makes CSC fast detector.

CMS CSC



Center of gravity of induced signal method.

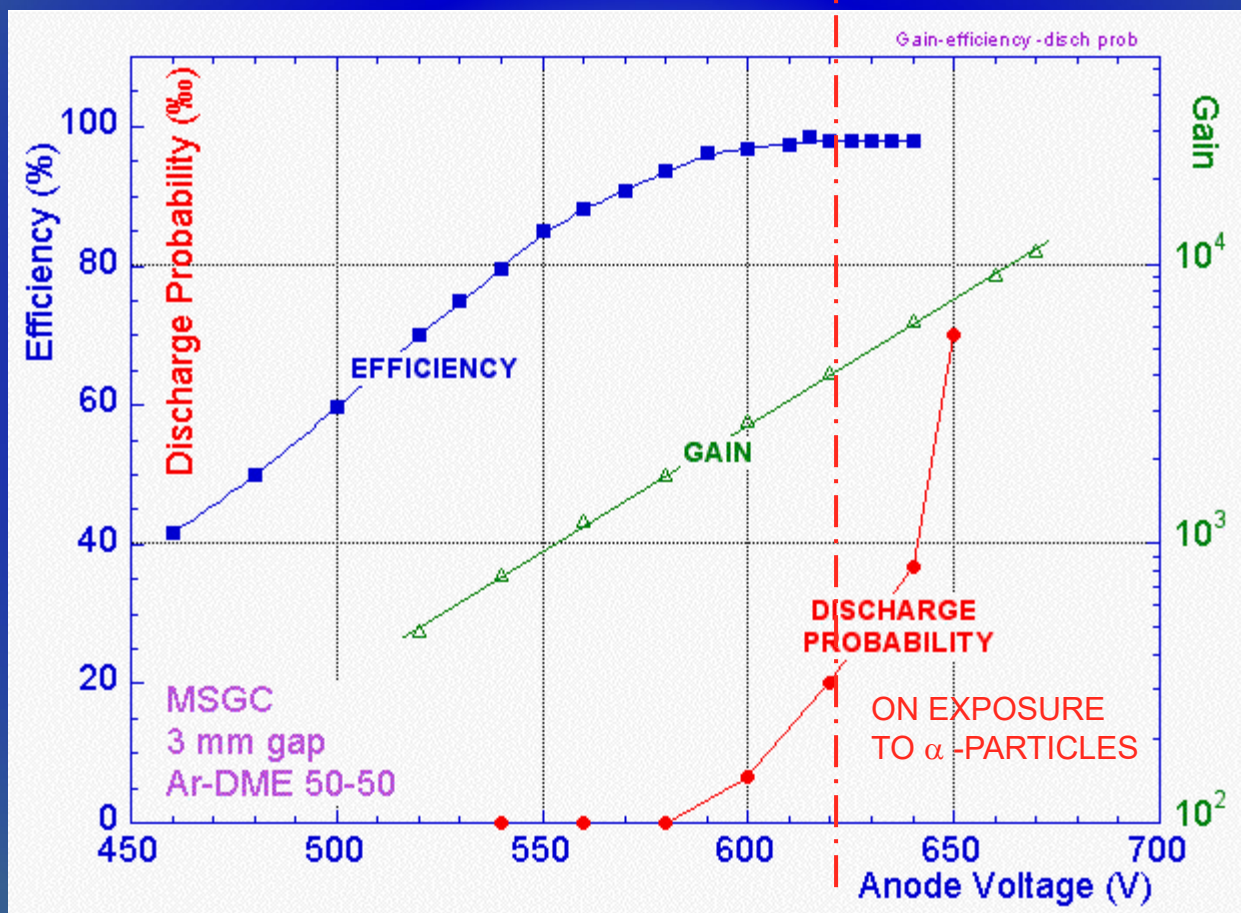
Space resolution



Micro-Strip Gas Chamber (MSGC): Discharge Problems

For efficient detection of minimum ionizing tracks a gain ~ 5000 is needed:

- No discharges with X-rays and electrons;
- Discharge probability is large \sim many per min (heavy ionizing particles)

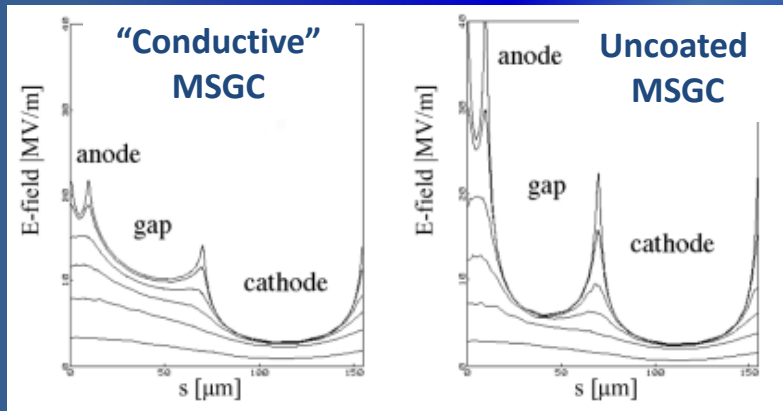


Induced discharges are intrinsic property of all single stage MPGDs in hadronic beams (MSGC turned out to be prone to irreversible damages)

Micro-Strip Gas Chamber (MSGC): Discharge Problems

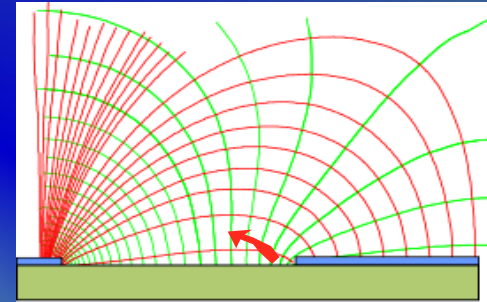
Major processes leading at high rates to MSGC operating instabilities:

- ✓ Substrate charging-up and time-dependent modification of the E field
→ slightly conductive support

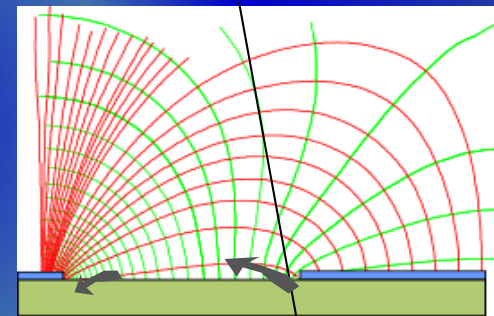


- ✓ Deposition of polymers (aging)
→ validation of gases, materials, gas systems
- ✓ Discharges under exposure to highly ionizing particles
→ multistage amplification, resistive anodes

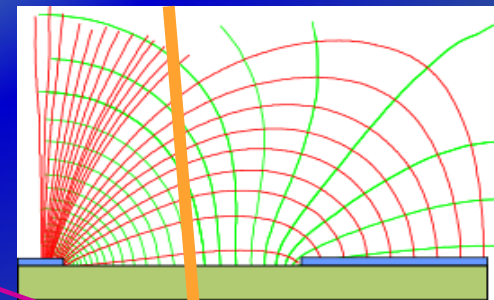
FIELD EMISSION FROM CATHODE EDGE



CHARGE PRE-AMPLIFICATION FOR IONIZATION RELEASED IN HIGH FIELD CLOSE TO CATHODE



VERY HIGH IONIZATION RELEASE FROM HEAVILY IONIZING PARTICLES



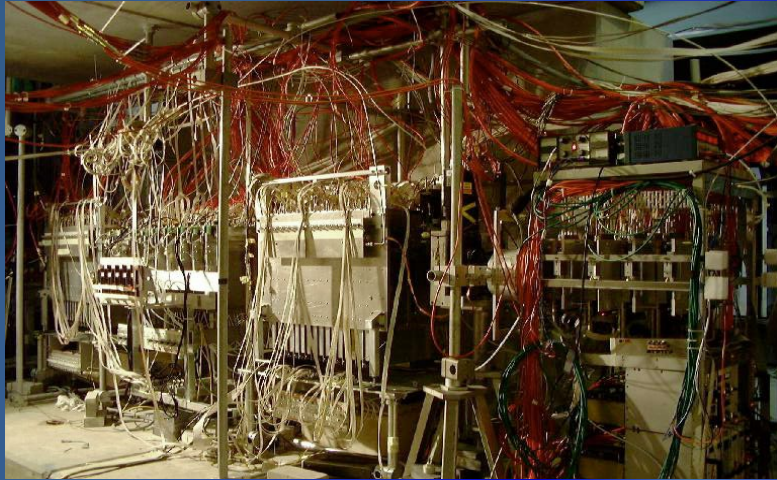
High Fields

Small Gap

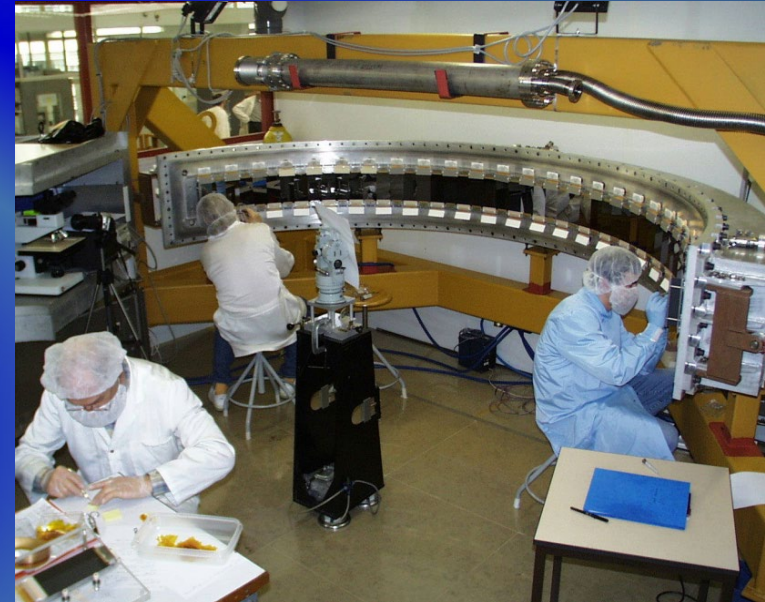
Discharge

Valid for all micro-pattern detectors
- Law of Nature!!!

MSGC In Experiments



Telescope of 32 MSGCs
tested at PSI in Nov99 (CMS Milestone)



HERA-B Inner Tracker

MSGC-GEM detectors

$R_{min} \sim 6 \text{ cm}$

$\Rightarrow 10^6 \text{ particles/cm}^2 \text{ s}$

300 μm pitch

184 chambers: max $25 \times 25 \text{ cm}^2$

$\sim 10 \text{ m}^2$; 140,000 channels

The D20 diffractometer MSGC
is working since Sept 2000

1D localisation

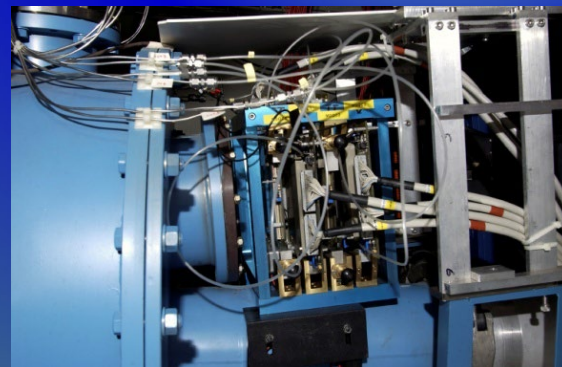
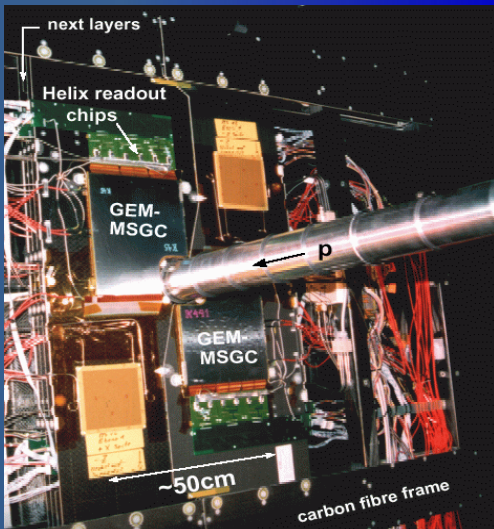
48 MSGC plates (8 cm x 15 cm)

Substrate: Schott S8900

Angular coverage : $160^\circ \times 5,8^\circ$

Position resolution : 2.57 mm ($0,1^\circ$)

5 cm gap; 1.2 bar CF_4 + 2.8 bars 3He



DIRAC

4 planes MSGC-GEM

Planes $10 \times 10 \text{ cm}^2$

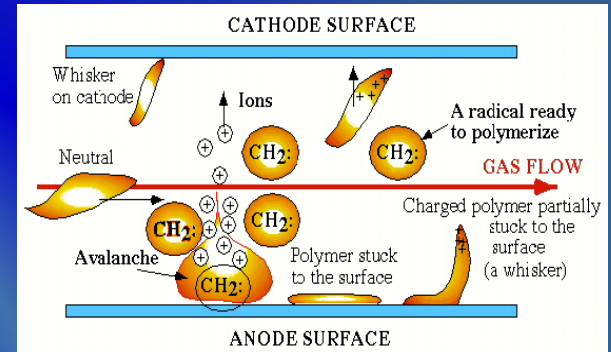
Aging Phenomena in Wire Chambers

Avalanche formation close to wire can be considered as a micro plasma discharge ...and plasma chemistry not well understood in general:

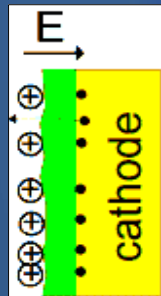
black magic...

Whereas most ionization processes require electron energies > 10 eV, the breaking of chemical bonds and formation of free radicals requires $\sim 3-4$ eV

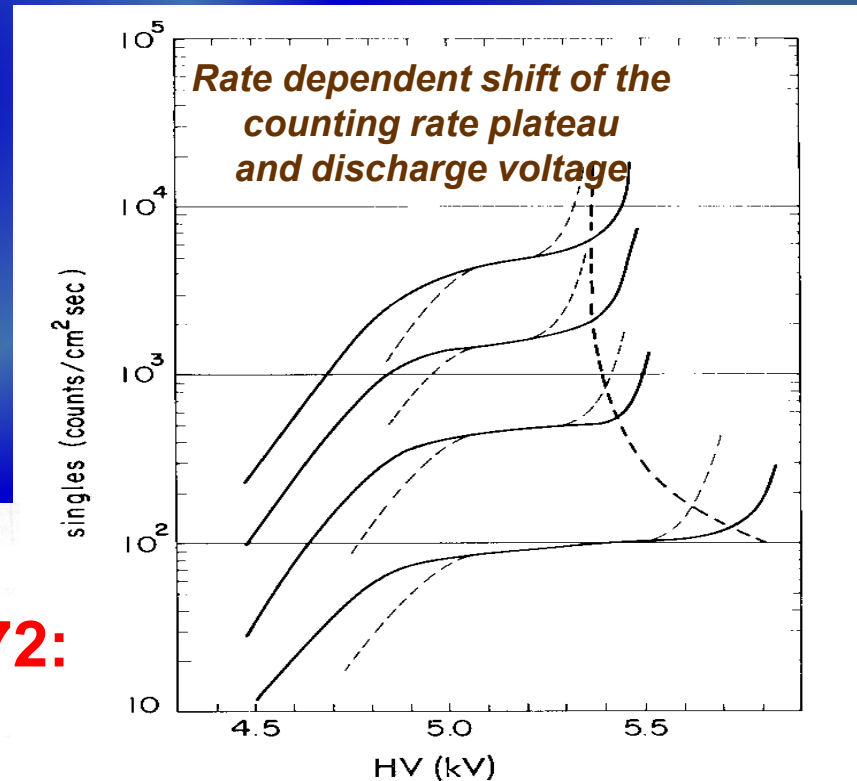
- ✓ dissociation of detector gas and pollutants
- ✓ formation of highly active radicals (many expected to have large dipole moments)
- ✓ polymerization of organic quenchers
- ✓ insulating deposits on anodes and cathodes



Anode: increase of wire diameter reduced and variable E-field variable gain and energy resolution



Cathode: ions on top of insulating layer cannot recombine built-up of strong E-field across insulating electron field emission and microdischarges (Malter Effect)



1972:

NUCLEAR INSTRUMENTS AND METHODS 99 (1972) 279-284; © NORTH-HOLLAND PUBLISHING CO.

TIME DEGENERACY OF MULTIWIRE PROPORTIONAL CHAMBERS

G. CHARPAK, H. G. FISHER, C. R. GRUHN, A. MINTEN, F. SAULI and G. PLCH

CERN, Geneva, Switzerland

and

G. FLÜGGE

II. Institut für Experimentalphysik, Hamburg, Germany

Received 28 May 1971

The deterioration with time of multiwire proportional chambers using isobutane as one component of the gas mixture is studied. It is shown that by addition of methylal among others, a long

lifetime can be obtained without changing the properties of the gas mixture. Irradiation tests of $5 \times 10^{10}/\text{cm}^2$ have not shown any alteration in the chamber performance.

Aging Phenomena in Wire Chambers: 1st Workshop (1986)

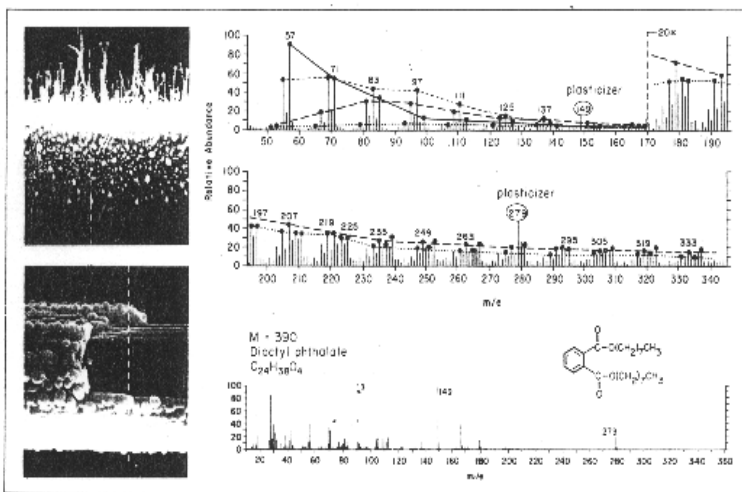
First systematic attempts to summarize aging results and to provide remedies minimizing wire chamber aging

Proceedings of the Workshop on Radiation Damage to Wire Chambers

1986:

Lawrence Berkeley Laboratory, Berkeley, California

January 16-17, 1986



April 1986

Lawrence Berkeley Laboratory
University of California
Berkeley, California 94720

Nuclear Instruments and Methods in Physics Research A252 (1986) 547-563
North-Holland, Amsterdam

547

REVIEW OF WIRE CHAMBER AGING *

J. VA'VRA

Stanford Linear Accelerator Center, Stanford University, Stanford, California 04305, USA

This paper makes an overview of the wire chamber aging problems as a function of various chamber design parameters. It emphasizes the chemistry point of view and many examples are drawn from the plasma chemistry field as a guidance for a possible effort in the wire chamber field. The paper emphasizes the necessity of tuning of variables, the importance of purity of the wire chamber environment as well as it provides a practical list of presently known recommendations. In addition, several models of the wire chamber aging are qualitatively discussed. The paper is based on a summary talk given at the Wire Chamber Aging Workshop held at LBL, Berkeley on January 16-17, 1986. Presented also at Wire Chamber Conference, Vienna, February 25-28, 1986.

436

Nuclear Instruments and Methods in Physics Research A300 (1991) 436-479
North-Holland

Wire chamber aging *

John A. Kadyk

Lawrence Berkeley Laboratory, 1 Cyclotron Road, Berkeley, CA 94720, USA

Received 27 June 1990

An overview of wire chamber aging is presented. A history of wire aging studies and the manifestations of wire aging are reviewed. Fundamental chemical principles relating to wire chamber operation are presented, and the dependences of wire aging on certain wire chamber operating parameters are discussed. Aging results from experimental detectors and laboratory experiments are summarized. Techniques for analysis of wire deposits and compositions of such deposits are discussed. Some effects of wire material and gas additives on wire aging are interpreted in chemical terms. A chemical model of wire aging is developed, and similarities of wire chamber plasmas to low-pressure rf-discharge plasmas are suggested. Procedures recommended for reducing wire aging effects are summarized.

**Harmful are: halogen or halocarbons, silicon compounds, oil, fats ...
CO₂ helps with water, and alcohol admixtures**



Aging Phenomena in Gaseous Detectors: 2nd Workshop (2001)

Summary and Outlook of the International Workshop on Aging Phenomena in Gaseous Detectors (DESY, Hamburg, October 2001)

M. Titov, M. Hohlmann, C. Padilla, and N. Tesch

arXiv:physics/0403055 v1 9 March 2004

RADIATION DAMAGE AND LONG-TERM AGING IN GAS DETECTORS¹

MAXIM TITOV

Institute of Physics, Albert-Ludwigs University of Freiburg, Hermann-Herder Str. 3, Freiburg, D79104, Germany and

Institute of Theoretical and Experimental Physics (ITEP), B. Chermushkinskaya, 25, Moscow, 117259, Russia

✓ The **HERA-B Experiment** was the first high-rate experiment, which addressed **SYSTEMATICALLY** aging phenomena in gas detectors, followed later by ALL LHC experiments

✓ Many **ORIGINAL PROBLEMS** in HIGH RATE GAS DETECTORS were due to CASUAL SELECTION of chamber designs, gas mixtures, materials and gas system components, which worked at “low rates”, but failed in high-rate environments

International Workshop on AGING PHENOMENA IN GASEOUS DETECTORS

DESY, Hamburg October 2-5, 2001

Topics will include:

- Coping with classical aging problems
- New aging effects
- Models and new insights from plasma chemistry
- Materials: Lessons for detectors and gas systems
- Experiences with large detector systems
- Recommendations for future detectors

Deadline for registration: August 1, 2001

Deadline for submission of abstracts: June 29, 2001

Proceedings to be published in Nuclear Instruments and Methods A

International Advisory Committee

M. Danilov (ITEP Moscow) V. Peskov (Lund)
 B. Dolgoshein (MEPHI Moscow) F. Sauli (CERN)
 D. Froidevaux (CERN) I. Shipsey (Purdue)
 J. Kadyk (LBL) J. Va'va (SLAC)
 P. Krizan (Ljubljana) A. Wagner (DESY)

Local Organizing Committee

M. Hohlmann (chair, DESY)
 C. Padilla (DESY)
 N. Tesch (DESY)
 M. Titov (ITEP Moscow)
 I. Kerkhoff, R. Matthes (secretaries)

Registration, Contact & Info

Register and submit abstracts online at <http://www.desy.de/agingworkshop>
 Contact: agingworkshop@desy.de
 Tel.: +49 40 8998-4600
 FAX: +49 40 8998-4900

Table 1. Aging results with wire detector prototypes for the use at high energy physics facilities.

Experiment, Detector, Reference	Gas Mixture	Gas reduction/etching	Cathode aging	Charge C/cm	Gas gain(G), Current density(I), Rate (R), Irradiated area (S)
HERA-B OTR [34]	Ar/CF ₄ /CO ₂ (65:30:5)	No/Au damage	No	0.6	G-3*10 ⁵ ; I-0.4-0.9 μA/cm; 100MeV n-beam; S-50cm ²
HERA-B MUON [35]	Ar/CF ₄ /CO ₂ (65:30:5)	No	No/F-film on Al cath.	0.7	G-10 ⁵ ; I-0.3 μA/cm; R<10 ⁶ Hz/cm ² ; S-1200cm ²
HERA-B MUON [35]	Ar/CF ₄ (70:30)	No	No	0.07	G-10 ⁵ ; I-0.15 μA/cm; R-10 ⁶ Hz/cm ² ; S-150cm ²
ATLAS TRT [15,48]	Xe/CF ₄ /CO ₂ (70:20:10)	No	No	20	G-3*10 ⁵ ; I-0.7 μA/cm; S-24cm ²
Straw R&D [45]	Ar/CF ₄ /CO ₂ (70:20:10)	No/Au	No	9	G-3*10 ⁵ ; I-1.7 μA/cm; S-1cm ²
Straw R&D [45]	Ar/CF ₄ (60:10:30)	No	No	1	G-10 ⁵ ; I-0.1 μA/cm; S-1cm ²
CMS MUON [14]	Ar/CF ₄ /CO ₂ (40:10:50)	crucass	on Cu cath.	0.4	R-2*10 ⁶ Hz/cm ² ; S-3cm ²
CMS MUON [46]	Ar/CF ₄ /CO ₂ (40:10:50)	No	Si-F film on Cu cath.	0.4	G-10 ⁵ ; I < 0.05 μA/cm; R-2*10 ⁶ Hz/cm ² ; S-21000cm ²
LHC-B MUON [52]	Ar/CF ₄ /CO ₂ (40:10:50)	No	Etching of FR4 bars	0.25	G-10 ⁵ ; I < 0.03 μA/cm; R-3*10 ⁶ Hz/cm ² ; S-1500cm ²
COMPASS Straws [53]	Ar/CF ₄ /CO ₂ (74:20:6)	No/Si traces	No	1.1	G-4*10 ⁵ ; I-4 μA/cm; R-2*10 ⁶ Hz/cm ² ; S-3cm ²
HERMES FD [47]	Ar/CF ₄ /CO ₂ (60:55:5)	No	Al etching/Cl deposits	9	G-5*10 ⁵ ; I-1 μA/cm; R-10 ⁶ Hz/cm ² ; S-7cm ²
ATLAS TRT [16]	Xe/CO ₂ /O ₂ (70:27:3)	No	No	11	G-3*10 ⁵ ; I-1-1.3 μA/cm; S-1cm ²
ATLAS TRT [16]	Xe/CO ₂ /O ₂ (70:27:3)	No/Si deposits	No	0.3	G-3*10 ⁵ ; I-0.1 μA/cm; S-1cm ²
ATLAS MDT [55]	Ar/CO ₂ (90:10)	No	No	0.7	I-0.1 μA/cm; R-4*10 ⁶ Hz/cm ² ; S-7500cm ²
ATLAS MDT [56]	Ar/CO ₂ (93:7)	No	No	>1.5	G-2*10 ⁵ ; I-0.05-0.2 μA/cm; R-8*10 ⁶ Hz/cm ² ; S-90cm ²
ATLAS MDT [57]	Ar/CO ₂ (93:7)	Yes/Si deposits	No	0.2	G-9*10 ⁵ ; I-0.02 μA/cm; R-5*10 ⁶ Hz/cm ² ; S-15000cm ²
CMS MUON [14]	Ar/CO ₂ (30:70)	Yes/Si deposits	No	0.76	G-6*10 ⁵ ; I-1-2 μA/cm; R-2*10 ⁶ Hz/cm ² ; S-1cm ²

Wire chambers

Table 2. Summary of aging experience with Micro-Pattern Gas Detectors.

Detector type	Mixture	Gas reduction ΔCFG	Charge in C/cm ²	Current density, μA/mm ²	Irradiate dose, 10 ¹⁴ MeV/cm ²	Irrad. source
MS GC [65,104]	Ar/DME (90:10)	No	200	10	3 mm ² , 10 ¹⁴ MeV/cm ²	6.4 keV X-rays
MS GC [66]	Ar/DME (90:50)	No	40	63	0.3*0.8 mm ² , 0.3*0.8 mm ² , 2.5*0.8 mm ²	5.4 keV X-rays
MS GC [66]	Ar/DME (90:50)	Anode deposit	50	9	0.3*0.8 mm ² , 2.5*0.8 mm ²	5.4 keV X-rays
MS GC+GEM [66]	Ar/DME (90:10)	No	70	63	0.3*0.8 mm ² , 2*10 ³ Hz/mm ²	5.4 keV X-rays
MS GC+GEM [51]	Ar/DME (90:50)	No	5	2	~113 mm ² , 2*10 ³ Hz/mm ²	8keV X-rays
MS GC+GEM [51]	Ar/DME (90:50)	Yes	0.5	1	~900 mm ² , 2*10 ³ Hz/mm ²	8keV X-rays
MS GC+GEM [51]	Ar/DME (90:50)	No	-	2	350 mm ² , 2*10 ³ Hz/mm ²	8keV X-rays
Double GEM [67]	Ar/CO ₂ (70:30)	No	12	4	200 mm ² , 5*10 ⁶ Hz/mm ²	6keV X-rays
Triple GEM [68]	Ar/CO ₂ (70:30)	No	11	10	1260 mm ² , 2*10 ³ Hz/mm ²	5.9 keV X-rays
Triple GEM [71,72]	Ar/CF ₄ /CO ₂ (60:20:20)	< 5%	230	270	1 mm ² , 5*10 ⁶ Hz/mm ²	5.9 keV X-rays
Triple GEM [72]	Ar/CF ₄ /CO ₂ (45:40:15)	< 5%	45	160	1 mm ² , 5*10 ⁶ Hz/mm ²	5.9 keV X-rays
Triple GEM [73]	Ar/CF ₄ /CO ₂ (45:40:15)	Yes/56%	20	20	200*240 mm ² , 25 kV ² Co	5.9 keV X-rays
Triple GEM [72]	Ar/CF ₄ /CO ₂ (65:25:7)	~10%	110	160	1 mm ² , 5*10 ⁶ Hz/mm ²	5.9 keV X-rays
Triple GEM+CsI [88]	Ar/CF ₄ /CO ₂ (100)	No	0.1	3	100 mm ² , 10 ¹⁴ MeV/cm ²	Hg UV Lamp
Micronegas [74]	Ne/C ₂ H ₆ (91:9)	Yes/35%	10	50	16 mm ² , 33Hz quench rate	5.3 MeV X-rays
Micronegas [75]	Ar/CF ₄ (95:5)	No	2	10	-----	8keV X-rays
Micronegas [76]	CF ₄ /C ₂ H ₆ (94:6)	No	1.6	25	20 mm ² , ~10 ⁶ Hz/mm ²	8keV X-rays
Micronegas [76]	Ar/C ₂ H ₆ (2:6)	No	18	20	20 mm ² , 2*10 ³ Hz/mm ²	8keV X-rays
Micronegas+GEM [77]	Ar/CO ₂ (70:30)	No	23	17	3 mm ²	5.4 keV X-rays
MS GC+GEM [78]	Ar/DME (90:40)	10% off. decay	0.01	0.05	100*160 mm ² , 2*10 ³ Hz/mm ²	24 GeV protons
3 GEM [78]	Ar/CO ₂ (70:30)	No	2.3	--	310*310 mm ² , 2*10 ³ Hz/mm ²	Compass Beam

MPGDs

Aging Phenomena in Gaseous Detectors

Implicit assumption: aging rate is proportional only to the total accumulated charge

$$R = - (1/G)(dG/dQ) \quad (\% \text{ per C/cm}) \quad (\text{Kadyk'1985})$$

Aging phenomena depends on many highly correlated parameters:

Microscopic parameters:

- ✓ Cross-sections
- ✓ Electron or photon energies
- ✓ Electron, ion, radical densities
- ✓ ...



Macroscopic parameters:

- ✓ Gas mixture (nature of gas, trace contaminants)
- ✓ Gas flow & Pressure
- ✓ Geometry/material of electrodes & configuration of electric field
- ✓ Construction materials
- ✓ Radiation intensity
- ✓ Gas gain, ionization density
- ✓ Size of irradiation area

~1980
CLASSICAL AGING:

'NEW AGING' EFFECTS:

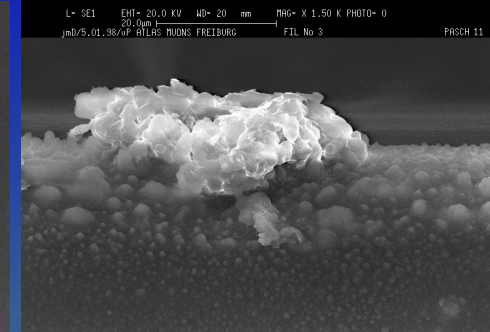
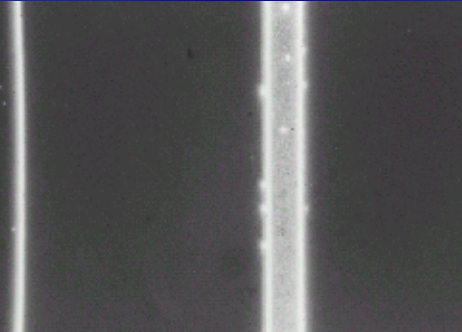
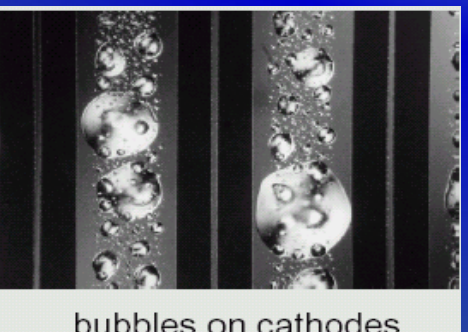
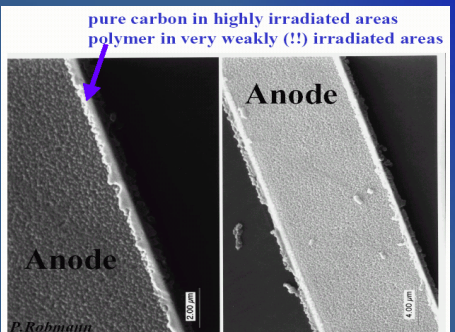
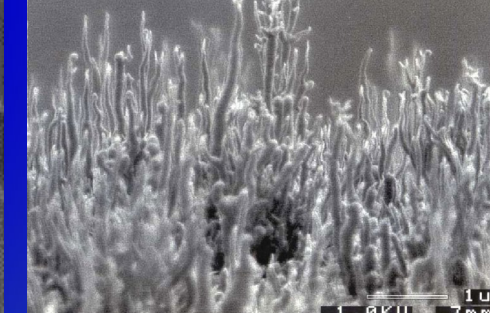
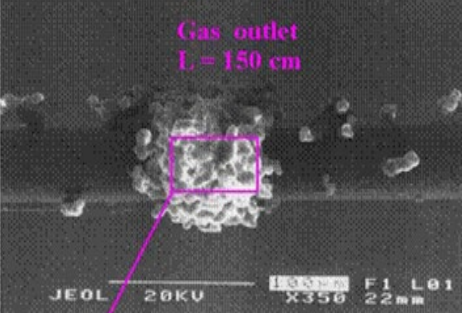
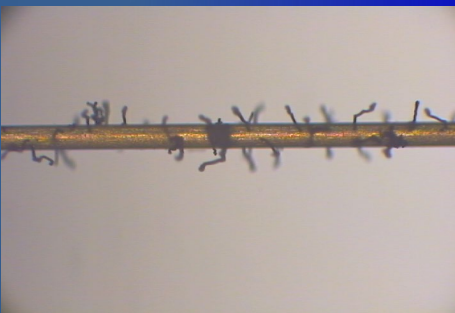
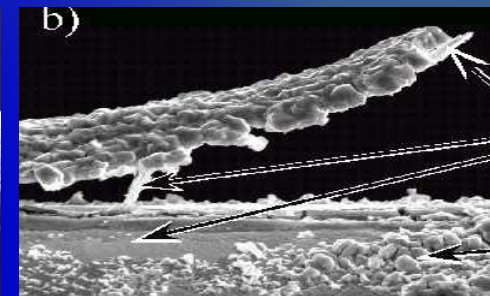
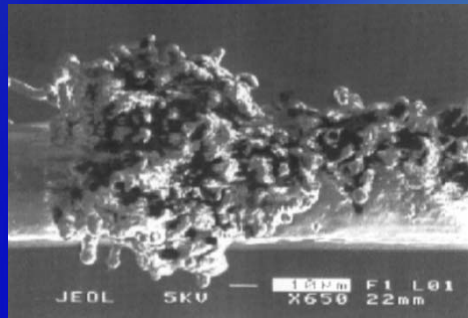
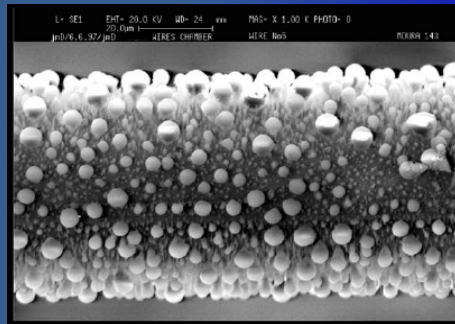
~2000

There are simply too many variables in the problem →

would be too naive to expect that one can express the aging rate using a single variable (C/cm)

Aging Phenomena in Gaseous Detectors

- ✓ Early aging studies of MSGCs indicated that they are much more susceptible to aging than wire chambers, potentially due to the filigree nature of MSGC structures and catalytic effects on the MSGC substrate
- ✓ More robust detectors (GEM, Micromegas) are better suited for the high-rate environments than MSGC and Wire-type detectors



Building Radiation-Hard Gas Detector (2001): Rules of Thumb

- ✓ *Build a “full-size prototype” (the smallest independent element of your detector)*
- ✓ *Expose full detector area of to the real radiation profile (particle type, gas gain, ionization density)*
- ✓ *Choose your gas mixtures (hydrocarbons are not trustable) and materials very carefully*
- ✓ *Vary all parameters systematically (gas gain, irradiation intensity, gas flow, ...) and verify your assumptions → make aging studies on several identical prototypes*
- ✓ *Do not extrapolate aging results for any given parameter by more than an order of magnitude*
- ✓ *If you observed unexpected result - understand the reason – and reproduce results ...*

International Conference on Detector Stability and Aging Phenomena in Gaseous Detectors

6–10 Nov 2023
CERN
Europe/Zurich timezone

3rd Conference on Detector Stability and Aging Phenomena in Gaseous Detectors (Nov 6-10, 2023, CERN)

Overview

Local Organizing Committee and International Program Committee

Official news and bulletins

Contact

✉ roberto.guida@cern.ch

Gaseous detectors for particle physics are entering a phase where operation at current experiments and future facilities will require the capacity to work at unprecedented particle rate, higher rate capability, integrated charge and improved time resolution. In addition, new materials are in many cases needed to achieve these new requirements. Finally, the need to replace environmentally unfriendly gases has set an additional challenge to the community.

The third International Conference on Detector Stability and Aging Phenomena in Gaseous Detectors aims in offering an occasion for sharing new results, new ideas, new facility requirements, ...

The conference will be held at CERN in the main Auditorium from November 6th to 10th, 2023.

The conference will continue the initiative started in 1986 with the first workshop held at LBL (Berkeley) and in 2001 at DESY (Hamburg).

Conference topics will include:

- Detector stability and performance
- Aging phenomena
- Radiation hardness
- Material outgassing
- Novel materials
- Electrodes
- Photocathodes
- Plasma chemistry
- Environmentally friendly gases
- Gas and material analysis, characterisation, instruments
- Discharge damage and mitigation
- Test facilities
- Front End Electronics for detector stability and aging mitigation

<https://indico.cern.ch/event/1237829>

The conference will have invited reviews and selected contributions, as well as a poster session.

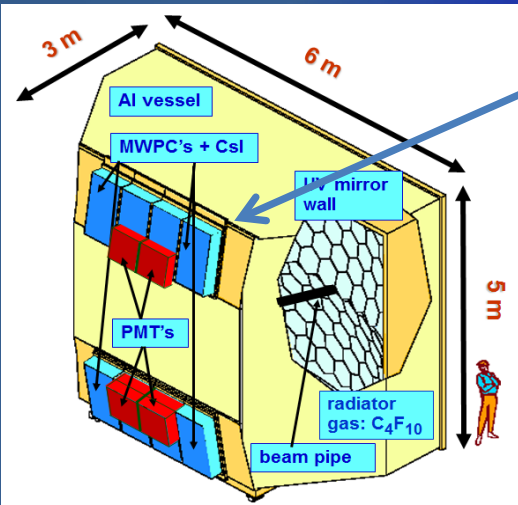
The conference proceeding will be published in peer-reviewed journal.

COMPASS RICH Upgrade: Hybrid THGEM + MM with CsI PC

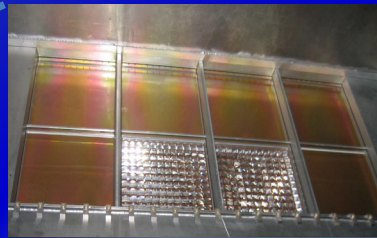
COMPASS RICH I: 8 MWPC with CsI since 2000

8 Years of Dedicated R&D: THGEM+ CsI

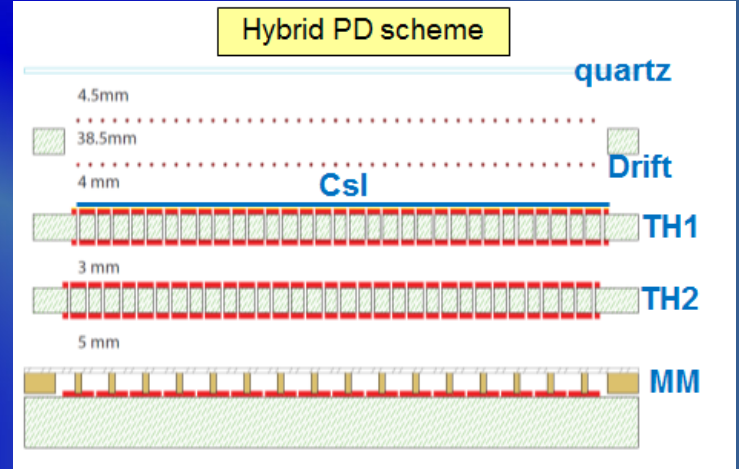
New Hybrid THGEM + MM PDs:



MWPC's + CsI

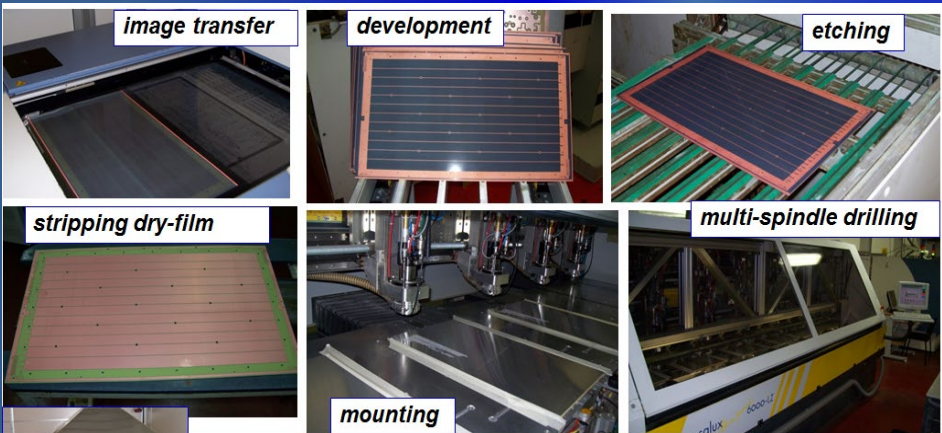


MWPC+CSI: successful but with performance limitations for central chambers

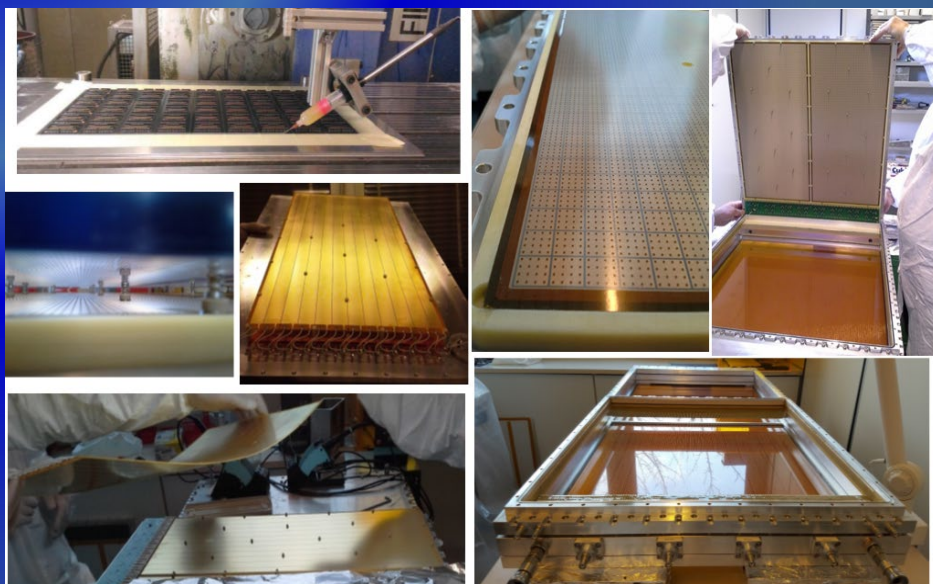
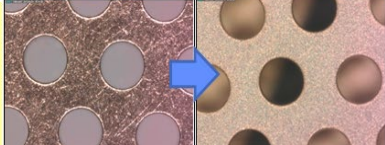


Production THGEM @ ELTOS Company:

Assembly of Hybrid THGEM +MM:



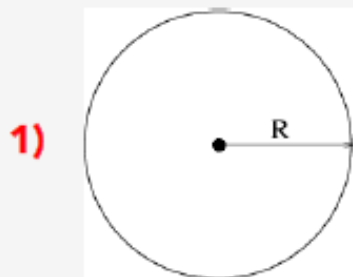
In Trieste a specific cleaning procedure is applied : polish with fine grain pumice powder, pressure water cleaning, ultrasonic Bath with Sonica PCB solution (PH11), distilled water rinsing and oven @ 160 °C



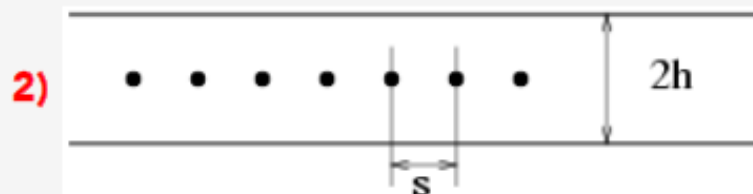
Summary & conclusion

Christian Lippmann, 2nd ECFA High Luminosity LHC Experiments Workshop, Aix-les-bains, France, October 21-23 (2014)

**Geiger- Müller (1908), 1928
Drift Tube (1968)**



**G. Charpak, 1968
Multi Wire Proportional Chamber**

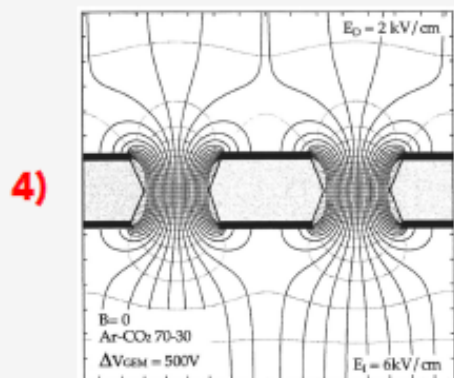


**R. Santonico, 1980
Resistive Plate Chamber**

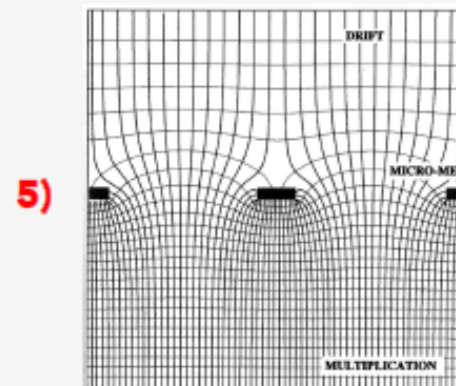


... will at HL-LHC be joined by:

**F. Sauli (1997)
Gas Electron Multiplier**



**I. Giomataris et al. (1996)
Micro-mesh gaseous chamber (Micromegas)**



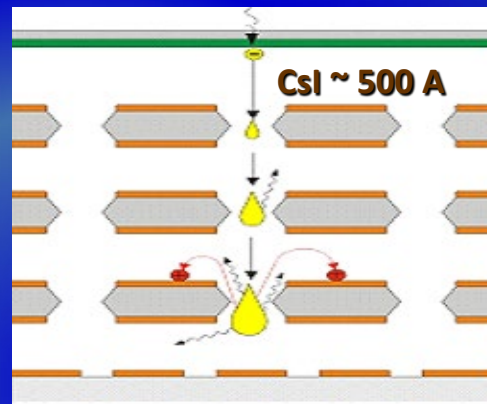
MPGD-Based Gaseous Photomultipliers

GEM or THGEM Gaseous Photomultipliers (CsI -PC) to detect single photoelectrons

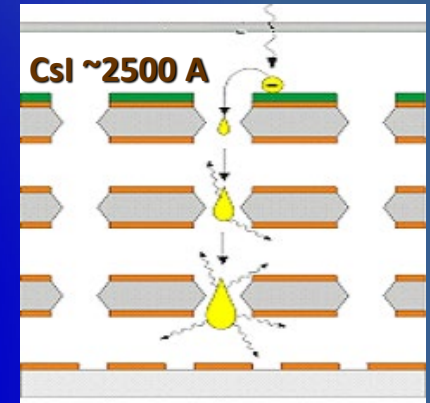
Multi-GEM (THGEM) Gaseous Photomultipliers:

- ✓ Largely reduced photon feedback (can operate in pure noble gas & CF_4)
- ✓ Fast signals [ns] → good timing
- ✓ Excellent localization response
- ✓ Able to operate at cryogenic T

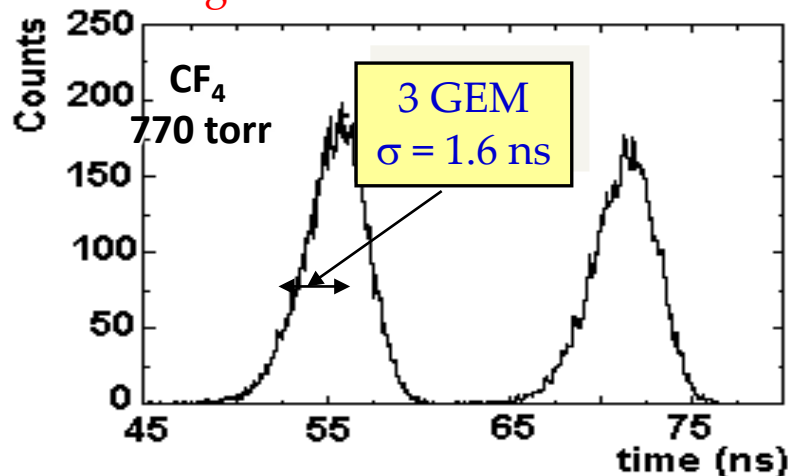
Semitransparent Photocathode (PC)



Reflective Photocathode (PC)

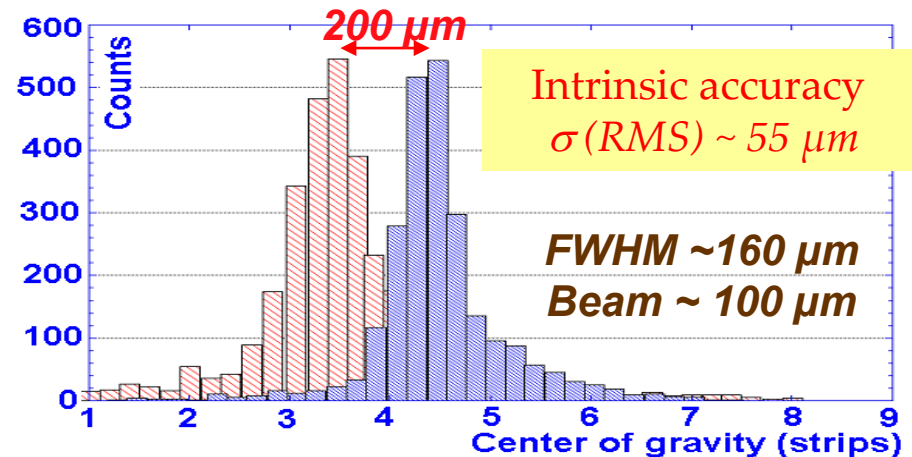


Single Photon Time Resolution:



Micromegas: $\sigma \sim 0.7$ ns with MIPs

Single Photon Position Accuracy:



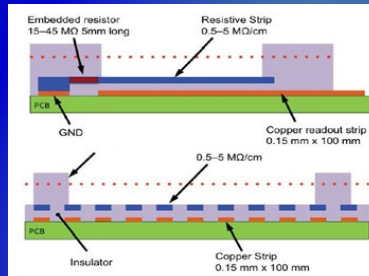
Large-Area MM / GEM Detectors for ATLAS / CMS Upgrade

Resistive MM for ATLAS NSW Muon Upgrade:

Standard Bulk MM suffers from limited efficiency at high rates due to discharges induced dead time

Solution: Resistive Micromegas technology

- Add a layer of resistive strips above the readout strips
- Spark neutralization/suppression (sparks still occur, but become inoffensive)



Still, main issue encountered: HV instability

==> found to be correlated to low resistance of resistive strip anode
 ==> applied solutions + passivation in order to deactivate the region where $R < 0.8 \text{ M}\Omega$

Production, sector integration (~1200m² resistive MM):

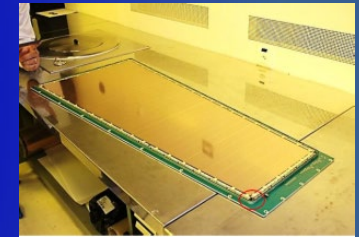
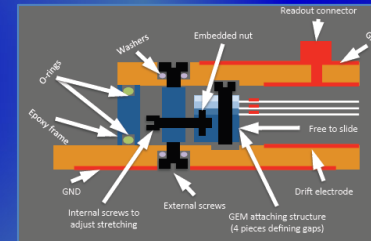


GEMs for CMS Muon System Upgrade:

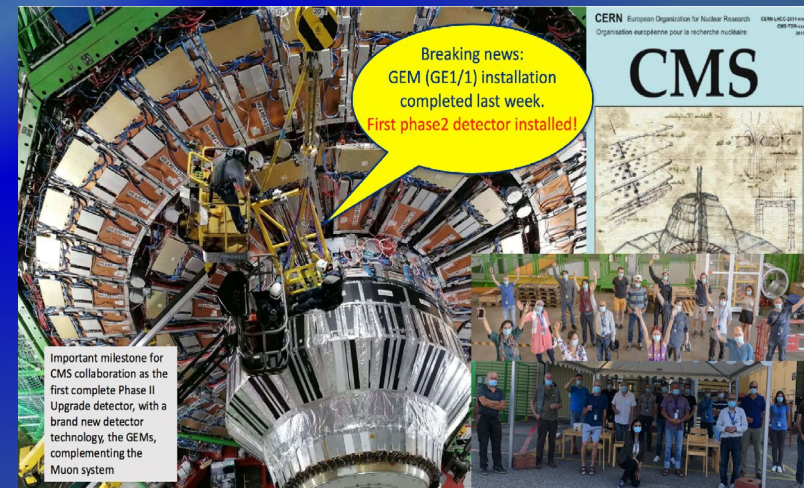
- Single-mask GEM technology (instead of double-mask)
 → Reduces cost /allows production of large-area GEM



- Assembly optimization: self-stretching technique:
 → assembly time reduction to 1 day



September 2020: 144 GEM chambers installed



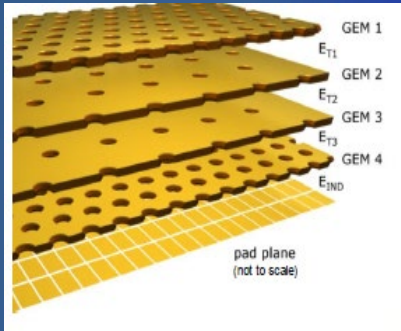
Important milestone for CMS collaboration as the first complete Phase II Upgrade detector, with a brand new detector technology, the GEMs, complementing the Muon system

CERN European Organization for Nuclear Research
 Organisation européenne pour la recherche nucléaire

CMS

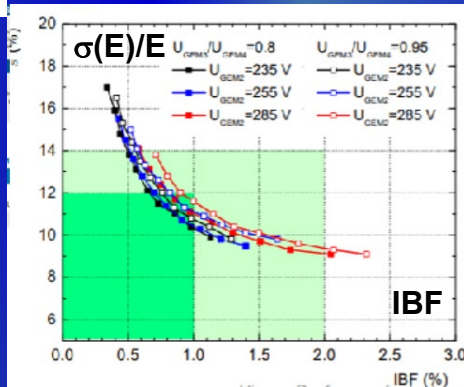
TPC with MPGD Readout for ALICE Upgrade and ILC

ALICE TPC → replace MWPC with 4-GEM staggered holes (to limit space-charge effects)



- Upgrade for continuous TPC readout @ 50 kHz Pb-Pb collisions
- Phys. requirements:
IBF < 1%,
Energy res. $\sigma(E)E < 12\%$

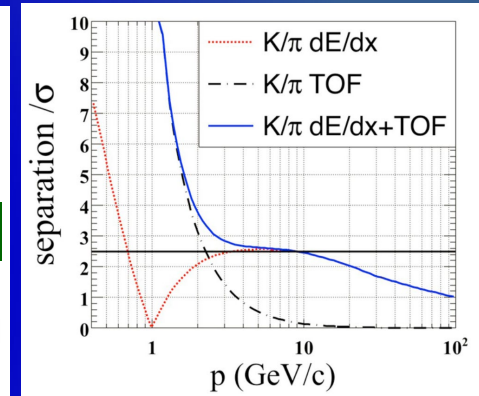
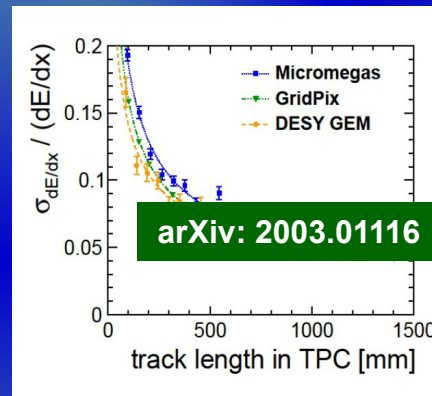
TPC reinstallation in the ALICE cavern (August 2020)



ILC –TPC with MPGD-based Readout

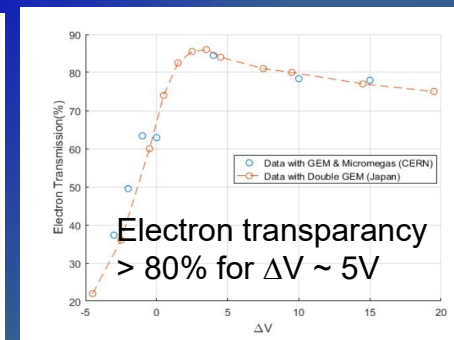
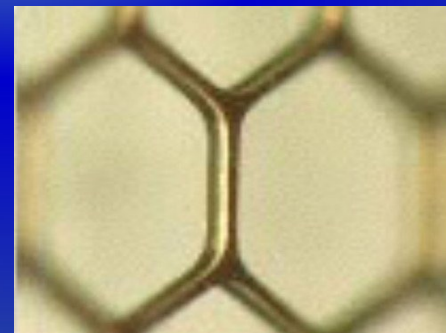
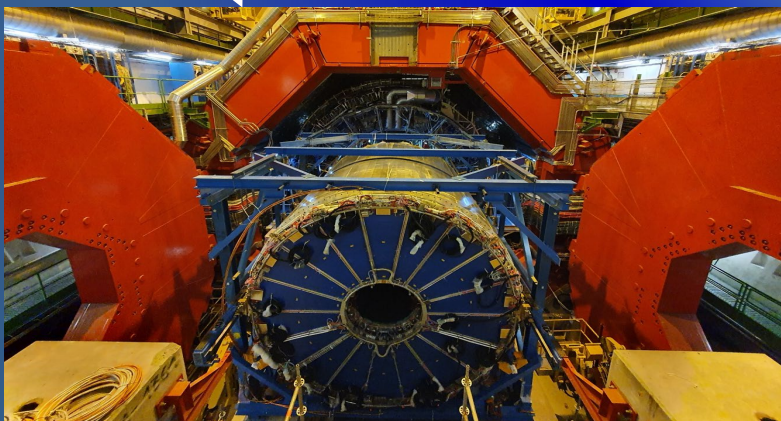
Target requirement of a spatial resolution of 100 um in transverse plane and dE/dx resolution < 5% have been reached with all technologies (GEM, MM and GridPix)

If dE/dx combined with ToF using SiECAL, $P < 10\text{GeV}$ region for pion-K separation covered



ILC: gating scheme, based on large-aperture GEM

- Machine-induced background and ions from gas amplific.
- Exploit ILC bunch structure (gate opens 50 us before the first bunch and closes 50 us after the last bunch)



Advanced Concepts Picosecond (a few 10's) Timing Detectors

Several types of technologies are considered for "Picosecond-Timing Frontier":

- **Ionization detectors** (silicon detectors or gas-based devices)
- **Light-based devices** (scintillating crystals coupled to SiPMs, Cherenkov absorbers coupled to photodetectors with amplification, or vacuum devices)

CONVENTIONAL MCP – PMT APPLICATIONS:

ATLAS HGTD (CMS ETL) TIMING WITH LGAD:

BELLE II TOP:

LHCb TORCH DIRC:

PANDA ENDCAP:

CMS BTL TIMING WITH LYSO:Ce / SiPMs:

LAPPD TIMING PROJECT:

GASEOUS DETECTORS APPLICATIONS:

ALICE MPRC TOF:

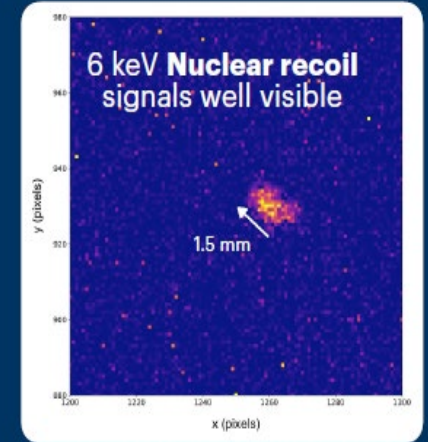
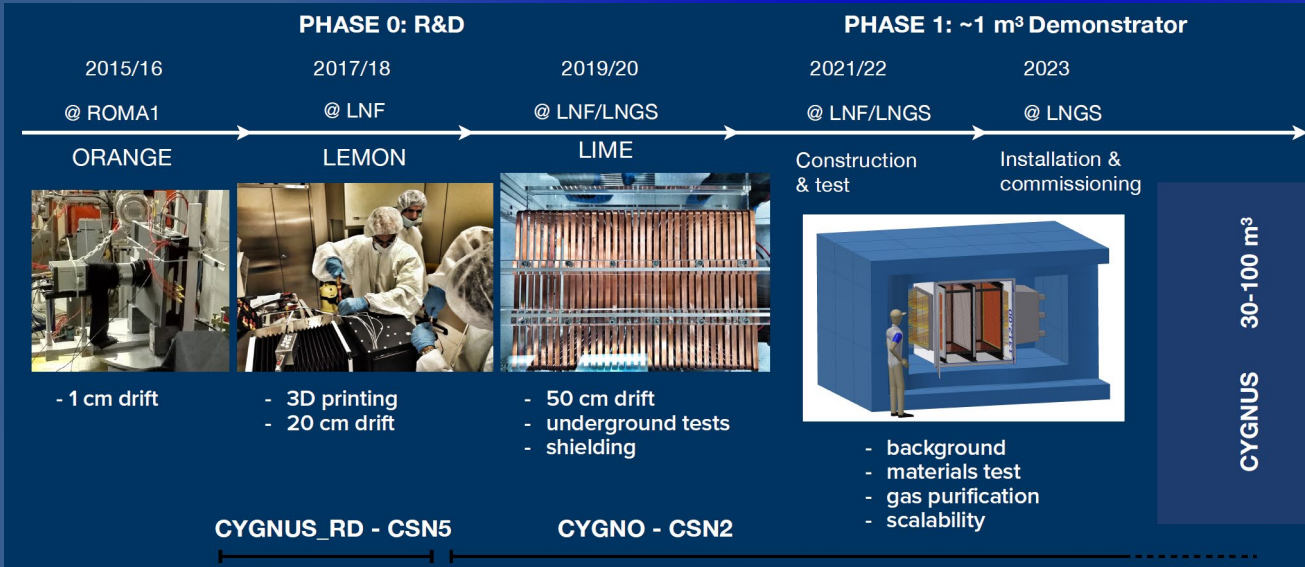
PICOSEC - MICROMEGAS:

Examples of timing detectors at a level of ~ 30 ps for MIPs and ~ 100 ps for single photons

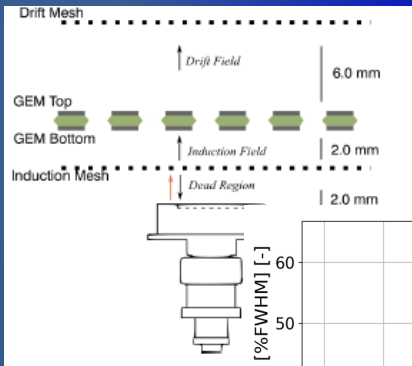
The CYGNO TPC: Optical Readout for Directional Study of Rare Events

CYGNO is working in the framework of CYGNUS: international Collaboration for realization of Multi-side Recoil Directional Observatory for WIMPs & ν 's

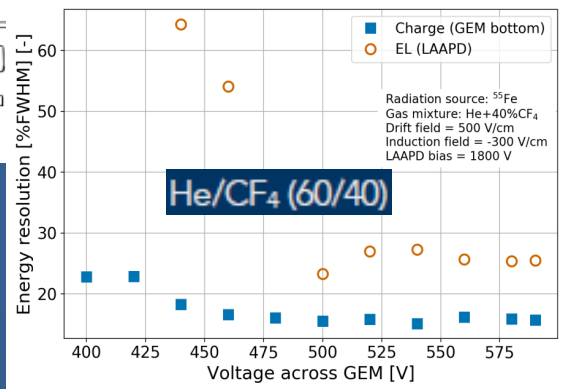
GEM Optical readout: Promising performance in a few keV region



A sizeable efficiency in the range 5-10 keV was measured while more than **95% (99%)** ⁵⁵Fe photons were rejected



Electroluminescence studies: readout light produced during multiplication process in GEMs

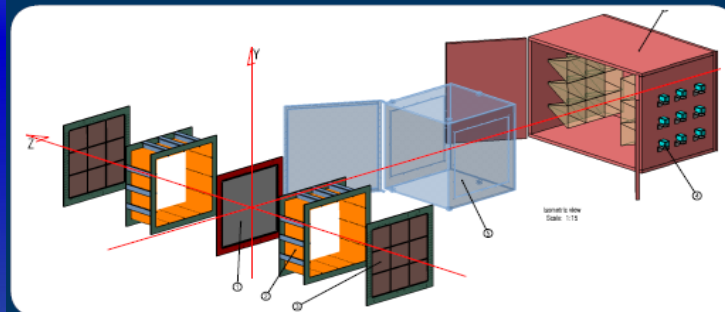


Optically readout TPC: 3D tracking (position and direction); total released energy measurement and dE/dx profile;

1m³ DEMONSTRATOR: BASELINE LAYOUT

1 m³ of He/CF₄ 60/40 (1.6 kg) at atmospheric pressure with a composed by two 50 cm long TPC with a central cathode and a drift field of about 1 kV/cm;

Acrylic vessel ensuring gas tightness and high voltage insulation;



Each side equipped by a 3x3 matrix of LIME-like:

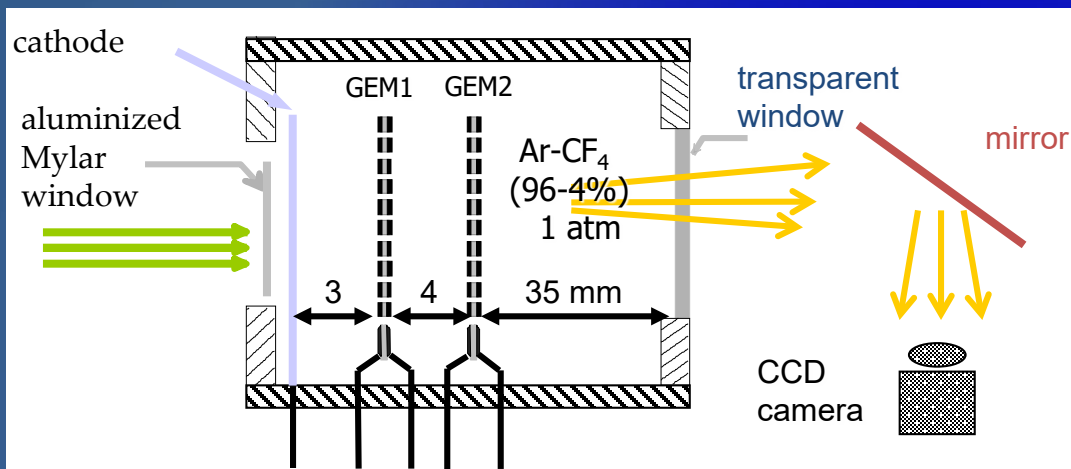
- sCMOS sensor 65 cm away;
- Almost 10⁸ readout pixels 165 x 165 μ m²
- Fast light detector (PMT or SiPM).

Radioactivity shielding:

- 5 cm thick copper box (Faraday cage too);
- 200 cm of water.

Scintillating GEM for Dose Imaging in Radiotherapy

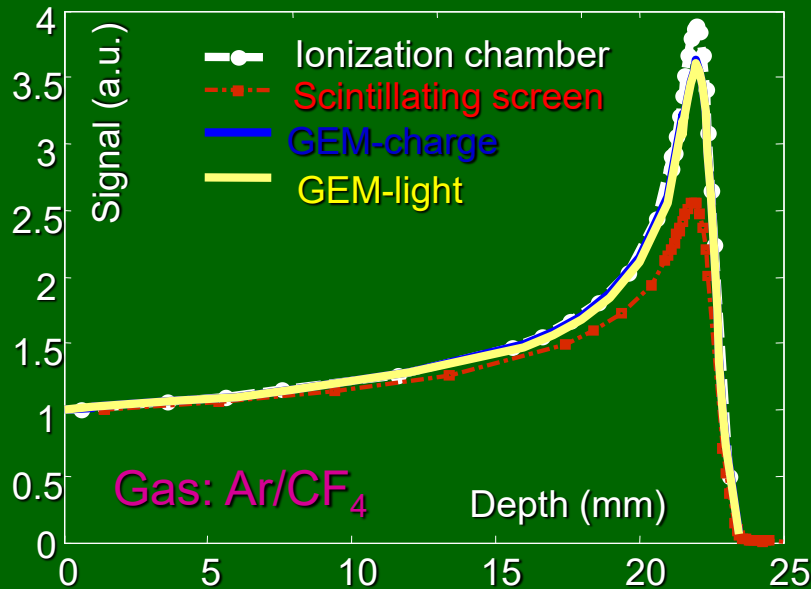
Scintillation Light (Optical) & Charge Readout:



Light output for 138 MeV protons:

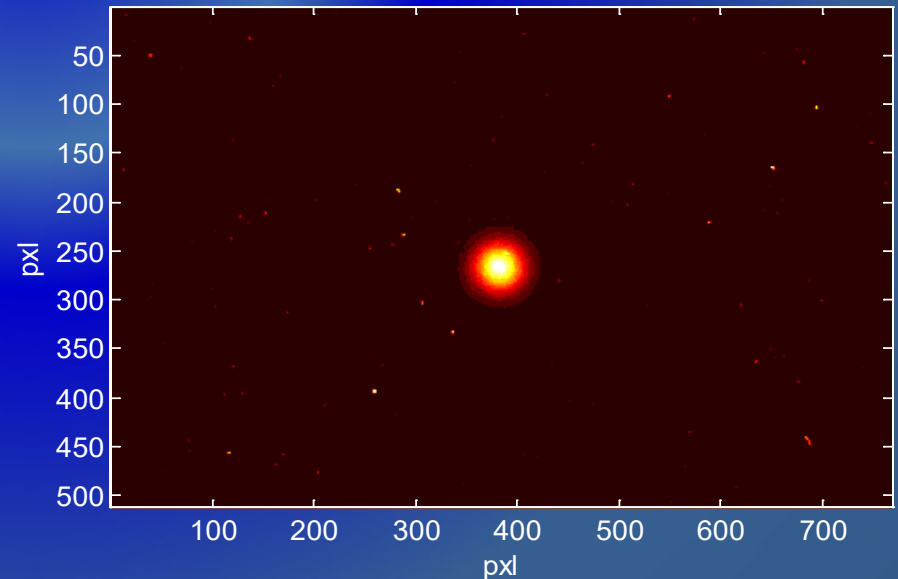
Scintillation type	Gas gain	Light signal (CCD) at 1Gy proton dose (ADU)
Screen (Gd ₂ O ₂ S:Tb)		2670
Ar/CO ₂ (90:10)	3000	270
Ar/CF ₄ (90:10)	1400	2350
Ar/CF ₄ (95:5)	1300	4000
Ar/CF ₄ (97,5:2,5)	770	2000

Bragg curve with 360 MeV α -beam



LIGHT SIGNAL FROM GEM:

(only 4% smaller than ionization chamber signal)

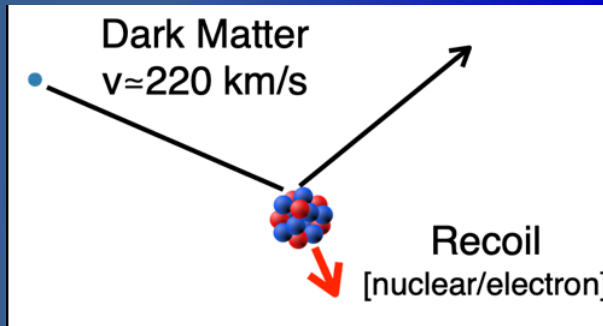


NEWS-G: Search for Dark Matter with Spherical Proportional Counters

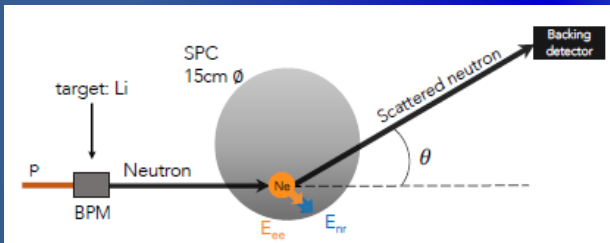
NEWS-G Collaboration: 5 countries, 10 institutes, ~40 collaborators

Three underground laboratories:

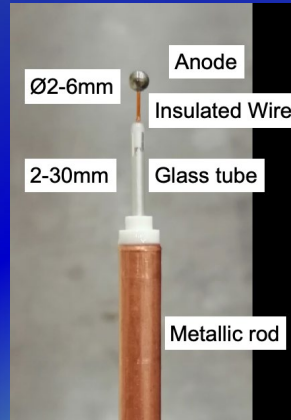
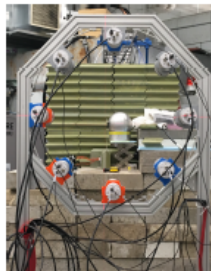
- ✓ SNOLAB
- ✓ Laboratoire Souterrain de Modane
- ✓ Boulby Underground Laboratory



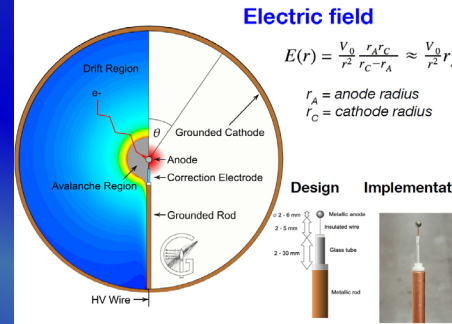
Nuclear Quenching Factor measurements:



Run	E_{nr} [keV $_{nr}$]	θ [°]
8	6.8	29.02
7	2.93	18.84
14	2.02	15.63
9	1.7	14.33
10	1.3	12.48
14	1.03	11.13
11	0.74	9.4
14	0.34	6.33



The Spherical Proportional Counter



Basic advantages

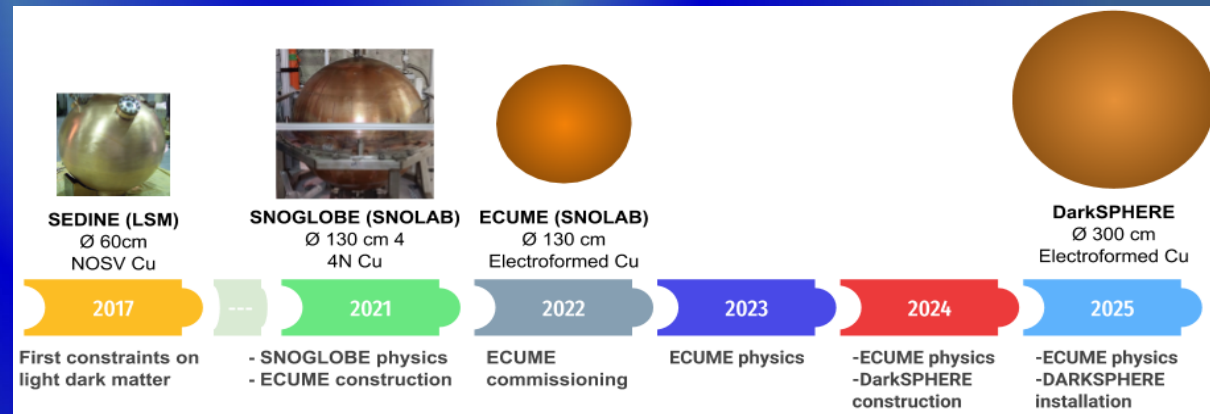
- Large volume/ few read-out channels
- Single electron threshold:
 - Low capacitance
 - High gain
- Radio-pure construction
- Background rejection handles
- Flexible operation
 - Swappable gases-targets
 - Variable pressure choice



L. Giomataris et al., JINST, 2008, P09007.

Increasing Target Mass and Reducing Background:

- ✓ ACHINOS, electroformation, ...
- ✓ Several detectors scheduled for the coming years
- ✓ Eventually sensitivity could reach neutrino floor



CEvNS & NEWS-G

- **CEvNS opens a window to investigation non-standard neutrino interactions**
 - ▶ First observations by COHERENT in NaI (2017) and Ar (2020)
 - ▶ Unique complementarity with DM searches as sensitivity reaches the neutrino floor
- **NEWS-G3: A low-threshold low-background sea-level facility**
 - ▶ Environmental and cosmogenic background studies towards reactor CEvNS studies
 - ▶ Shielding: Layers of pure copper, polyethylene, and lead, with active muon veto
 - ▶ Commissioning in 2021